Project No. 12-69 **COPY NO.**

___

DESIGN AND CONSTRUCTION GUIDELINES FOR LONG-SPAN DECKED PRECAST, PRESTRESSED CONCRETE GIRDER BRIDGES

FINAL REPORT

Prepared for
National Cooperative Highway Research Program
Transportation Research Board
National Research Council

R.G. Oesterle and A.F. Elremaily
Construction Technology Laboratories, Inc
5400 Old Orchard Road, Skokie, IL 60077

In Association with:
Z. John Ma, University of Tennessee, Knoxville
Roy Eriksson, Eriksson Technologies, Inc.
Chuck Prussack

July 30, 2009

Project No. 12-69

DESIGN AND CONSTRUCTION GUIDELINES FOR LONG-SPAN DECKED PRECAST, PRESTRESSED CONCRETE GIRDER BRIDGES

FINAL REPORT

Prepared for
National Cooperative Highway Research Program
Transportation Research Board
National Research Council

R.G. Oesterle and A.F. Elremaily
Construction Technology Laboratories, Inc
5400 Old Orchard Road, Skokie, IL 60077

In Association with:
Z. John Ma, University of Tennessee, Knoxville
Roy Eriksson, Eriksson Technologies, Inc.
Chuck Prussack

July 30, 2009

ACKNOWLEDGMENT OF SPONSORSHIP

This work was sponsored by the American Association of State Highway and Transportation Officials, in cooperation with the Federal Highway Administration, and was conducted in the National Cooperative Highway Research Program, which is administered by the Transportation Research Board of the National Research Council.

TABLE OF CONTENTS

TABLE OF CONTENTS (continued)

LIST OF TABLES

LIST OF FIGURES

LIST OF FIGURES (continued)

LIST OF FIGURES (continued)

AUTHOR ACKNOWLEDGEMENTS

The research reported herein was performed under NCHRP Project 12-69 by Construction Technology Laboratories, Inc (CTLGroup). Dr. Ralph G. Oesterle, Senior Principal Structural Engineer at CTLGroup was Principal Investigator. The other authors of the report are Dr. Ahmed Elremaily, Senior Structural Engineer, CTLGroup, Dr. Z. John Ma, Associate Professor, University of Tennessee (UTK), Lungui Li, Ph.D. Candidate at UTK, Roy Eriksson, President and CEO, Eriksson Technologies, Inc., and Chuck Prussack, President, Central Pre-Mix Prestress Co.

The author would also like to acknowledge Mary Griffey, Austin Bateman, Ken Thomas and Larry Roberts, Research Assistants at UTK for their assistance with the testing. Ross Prestressed Concrete, Inc. donated the concrete materials and helped with the casting of the specimens. Headed Reinforcement Corporation donated the headed bar reinforcement, and Oklahoma Steel and Wire Co., Inc. provided the welded wire reinforcement (WWR).

ABSTRACT

This report documents results of a study of decked, precast, prestressed, concrete bridge girders. This type of bridge provides benefits of rapid construction, and improved structural performance. The research was performed to develop guidelines for design and construction and to address issues that significantly influence performance. The first goal was accomplished by development of guidelines for design, construction, and geometry control based on successful methodology currently being used. The second goal of the project was to develop an improved longitudinal joint system. The performance of longitudinal joints between the flanges of adjacent decked girders was defined as a major issue inhibiting the general use of decked girders. An analytical study was performed to develop an optimized family of girder section with consideration for future re-decking. Analytical studies were carried out using the optimized section to define live load and camber leveling load demand on the flange-to-flange joint. A study of potential joint systems was used to define trial alternate joints, Laboratory testing of trial joints was used to identify an improved alternate joint, and full-scale panel tests of the selected alternate joint were conducted to investigate the performance under static and fatigue flexural and flexure-shear loading. The improved joint includes headed reinforcing bars lapped spliced to develop moment and shear continuity in narrow grouted joints. The findings of the longitudinal joint study indicate that the improved joint detail is a viable connection system to transfer the force between adjacent decked bulb tee girders.

EXECUTIVE SUMMARY

A "decked" concrete girder is a precast, prestressed concrete I-beam, bulb-tee, or multi-stemmed girder with an integral deck that is cast monolithically and prestressed with the girder. These girders are manufactured in precast concrete plants under closely controlled and monitored conditions, transported to the construction site, and erected such that flanges of adjacent units abut each other. Load transfer between adjacent units is provided using specially designed connections along with a grouted shear key. Sections that are not too long or too heavy for transportation by truck can be used to construct long-span girder bridges. This type of bridge construction provides the benefits of rapid construction, improved safety for construction personnel and the public, and improved structural performance and durability.

In spite of their benefits, the use of decked precast, prestressed concrete girders has been limited because of concerns about certain design and construction issues that are perceived to influence the structural integrity of the bridge system. These issues include connections between adjacent units, longitudinal joints, longitudinal camber, cross slope, live load distribution, continuity for live load, lateral load resistance, skew effects, maintenance, replaceability and other factors that influence constructability and performance.

The primary objective of NCHRP Project 12-69 is to develop guidelines for design and construction for long-span decked precast, prestressed concrete girder bridges. These guidelines will provide highway agencies with the information necessary for considering a bridge construction method that is expected to reduce the total construction time, improve public acceptance, reduce accident risk, and yield economic and environmental benefits.

In developing these guidelines, the NCHRP Project 12-69 had two goals. The first was to provide guidelines for design, construction, and geometry control based on successful methodology currently being used. To date, use of long-span decked precast, prestressed concrete girder bridges has mostly been limited to the northwest region of the United States where this type of bridge has been used very successfully. The first goal of the NCHRP project is to document the successful methodologies. This has been accomplished by interviews with knowledgeable designers and precasters, by collecting and reviewing existing design and construction practices, and presenting the collected information within a separate guideline document.

The second goal was to develop an improved longitudinal joint system. Currently, the most widely used longitudinal connection between precast concrete members is a combination of a continuously grouted shear key and welded connectors spaced at intervals from 4 ft to 8 ft on-center. This type of connection is intended to transfer shear and prevent relative vertical displacements across the longitudinal joints.

Implications from a survey of issues performed as part of the NCHRP Project12-69 indicated that, if this type of joint is properly designed and constructed, the performance can be good to excellent. Therefore, the guidelines for methodology currently being used address this type of connection. However, there is also a perception of cracking and leakage with this type of longitudinal joint. Therefore, an improved type of joint was a second goal within the NCHRP Project 12-69. This goal was accomplished with an improved joint that includes headed reinforcement bars lap spliced and grouted within a narrow joint preformed into the longitudinal edges of the precast deck portion of the precast girders. This type of joint transfers both moment and shear between the precast elements. The work done to develop and demonstrate the viability of the improved longitudinal joint system is documented and described within this document

Work in the NCHRP Project 12-69 has focused on the decked bulb tee (DBT) because of the structural efficiency of this section and because this is the section that is most common in current use. Most of the procedures in use for designing and fabricating DBT girders are the same as or similar to those used for other types of precast, prestressed bridge girders, such as conventional bulb tees. This document will present design and detailing guidelines for DBT girders with emphasis on those areas that are specific to DBT's.

CHAPTER 1

BACKGROUND

PROBLEM STATEMENT AND RESEARCH OBJECTIVES

A "decked" concrete girder is a precast, prestressed concrete I-beam, bulb-tee, or multi-stemmed girder with an integral deck that is cast and prestressed with the girder. These girders are manufactured in precast concrete plants under closely controlled and monitored conditions, transported to the construction site, and erected such that flanges of adjacent units abut each other. Load transfer between adjacent units is provided using specially designed connections. Sections that are not too long or too heavy for transportation by truck can be used to construct long-span girder bridges. This type of bridge construction provides the benefits of rapid construction, improved safety for construction personnel and the public, and improved structural performance and durability.

In spite of their benefits, the use of decked precast, prestressed concrete girders (DPPCG) has been limited because of concerns about certain design and construction issues that are perceived to influence the structural integrity of the bridge system. These issues include connections between adjacent units, longitudinal joints, longitudinal camber and cross slope, live load distribution, continuity for live load, lateral load resistance, skew effects, maintenance, replaceability and other factors that influence constructibility and performance.

Research is needed to address the issues that significantly influence the performance of long-span decked precast, prestressed concrete girder bridges and to develop guidelines for their design and construction. These guidelines will provide highway agencies with the information necessary for considering a bridge construction method that is expected to reduce the total construction time, improve public acceptance, reduce accident risk, and yield economic and environmental benefits.

The objective of this research is to develop design and construction guidelines for long-span decked precast, prestressed concrete girder bridges. The guidelines shall be prepared in a format suitable for consideration and adoption by the American Association of State Highway and Transportation Officials (AASHTO) as part of the *AASHTO LRFD Bridge Design Specifications*.

SCOPE OF STUDY

To address the issues and objectives regarding use of DPPCG in long-span bridge construction, NCHRP has identified the following tasks to accomplish this project:

Task 1 – Collect and Review Relevant Literature

Collect and review relevant specifications, research findings, current practices, and other information relative to the design, fabrication, and construction of DPPCG bridges. Information must be assembled from published and unpublished reports, contacts with transportation agencies and industry organizations, and other domestic and foreign sources.

Task 2 – Identification of Design and Construction Issues

Based on the information gathered in Task 1, identify and discuss the issues related to design and construction that hamper widespread use of DPPCG systems. These issues would include, but not limited to, connections between adjacent units, longitudinal joints, longitudinal camber and cross slope, live load distribution, continuity for live load, lateral load resistance, skew effects, maintenance, and replaceability.

Task 3 – Assessment and Prioritization of Issues

Assess the relevance and importance of the issues identified in Task 2 to the implementation of the DPPCG systems, and develop a prioritized list of these issues. Also, identify those issues recommended for further research in Phase II.

Task 4 – Detailed Work Plan

Prepare an updated, detailed work plan for Phase II that includes theoretical and experimental investigations for addressing the issues recommended in Task 3. The experimental investigation shall include full-scale testing of components and assemblies, and associated analysis.

Task 5 – Interim Report

Prepare an interim report that documents the research performed in Phase I and includes the updated work plan for Phase II. Following review of the interim report by the panel, the research team will meet with the project panel. Work on Phase II of the project will not begin until the interim report is approved and the Phase II work plan is authorized by NCHRP.

Task 6 – Execution of Work Plan

Execute the plan approved in Task 5. Based on the results of this work, recommend design and construction guidelines for long-span DPPCG bridges. Include design examples for a simple span and a skewed three-span continuous bridge to demonstrate the use of the recommended guidelines. Also, provide typical details for construction of these bridges.

Task 7 – Final Report

Submit a final report that documents the entire research effort. The report shall include an implementation plan for moving the results of this research into practice. The plan shall include supporting documents to facilitate incorporation of the recommended guidelines into the AASHTO LRFD Bridge Design Specification.

CHAPTER 2

RESEARCH APPROACH

INTRODUCTION

Summary of Objectives and Approach

Design and construction issues that have negatively affected the widespread use of DPPCG for rapid construction of long-span bridges have been identified in Task 2 through review of literature, a questionnaire, and interviews. In Task 3, Assessment and Prioritization of Issues, this information has been assessed to determine issues for further study and inclusion in the Detailed Work Plan. In accomplishing this assessment, the research team's primary philosophy has been that increasing the understanding of existing systems and well-served practices will provide the maximum returns for the bridge engineering community. The primary emphasis should be on documenting and demonstrating the use and performance of existing systems by developing design and construction guidelines and examples based on the best of current practice. However, Task 2 has identified issues of concern regarding performance and durability of details used in the existing systems, particularly the longitudinal joints. Therefore, emphasis is also placed on exploring potential improvements for these joints.

The overall objective of the research is to provide results that will lead to increased understanding and confidence in the DPPCG concept that will promote more widespread use of this type of structure. However, intrinsic to the approach used to assess and prioritize issues for further study was the need to reconcile the scope of work for the research with the established budget for this project.

General List of Issues

The potential issues and/or important factors affecting the use of DPPCG for long-span bridge construction previously identified (1) are categorized in four groups, namely analysis and design, fabrication, transportation/erection/construction, and maintenance and listed below:

Analysis and Design:

1. Analysis for long-term effects
2. Camber analysis
3. Variable girder camber and differential camber among girders
4. Section optimization (includes I-, T-, Bulb-T, and multi-stem beam configurations)
5. Design using high performance/high strength concrete
6. Design for lighter deck profiles and lightweight material for deck
7. Design for increased number and sizes of prestressing and post-tensioning strands
8. Shear design and web thickness
9. Loss of prestress and post-tensioning stresses
10. Design of asymmetric girders for transverse slope
11. Lateral stability
12. Transfer length and crack development
13. Live load transverse distribution
14. Live load continuity for bridges made continuous
15. Lateral load resistance including seismic performance
16. Effect of skew
17. Analysis of diaphragm effects
18. Analysis for transportation and erection
19. Girder splicing and segmental construction
20. Design of shear keys and grouting for transverse continuity
21. Use of post-tensioning for transverse continuity
22. Design of connections for longitudinal continuity
23. Provisions for bridge widening

Fabrication:

1. Strand concentration in the bottom flange
2. Workability of high performance/high strength concrete
3. Narrow webs and concrete consolidation
4. Quality control
5. Attachment of rail system
6. Geometry control issues (cross-slope, skew, camber)

Transportation/Erection/Construction:

1- Weight and length limitations for loading, transportation, and erection
2- Lateral stability during transportation
3- Erection schemes
4- Finished cost
5- Planning for speed of construction
6- Geometry control issues (cross-slope, skew, camber)

Maintenance:

1. Deck cracking along longitudinal and transverse joints
2. Deck replacement possibilities
3. Future bridge widening

The following section of this report describes the issues given highest priority and the rational for the Detailed Work Plan to further investigate these issues.

RESEARCH FOR PHASE II

Detailed Work Plan for Task 6

Based on results of Tasks 1, 2 and 3 the following specific tasks and subtasks were planned to study the primary issues in Task 6.

Task 6.1 – Develop Optimized Family of Girder Sections with Consideration for Future Deck Replacement.

Task 6.1 Background. The most common obstacle cited in the responses to the questionnaire survey is weight. Strategies for reducing haul weight need to be addressed. One strategy is to develop an appropriately efficient structural section. Therefore, development of an optimized family of girder sections was given high priority by the project team.

Another obstacle that will hamper the use of DPPCG bridges nationwide will be the acquisition costs of new forms by precast fabricators. Since the decked bulb tee is one of the most commonly used sections by those who use DPPCG bridges, and since bulb tee girders are perhaps the most common and structurally efficient types of girder in current use for girders with cast-in-place decks, the decked bulb tee was selected as the type of section to optimize.

To accomplish this optimization of girder section, Task 6.1 was included in the Detailed Work Plan. The study addressed many of the material and section geometry issues in the General List of Issue presented in the Introduction of this report.

Also, parameters to facilitate full deck replacement were included in Task 6.1. Based on the work accomplished in Task 2, deck replacement of DPPCG bridges is an important issue that has been raised as a possible impediment to their use. From the questionnaire survey, of the 22 respondents who did not use DPPCG bridges, 8 listed difficulties in future deck replacement as a reason DPPCG is not used.

The need for deck replacement is covered in Section 2.5.2.3 of AASHTO LRFD (2). This section of the specification states:

Structural systems whose maintenance is expected to be difficult should be avoided. Where the climatic and/or traffic environment is such that the bridge deck may need to be replaced before the required service life, either the provisions shall be shown on the contract plans for the replacement of the deck or additional structural resistance shall be provided.

The questionnaire survey responses indicate that current practice does not consider future deck replacement. Of the 14 respondents who did use DPPCG bridges, 12 provided information regarding accommodation of future deck replacement. Of these, 11 indicated they do not accommodate future deck replacement and one respondent discussed use of a partial deck replacement scheme involving grinding off and replacing 2 in. of the deck. A major reason cited for not considering deck replacement is that the deck concrete is of the same high quality concrete as the girder with 30 years of success without any need to replace the deck. However, since this experience is primarily with DPPCG bridges with low volume traffic, this is not a convincing reason if increased use in higher traffic volume applications is a goal.

Another reason cited for not considering deck replacement is that deck replacement requires shoring and the integrity of the finished girder may not be as expected. However, this reason indicates it is a system whose maintenance is expected to be difficult. Therefore, it indicates perhaps that this is a system to be avoided.

To understand further the difficulties in deck replacement in DPPCG bridges, a parametric study was conducted in Task 2 to investigate the feasibility of re-decking by removing and replacing the entire top flange of the girders. This study indicated that, for conventionally designed decked bulb tee girders, the deck (top flange) could typically be removed without overstressing the girder provided proper support for lateral stability is in place. However, since a new cast-in-place deck or precast deck is not composite for the dead load from the new deck, (whereas the top flange of the original girder is) the re-decked girder will be overstressed unless the bridge is shored during the retrofit work. Therefore, the initial design must accommodate the future deck removal. This requires additional prestressing and part of the deck to be left in place or a two-stage casting procedure.

The main strength of the DPPCG system and the reason it is being investigated in this NCHRP Project is one potential resolution of the deck replacement issue. This system is being investigated because, as included in the first line of the Problem Statement, speed of construction, particularly for the bridge replacement and repair projects, has arisen as a much more critical issue than ever before. If and when the deck of DPPCG bridges deteriorates to a

state requiring replacement, it may be much more efficient, expeditious, and economical to replace the entire girder rather than replace just the deck.

However, there may be situations where replacement of the entire girder is not practical. Therefore, full deck parameters were included in the development of an optimized family of girder sections in Task 6.1 described in the following: The methods and procedures described in NCHRP Report 407, Rapid Replacement of Bridge Decks (3) were used as a basis for deck replacement parameters. Other more current literature was also reviewed.

Task 6.1 Work Plan

Objectives: To develop efficient DPPCG girder sections including consideration for future full depth deck replacement.

Subtask 6.1-A – Full Depth Deck Replacement

Objectives: To document viable methods and details to accommodate rapid full deck replacement.

Scope:

- Review current literature for methods and details to accommodate rapid full deck replacement.
- Evaluate methods and details based on:
  - Constructibility.
  - Available performance data including laboratory test data and in-service data, if available.
- Identify viable methods and parameters that need to be considered in design.

Results:

Recommendations for details and methods to accommodate future full deck replacement.

Subtask 6.1-B – Optimized Girder Study

Objective: To develop efficient DPPCG girder sections.

Scope:

- Review existing girder sections and previous parametric studies and carry out a parametric study of their structural efficiency, if necessary.
- Select a basic shape for further study considering:
  - Effect on costs of formwork and/or modification of existing forms.
  - Full deck replacement which will include:
    - Shape of the top flange
    - Two stage casting
    - Two different materials for deck and girder
    - Debonded joint between deck and girder
    - Shear transfer details between deck and girder
    - Shear keys
    - Strand release after casting-deck.
  - Other fabrication issues.
- Carry out a parametric study varying:
  - Bottom flange geometry
  - Web thickness
  - Top flange geometry
  - Different materials for girder and deck
- Assess results and select a family of sections considering:

- Stresses at release
- Stresses at service load and strength of initial girder
    - Simple spans
- Camber
- Transportation and erection issues
    - Girder weight and length
    - Lateral stability
- Stresses at removal and replacement of initial deck

Results:

Recommendations for an efficient family of DPPCG Girder Sections.

Task 6.2 – Development of Durable Longitudinal Joints

Task 6.2 Background. The performance of longitudinal joints and connections was preliminarily identified in the proposal stage of this project as an issue with higher priority and likely to be addressed extensively. Based on the work accomplished in Task 2, performance of the longitudinal joints is the most important issue that needs addressing in this investigation. From the questionnaire survey, of the 22 respondents who did not use DPPCG bridges, six listed unsatisfactory performance of joints between adjacent units as a reason DPPCG is not used. Seven respondents of 14 that had experience with the DPPCG bridge system reported problems encountered. Of these seven respondents, six reported problems related to longitudinal joint cracking. However of these 6 respondents, two reported “excellent” for overall evaluation and two reported “good” for overall evaluation. The implication from the respondents’ comments is that, if the joints are properly designed and constructed, the performance can be good to excellent.

However, because of the concern and interest in the durability of the type of longitudinal joints currently being used, the research team concluded that the study should include an

investigation of a potential improved joint. It is anticipated that behavior of DPPCG bridges can be improved by providing improved moment continuity in the longitudinal joints. Two methods were considered for potential testing. One method includes transverse post-tensioning of the deck. A second method includes connecting or splicing the top and bottom transverse deck reinforcement. An example of a joint detail for this type of connection is the loop bar detail shown in Figure 2.1. Based on complexity involved in construction and the anticipated behavior, the research team selected the connection of top and bottom rebar method for further investigation.

Task 6.2 includes subtasks to define connection loads, select trial connections, test trial joint assemblies, and test selected full scale joint connection details as described in the following work plan.

Task 6.2 Work Plan

Objectives: To develop a longitudinal joint including consideration for transverse continuity for moment and shear.

Subtask 6.2-A – Analytical Program

Objectives:

- Determine service load demands on flange-to-flange longitudinal connections for fully continuous transverse deck behavior including critical combinations of moment and shear considering.
  - Camber leveling forces
  - Live load forces
- Develop test procedures for static and fatigue loading of laboratory test specimens.

Subtask 6.2-A1 – Study for Camber Leveling Forces

Objective: Determine load demands on continuous longitudinal joints resulting from leveling of differential camber.

Scope:

- Select a value for maximum differential camber between adjacent girders based on accepted construction tolerances.
- Use the finite element model to simulate the different stages of the leveling process.
- Perform a parametric study to determine range of forces in the connection for different girder geometry and leveling procedures.

Results:

Database to use in the determination of appropriate design guidelines for loads due to camber leveling.

Subtask 6.2-A2 – Study for Live Load Forces

Objective: Determine load demand on continuous longitudinal joints due to service level live load.

Scope:

- Perform a parametric study for live load forces on the longitudinal joint considering the following variables:
  - Girder depth, span, and spacing.
  - Single-lane and multi-lane loading.
  - Skew.
  - Diaphragm spacing and stiffness.

Results:

Database for bending moments, in-plane shear and tension and out-of-plane shear for determination of appropriate design guidelines for connection loads due to live load.

Subtask 6.2-A3 – Development of Laboratory Testing Protocol

Objective: To define details of testing apparatus, to determine the level of load, load variation, and locations of load points to be used in static and fatigue load tests for continuous longitudinal joints.

Scope:

- Use the analytical models of the deck component test setup in Task 6.2-C combined with results of Task 6.2-A1 and 6.1-A2 to define loading criteria for static and fatigue load testing of connection specimens.

Results:

Data to define loading for laboratory tests in Task 6.2-C.

Subtask 6.2-B Selection of Trial Alternate Longitudinal Joint Systems

Objectives: To define alternate longitudinal joint systems for joint.

Scope:

- Continue literature review beyond the AASHTO/FHWA Scanning Tour Report to search for test data/performance survey data on the types of joints used in Europe and Japan.
- Review results of on-going Texas DOT Research Project 4122: Behavior of Cast-in Place Slabs Connecting Precast and Steel Girder Assemblies
- Contact other state DOT's and DPPCG precasters regarding experience with alternate longitudinal joint systems.
- Review potential joint systems based on:
  - Constructability

- Available performance data including laboratory test data and in-service data.
- Minimizing shipping weight, (i.e. maintaining minimum flange thickness).
- Costs

- Identify trial joint details for further testing.

Subtask 6.2-C – Laboratory Testing

Objectives:

- Investigate performance of selected alternate longitudinal joint systems under static and fatigue loading.
- Demonstrate performance of proposed improved joint system with full-scale girder tests.

Subtask 6.2-C1 – Laboratory Testing of Trial Joints

Objective: To select trial joint details based on simple joint tests.

Scope:

- Perform both static tests using simple loading apparatus and simple specimens including tension tests and/or bending tests as illustrated in Figures 2.2 –2.6. These figures show examples of potential connection details and testing variables as follows:
  - Splice bar details (as shown in Figures 2.2 and 2.3) with potential variables including: length of splice bar, spiral dimension, high strength non-shrink grout and transverse bar offset.
  - U-bar details (as shown in Figure 2.4) with potential variables including: bending U-bars on smaller radius

using materials by different WWR manufacturers, bending the bars again in elevation so that they miss each other coming from two adjacent beams.

- Tilted U- or Loop-bar details (as shown in Figures 2.5 and 2.6) with potential variables including: tilting angle of bars, amount of longitudinal bars crossing the loop and constructability of each detail.

- Other details identified in Subtask 6.2 – B with related design parameters as variables.

Results:

- Selection of a trial joint detail for further testing.

- Resulting data on load deformation relationships were available for further analytical research.

Subtask 6.2-C2 – Laboratory Testing of Joint Assemblies

Objectives:

- Determine load-deformation relationship and static load strengths for selected alternate longitudinal joint system.

- Determine fatigue characteristics for selected alternate longitudinal joint system.

Scope:

- Use loading apparatus as shown in Figure 2.7 to 2.9 to test trial joint assemblies. The joint assemblies were made with two panels simply supported on steel beams. The two panels were connected at midspan with the trial connection.

- Two sets of trial panel specimens were made. Each set consisted of two panels with the trial joint assembly detail on two edges of

each panel. Therefore each panel was used twice. One set was used for two static strength tests and the other set of two panels was used for two fatigue tests.

- For static strength tests, two panels were connected and incrementally loaded to failure under bending moment with no shear as shown in Figure 2.7a. The panels were then separated and re-connected along the opposite edges and retested under combined bending and shear as shown in Figure 2.7b. Specific test loading regimes will be defined in Subtask 6.2-A3.

- Fatigue tests were run with a set of duplicate panel. Loading included cyclic reversing moment with no shear as shown in Figure 2.8, and combined cyclic reversing moment and shear as shown in Figure 2.9. Following completion of the fatigue tests, the connections will be loaded to failure.

- Each specimen was instrumented to measure:

    - Joint opening on top and bottom across joints.

    - Strains in reinforcing steel.

    - Relative vertical displacements of slab on each side of test connection.

    - Vertical displacement of slabs at center span.

    - Applied loads.

Results:

- Resulting data on load deformation relationships for further analytical research.

- Trial test results from static and fatigue loading demonstrate a longitudinal joint system with significant durability and minimal cracking to be used in full-scale girders

Task 6.3- Design and Construction Guidelines

Task 6.3 Background. Based on the work accomplished in Task 2, construction and geometry control are identified as key issues for further work in Task 6. There are certain issues involved in erection/construction that are relatively unique to this type of bridge. Current non-users have little experience with these issues and need guidelines as to how to handle these issues. In particular, construction geometry control for differential camber, skewness and cross-slope need to be addressed. From the questionnaire survey, of the 22 respondents who did not use DPPCG bridges, 6 listed difficulty in construction geometry control as a reason DPPCG bridges are not used.

Therefore, Task 6.3 was included in the Detailed Work Plan. This task was carried out to document best practices for existing systems. Guidelines were developed for design and construction, including geometry control, based on successful methodology currently being used. In addition, the guidelines include design methodology for future re-decking developed as the result of Subtask 6.1-A.

Task 6.3 Work Plan

Subtask 6.3-A – Documentation of Design and Construction Practices

Objectives: To document best practices for design, construction, and geometry control including the effects of differential camber, skewness, and asymmetrical girders.

Scope:

- Collect and review existing construction practices.
- Interview designers, bridge erectors, precasters, and DOT's on experiences with selected practices.
- Based on results of interviews and the knowledge and experience of the research team, particularly of Mr. Chuck Prussack, assess the practicality of the existing practices.
- Provide written descriptions of selected practices to address:

- Geometry control issues (cross-slope, skew, camber).
- Weight and length limitation for loading, transportation, and erection.
- Lateral stability during transportation and erection.
- Erection schemes.
- Planning for speed of construction.
- Details and construction sequence for establishing continuity for live load.
- Girder splicing and segmental construction.
- Attachment of rail systems.
- Provisions for bridge widening.

Results:

Guidelines for Design and Construction.

Subtask 6.3-B – Design Examples

Objective: To develop examples of design and detailing procedures for selected bridges in a clear and step-by-step fashion with respect to the guidelines

Scope:

- Develop a design example for a simple-span bridge.

Results:

Step-by-step design examples that will illustrate all significant steps in the design process.

Subtask 6.3-C – Design Examples for Future Re-Decking

Objectives: Demonstrate the design of selected joint connection details in full-scale bridge girders.

Scope:

- Design full scale bridge girders with selected joint details.
- Girders were designed considering features for anticipated future deck replacement including two stage casting, debonded joint between deck and girder, shear transfer detail between deck and girder, and strand release after deck-casting. The design horizontal shear for the debonded joint between deck and girder was the maximum horizontal shear anticipated for this type of bridge girder based on the parametric studies in Subtask 6.1-B Optimized Girder Study
- Two girders were designed. The first considering the optimized section developed in Subtask 6.1-B and the second considered a typical AASHTO type section.

Results:

Determination of maximum reinforcement and shear key geometry required for selected connection details to feasibility of these connection details.

Task 7 – Final Report

This final report documenting the entire research study was completed. In addition, a separate report on Guidelines for Design and Construction of Decked Precast Prestressed Concrete Girder Bridges was completed.

.

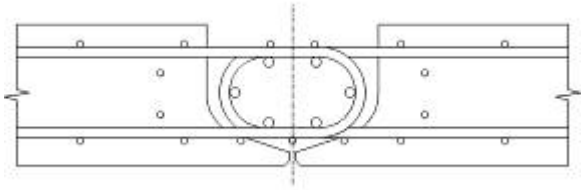

Figure 2.1 Example of concept for connection of top and bottom reinforcement for longitudinal joints

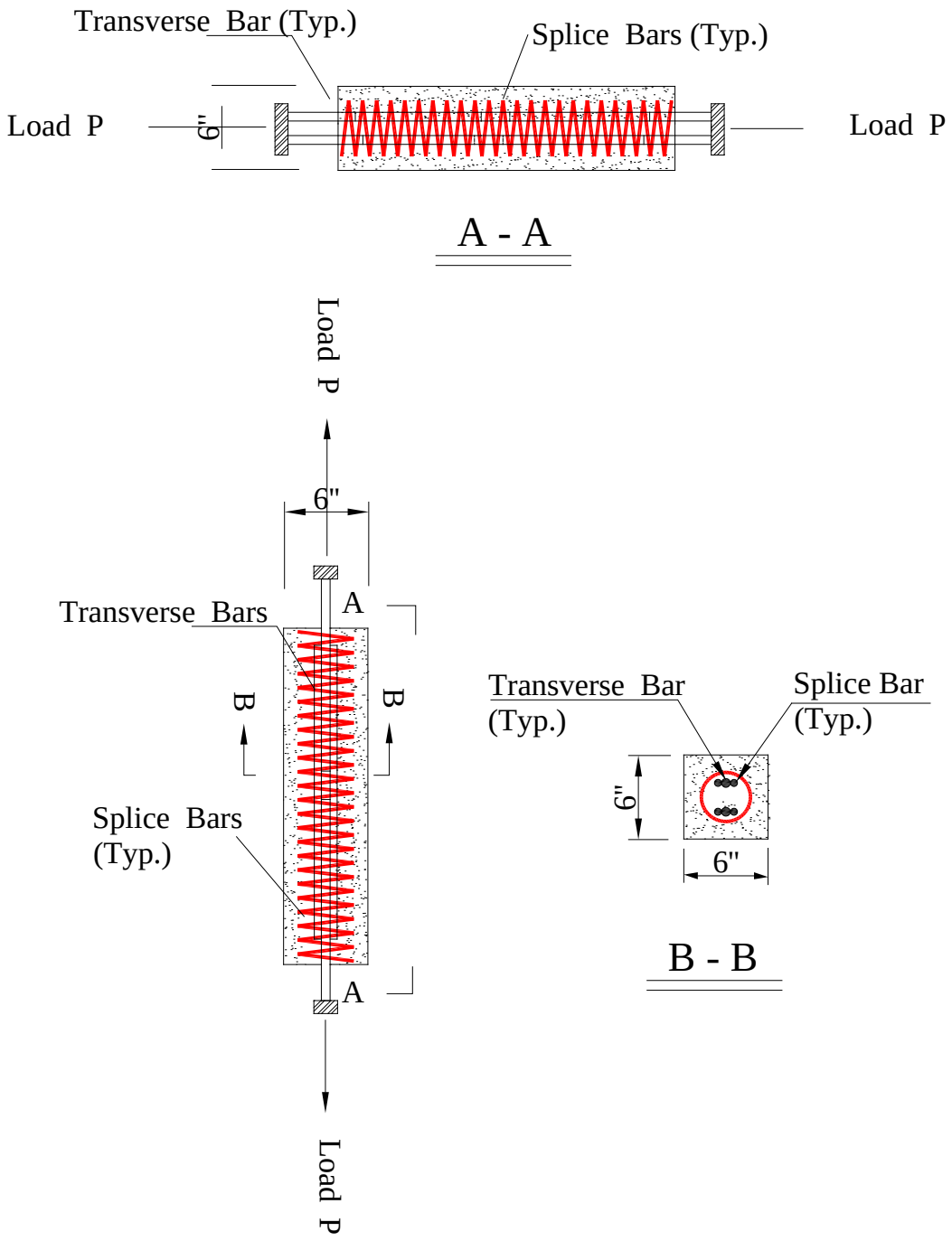

Figure 2.2 Single Joint Tension Test – Splice Bar Detail

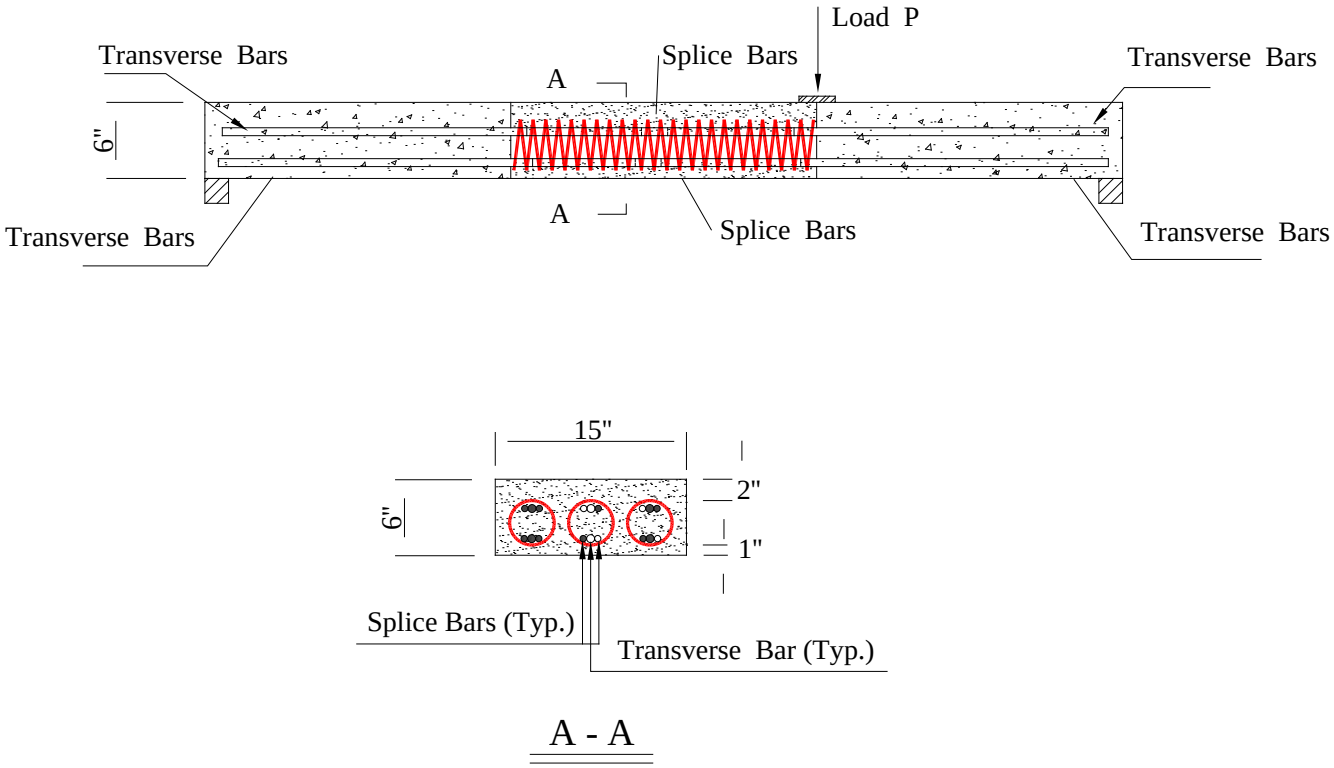

Figure 2.3 Wide Beam Test – Splice Bar Detail

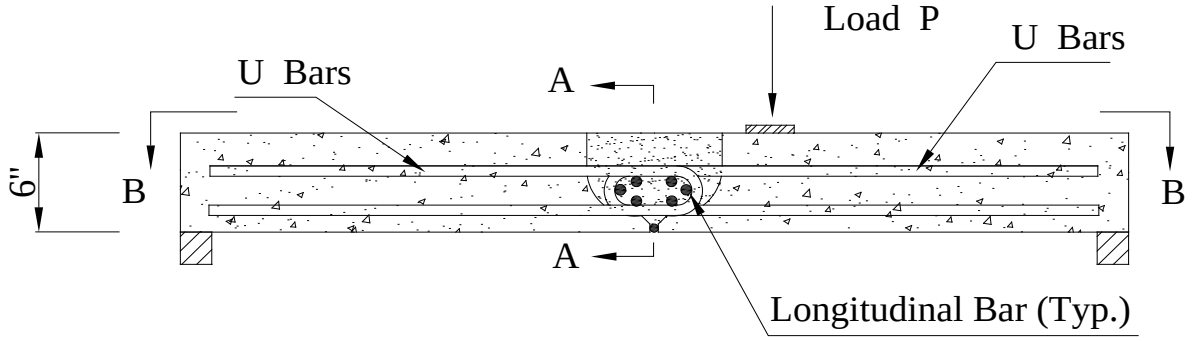

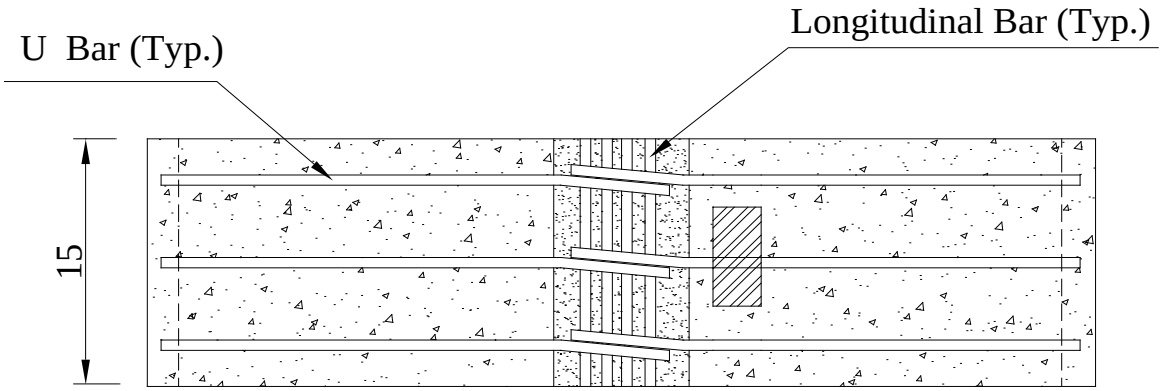

B - B

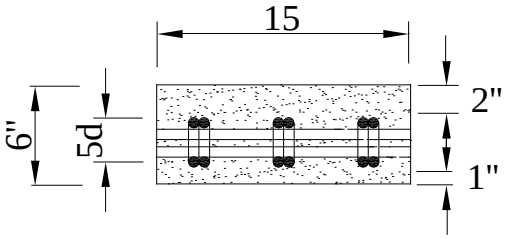

A - A

Figure 2.4 Wide Beam Test – U-Bar Detail

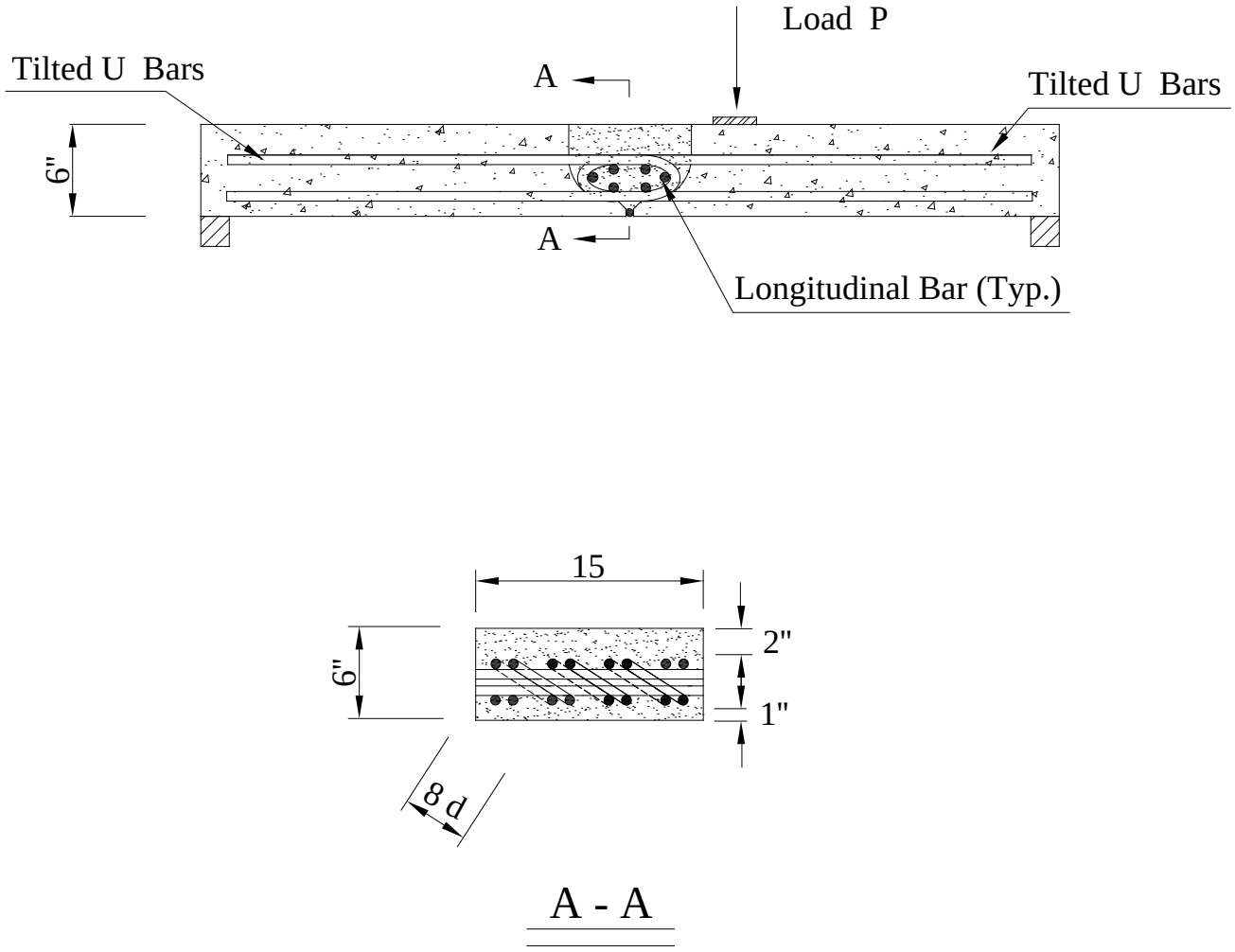

Figure 2.5 Wide Beam Test – Tilted U-Bar Detail

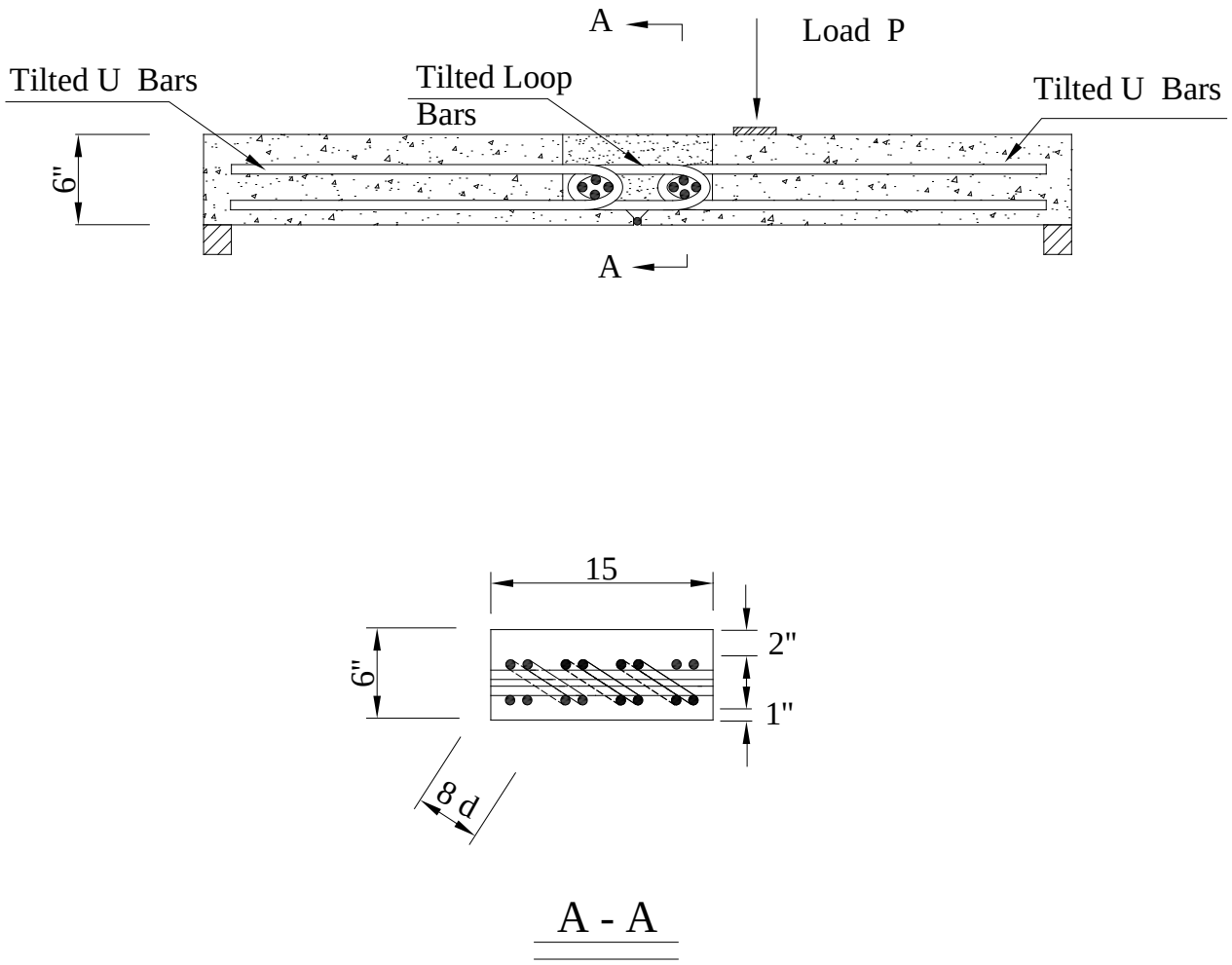

Figure 2.6 Wide Beam Test – Tilted Loop-Bar Detail

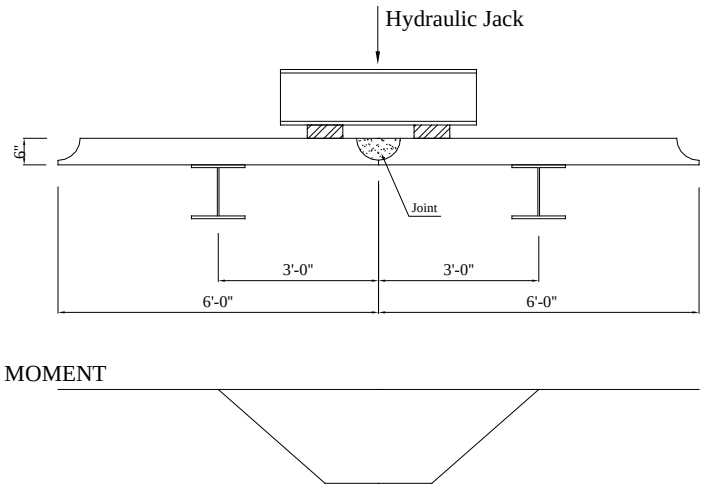

(a) MOMENT Only

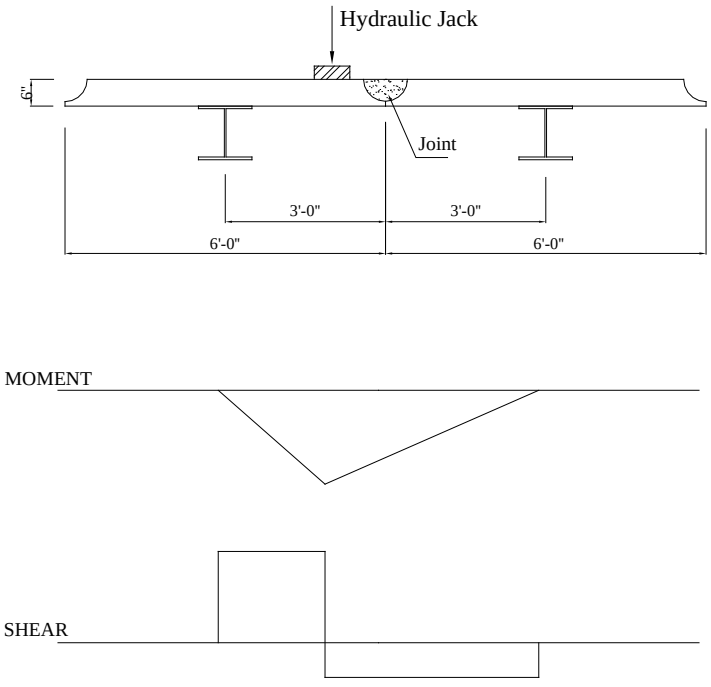

(b) MOMENT and SHEAR

Figure 2.7 Joint Assembly Static Test

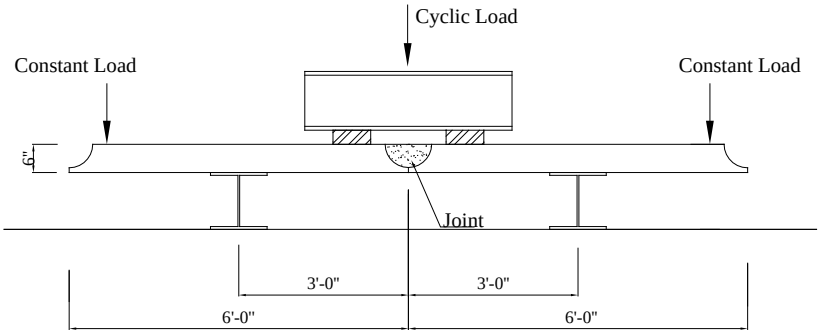

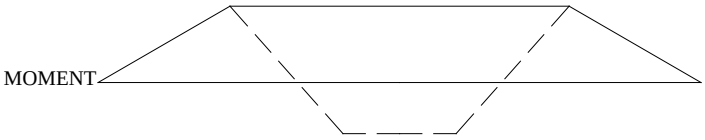

MOMENT Only

NOTE:

Due to Constant Load

Due to Cyclic Load

Figure 2.8 Joint Assembly Cyclic Test – Moment Only

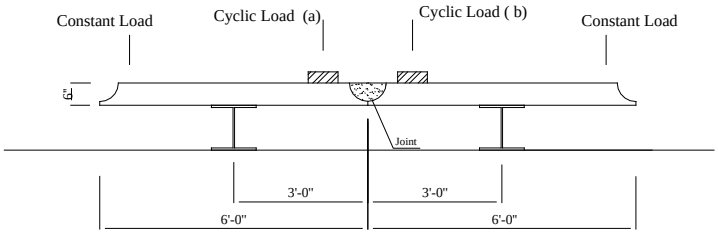

MOMENT and SHEAR
[Cyclic Load (a) is 180 degree out of Phase with Cyclic Load (b)]

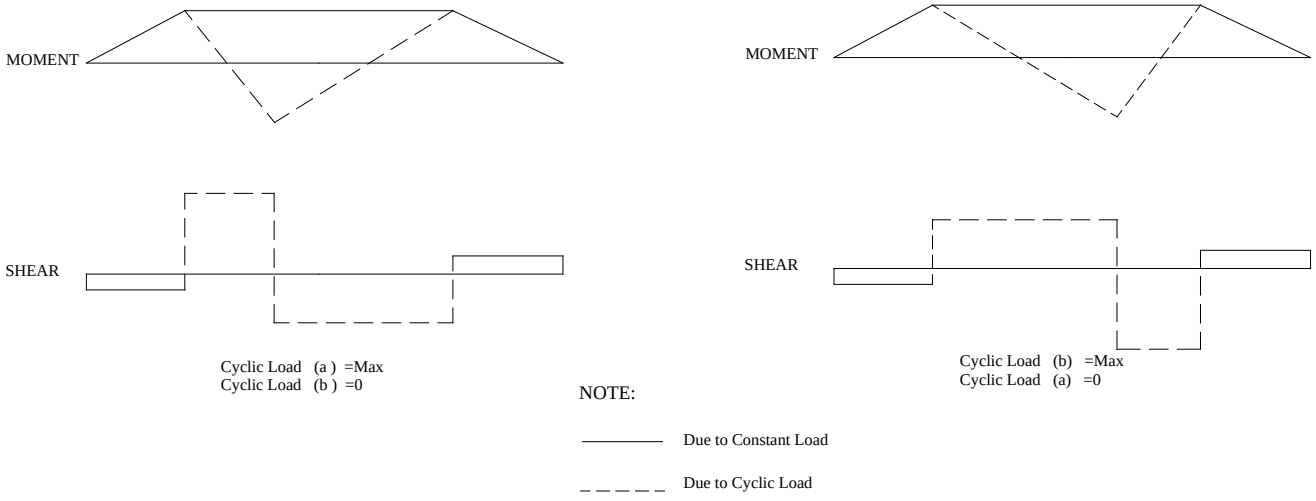

Figure 2.9 Joint Assembly Cyclic Test – Moment and Shear

CHAPTER 3

FINDINGS AND APPLICATION

TASK 1 – COLLECT AND REVIEW RELEVANT LITERATURE

The research team has carried out a comprehensive review of available current literature and data encompassing relevant papers and articles. Additionally, both AASHTO Standards Specifications and AASHTO LRFD Specifications were reviewed for references specifically related to DPPCG. General provisions that related to this type of bridge construction were identified and summarized. Also, bridge design specifications for the states of Alaska, Idaho, Oregon, and Washington were obtained and reviewed and the findings were summarized.

A summary of the findings from literature reviewed is provided in Appendix A of this report. A bibliography of documents reviewed is provided in this appendix.

To complement the data determined from the relevant literature, a survey was conducted among departments of transportation, design and consulting firms, researchers, and precasters. The survey was accomplished using a questionnaire. The survey was compiled and modified based on comments by the project panel and sent to 137 sources. The research team received and reviewed responses to the questionnaire. About 26 percent of total 137 surveyed responded. Among these, 14 respondents have answered yes to the use of DPPCG and provided useful information about the system and procedure. A webpage has been set up for the project and summary of the results posted for the use of all team members. The questionnaire used is provided in Appendix B. A summary of the findings is as follows.

Survey Results

In parallel to the published literature and practices research, first-hand information was collected via surveys and contacts with transportation agencies, industry organizations, and other sources. A questionnaire form was prepared and sent to transportation officials, designers, fabricators, and others to obtain knowledge on the current state of the practice in design and construction of decked precast prestressed concrete girder bridges. The questionnaire and a presentation and discussion of the survey results are provided in Appendix B.

Review of the results of the survey conducted indicates that decked bulb tee systems are used almost exclusively in the northwest region of the country. The principal states in which they are used include Alaska, Washington, Oregon, and Idaho. Other states in the country reported similar types of members, such as multi-stemmed channel sections, but not decked bulb tee systems. The survey results indicated a favorable performance of decked bridge systems. The major problem encountered during service is cracking of the longitudinal joints. The primary obstacles to the use of such system that were mentioned in the responses included girder weight, girder length, and the lack of available specifications for design and construction. Of these, the main obstacle cited was weight.

In addition to the questionnaire several individuals were contacted by telephone for further information including:

- Dr. Henry Russell and Dr. Shri Bhide regarding the results of the scanning tour (1) sponsored by the Federal Highway Administration (FHWA) and the American Association of State Highway and Transportation Officials (AASHTO). Based on the discussions, CTL obtained a copy of the draft report for use in planning scope-of-work for NCHRP Project 12-69.

- Mr. Michael Hyzak of Texas Department of Transportation regarding ongoing Research Project 4122 on development of closure pour connections for precast decks on steel girders. These closure pour connections for longitudinal joints in the deck may have application with DPPCG bridges. Mr. Hyzak provided a status report on this work.

- Dr. J. Puckett, Principal Investigator of NCHRP Project 12-62 Simplified Live-Load Distribution Factor Equations was contacted regarding applicability of the scope of work in Project 12-62 to the DPPCG type of bridge.

Also, Roy Eriksson, Co-investigator for Project 12-69 interviewed Mr. Stephen Sequirant, Director of Engineering for Concrete Technology Corporation, and Mr. Millard, Sales Manager, Heavy Construction. This organization had responded to the formal survey conducted for this project. However, since Concrete Technology Corporation is one of the three main producers (the others are Central Pre-Mix and Morse Bros.), a personal interview was warranted.

In this interview Key areas the design and construction of decked bulb tee girders were discussed, which were as follows:

Deck Replacement

In the states in which they do business, deck replacement is not done. Wear to the riding surface is handled by resurfacing. Normally, a membrane and asphalt riding surface are applied to the upper surface of the girders. When necessary, resurfacing is done rather than re-decking.

Joints

The opinion of Concrete Tech is that the most important element of DBT systems is the joints. It is here that the most value from research can be obtained. While they have experienced good performance over the years with the existing method of connection (weld plates + grouted longitudinal joints), they recognize that some of the states may require better joint performance to consider adopting the DBT system.

Currently, DBTs are not used on interstate bridges, but possibly could be in the future if durability issues are addressed.

Camber

Their experience is that camber is quite variable. They have their own procedure for estimating camber. Allowable camber differential is ¼". Since DBTs have no CIP deck, care must be taken to control differential camber. They employ a leveling procedure when necessary (previously noted by Central Pre-Mix) to equalize differential camber between adjacent members.

For span-to-span differential camber, Concrete Tech uses a cording procedure (Central Pre-Mix varies flange thickness) to minimize camber effects. Their forms are segmented every 20 feet to facilitate this.

Transportation & Erection

Maximum girder weight for hauling is about 200 kips. Maximum segment width is 8 feet. To accommodate longer spans, 2- and 3-point splicing has been used successfully.

Continuity

Span-to-span continuity is accomplished by splicing top girder rebar using angles

TASK 2 – IDENTIFICATION OF ISSUES

A comprehensive search was conducted to identify the design and construction issues that have negatively affected the widespread use of DPPCG in long-span bridge construction. The potential issues and/or important factors are categorized in four groups, namely analysis and design, fabrication, transportation/erection/construction, and maintenance. A general list of issues is provided in Chapter 2. A detailed summary of the areas investigated is provided in Appendix A.

TASK 3, 4 AND 5

Task 3 was carried out to assess the relevance and importance of the issues identified in Task 2 to the implementation of the DPPCG systems, and to develop a prioritized list of these issues. Also, Task 3 was conducted to identify those issues recommended for further research in Phase II.

Task 4 was conducted to prepare an updated, detailed work plan for Phase II that includes theoretical and experimental investigations for addressing the issues recommended in Task 3.

Task 5 was carried out to prepare an interim report that documents the research performed in Phase I and includes the updated work plan for Phase II.

Results of Tasks 3, 4, and 5 are presented in Chapter 2 of this report.

TASK 6 EXECUTION OF WORK PLAN

The work plan for Task 6, described in Chapter 2, was carried out. Results are presented in the following sections of this report

Task 6.1 – Develop Optimized Family of Girder Sections with Consideration for Future Deck Replacement

The objective of Task 6.1 was to develop an efficient DPPCG girder sections including consideration for future full depth deck replacement.

Subtask 6.1-A – Full Depth Deck Replacement

The parametric study conducted in Phase I of this project indicated that when replacing the deck of a DPPCG bridge, part of the deck, i.e. top flange, needs to be left in place in order to enable the deck replacement without shoring the bridge. To facilitate the removal of the deck, a two-stage casting procedure would be required. The connection between the two casting stages needs to provide full composite action while facilitating deck removal and replacement. The methods and procedures described in NCHRP Report 407, Rapid Replacement of Bridge Decks (3) were also identified in Phase I as the basis for deck replacement parameters to be used in the development of an optimized family of girder sections.

The NCHRP Report 407 was further reviewed in depth. The system proposed for precast concrete girder bridges consisted of a shear key system with a debonded interface between the precast girder and the cast-in-place deck. Extensive tests and field implementation showed that the shear key system has a comparable structural behavior with conventional roughened interface system. For DPPCG systems, this type of connection can be used at the interface between the two casting stages.

A literature review for more current documentation was also conducted. There is considerable amount of work done on full-depth precast deck panels for use in deck replacement projects as well as new construction. Although it is mentioned in some literature that this deck system can be used efficiently for concrete girder bridges, in all documented applications, steel girders were used as the supporting system. An investigation conducted by the University of Illinois in 1995 did not reveal any applications where precast concrete girders were used as supporting systems for full depth precast panels. Reviewing more recent literature did not reveal any such application either.

Accordingly, it is concluded that the concept of the debonded shear key and the cast-in-place deck as described in NCHRP Report 407 (3) is the current state-of-art for replacement of decks on concrete girders that has been sufficiently tested and documented. Therefore, it is the appropriate system to be incorporated in the development of optimized family of girder sections.

The debonded shear key system facilitates deck removal and replacement by minimizing the demolition effort and by providing a preconstructed shear interface system for the replacement deck. Demolition of bridge decks that are compositely connected with I-girders is one of the major time-consuming tasks in deck replacement. For new bridge superstructures,

the time required for deck demolition can be reduced by constructing bridges with connections that provide composite action and allow for easier deck removal. For precast concrete I-girders, a debonded interface with a shear key is placed in the top flange of the concrete girder and shear connectors of reinforcement bars at wide spacing are provided. A photograph of the recessed shear key system is shown in Figure 3.1. To accomplish the debonded interface, a debonding agent is applied to the hardened concrete using a brush or hand-held sprayer. The primary resistance mechanisms for the shear key are bearing and friction between the top flange and bottom of the deck, including the tensile and shear strength of steel connectors crossing the interface. In addition to extensive laboratory tests on push-off specimens, two full-scale girder tests were performed to compare the performance of the unbonded shear key system with that of a conventional system. Test results showed that this debonded surface in conjunction with extended vertical shear stirrups provided adequate horizontal shear transfer to ensure composite action. The design approach for the shear interface is provided in Reference (4). Further documentation of the work for Subtask 6.1-A is provided in Appendix C of this report. Examples of design calculations for the shear interface are provided in Appendix G.

Subtask 6.1-B – Optimized Girder Study

Introduction. Decked bulb tees have been used successfully for many years. Their cross sectional shape has evolved to accommodate varying bridge widths and span lengths. A generic shape that closely approximates the decked bulb tees in common use is shown in Figure 3.2. Overall girder widths range from approximately 4 ft 0 in. to 8 ft 0 in. Overall depths range from about 2 ft 11 in. to 6 ft 5 in.

As discussed above, the shear key system described in NCHRP Report 407 (3) is adopted and integrated into this girder system to make the system re-deckable.

Assessment of Existing Cross Sections. With minor variations the section family described in Figure 3.2 is the primary girder shape used today for most decked bulb tee bridges (5). Since this basic shape has functioned well and has had a good service history, this shape was used as the basic starting shape of this optimization study. The top flange, web and bottom bulb were each assessed for potential improvement.

Proposed Cross Section. Figures 3.3 and 3.4 show the dimensions of the two casting stages of the proposed girder shape. The girder shown in Figure 3.3 represents Stage 1 casting, which will also be the girder shape when the top portion of the system is removed for

future re-decking. The shape in Figure 3.4 includes Stage 2 casting, and represents the girder that will initially be used to construct the bridge. Release of prestress occurs after the proper cure of the Stage 2 casting.

Optimization Study Parameters. A parametric study was carried out considering the following parameters:

Bottom Bulb - The shape of the bottom bulb of the Washington State DOT standard (Figure 3.5) was assumed as a starting point for the optimization study. The width and depth of the bottom bulb were varied to accommodate the required number of strands to determine the most structurally efficient shape of the bulb

Web Width - The web width was held constant at 6 in.

Flange - The top portion of the girder consists of two parts: the sub-flange and the top flange (see Figures 3.3 and 3.4). The thickness of the sub-flange is dictated by the shear key depth, reinforcement layout, and concrete cover requirements. Based on these requirements, the edge thickness will be set at 3.5 in. The width of the sub-flange will be dictated by the force demands placed upon the shear key. However, the minimum width is set at 42 in., in order to fully develop transverse reinforcement in the sub-flange. Girder depths and lengths were varied within the specified ranges to determine the maximum forces on the shear key. The sub-flange width was set accordingly. The thickness of the top flange was held constant at 6 in. The width of the top flange was assumed to be 8 ft unless analysis indicates the need for a narrower flange.

Shear Keys - Top surface of the sub-flange shall have formed shear keys (see Figure 3.3). Shear keys shall be the width of the sub-flange of the girder less 2 in. on either side. Depth of shear keys shall be ¾ in. Spacing of shear keys along the longitudinal axis of the girder is dictated by the vertical shear steel requirements and shear friction steel (for composite action).

Girder Concrete - Two different concretes were used for the lower and upper portions of the girder. For the top portion of the girder, air-entrained concrete was used. The 28-day strength of both concretes will be 7.00 ksi. However, at release of the strands, the top portion is assumed to have reached a strength of 4.00 ksi. At the time the girder is re-decked; two different deck concrete strengths were investigated: 4.00 ksi and 6.00 ksi.

Study Methodology. As discussed above, for a given depth of girder (41 in., 53 in., or 65 in.), four different bottom bulb geometries were investigated: normal, tall, wide, and NU configurations. For each of these bottom bulb geometries, the steps in the investigation were as follows:

1. Generate a load table of span length versus required number of strands at 2-ft span increments for the initial, fully decked, fully prestressed phase of the bridge (Phase 1). Make note of the total long-term losses.

2. Generate a load table of span length versus required number of strands at 2-ft span increments for the phase in the life of the bridge when the top flange is removed and the bridge is re-decked with a 6 in. thick cast-in-place deck (Phase 2). Assume that f'_{ci} of the girders at the time of re-decking is equal to the f'_c. In lieu of calculating the prestress losses, assume that the prestress loss at the "release" stage (i.e., when the top flange is removed) is the lower range of the long-term losses determined in Step 1. For analysis of the re-decked section, assume the long-term losses for this step as the upper bound of the losses computed in Step 1. Preliminarily, assume the "release' and final losses to be 25% and 35%, respectively. Investigate deck concrete strengths of 4.00 ksi and 6.00 ksi.

3. Compare the results of Steps 1 and 2.

4. Adopt the maximum span length for a given girder depth and bottom bulb geometry as the lower of the maximum span for Phases 1 and 2.

5. Check shear key design based on maximum demand placed on shear key and adjust sub-flange width if needed.

6. Check stability of the maximum span for each girder depth (6, 7).

Further details regarding design criteria, materials, loads and construction sequence used in the study are provided in Appendix D. Also, a detailed summary of results for the effects of variable parameters is provided in Appendix D

Assessment of Results

Section Shape

Top Flange. A 6 in. top flange thickness was assumed based upon the historical thickness of the top flange of conventional decked bulb tee girders to minimize weight. An 8-ft width of flange was assumed in all cases to cause the highest force demands on the lower portion of the system (i.e., the Stage 1 casting). Design forces for exterior girders require No. 5 bars at 4 in. centers for transverse reinforcement.

Lateral stability checks for an 8-ft wide top flange showed that the system has adequate factors of safety for both hanging and supported conditions for all girder depths (6, 7). Narrower widths of top flange could be used to extend the span ranges, but would reduce the factor of safety against lateral instability.

At the re-decking phase, f'_c was assumed to be 4.00 ksi and 6.00 ksi, assuming a cast-in-place deck. This was a governing constraint on the span range. Increasing assumed f'_c for re-deck concrete increases the maximum span length.

Sub-flange. The sub-flange width was set based on a study of force demands placed on the flange. The required transverse reinforcement to resist the applied forces was No. 4 bars at 6 in. on center or a pair of No. 4 bars at 12 in. on center. Accounting for web width, cover, and rounding up to the nearest inch, the required total sub-flange width to fully develop the No. 4 bars was 42 in.

Force demands placed on the shear key on the top surface of the sub-flange were checked assuming a minimum 42 in. wide sub-flange. Both horizontal shear capacity and edge bearing were adequate.

Web. A 6 in. web width was maintained for all cases to accommodate two columns of draped strands, transverse reinforcement, and provide adequate cover. Maximum factored shear forces at the critical sections for the 41, 53, and 65 in. cases were 268, 314, and 361 kips. The corresponding maximum nominal shear resistances, V_n, permissible by the LRFD Specifications were 372, 480, and 550 kips, respectively. Therefore, a web width of 6 in. is adequate for all cases.

Bottom Bulb. The extra strand locations provided by making the standard bulb larger resulted in longer span ranges for each depth of girder studied. These extra strand locations enabled more of the concrete in the top portion of the system to be mobilized. Typically, the lowest strand locations in the girder are the most efficient places in which to add strands. Therefore, the wide flange configuration in which eight new strand locations were created at each of the bottom two levels of strands (Figure 3.5c) was more efficient than the tall case, where additional strand locations were also added, but at somewhat higher and therefore less efficient elevations (Figure 3.5b). However, the NU bulb shape was the most efficient of all the shapes.

For the 41 in. deep member, the moment of inertia of the initial section (i.e., before re-decking) with the normal bulb width was 191,823 in^4 with a cross-sectional area of 1086 in^2. With the tall bulb, the moment of inertia increased to 206,962 in^4 with an area of 1126 in^2. With the wide bulb, the moment of inertia increased to 226,203 in^4 with an area of 1146 in^2. Therefore, increasing the depth of the bulb resulted in an increase in the moment of inertia of 7.9%, with a corresponding increase in area of 3.7%. Increasing the width of the bulb resulted in an increase in the moment of inertia of 17.9%, with a corresponding increase in area of 5.5%. Similar results were observed for the 53 and 65 in. cases.

For the normal, tall, wide bulb, and NU configurations (Figure 3.5), the maximum span lengths were achieved in all cases using the NU bulb. For the 41, 53, and 65 in. deep girders, the maximum spans were 118, 148, and 176 ft, respectively for the initial phase of construction. For the re-decked phase using 4.00 ksi deck concrete, the maximum span lengths were 98, 118, and 134 ft, respectively. For the re-decked phase using 6.00 ksi deck concrete, the maximum span lengths were 114, 138, and 160 ft, respectively. Based on the maximum spans achievable, the NU bottom bulb proved to be the most efficient shape.

Deck Replacement - Longer span lengths were possible for the initial phase of the bridge. Therefore, if re-decking capabilities are to be incorporated into the system, significantly shorter span capabilities will result. Use of higher strength concrete for the future re-decking phase will increase span capabilities. Also, span capabilities increase if total superstructure replacement is considered as the future "deck replacement" scheme in lieu of removal and replacement of the top flange.

Task 6.1 Findings and Recommendations. Based on this study, it is recommended that the girder shape shown in Figure 3.4 be adopted with the modified NU bulb configuration shown in Figure 3.5 d) incorporated. This shape is structurally efficient and facilitates future re-decking of the system. However, the analyses in this study show that the efficiency of these girders is decreased when the re-decking option is considered. To use the re-decking option, a two-stage casting procedure is required and to attain the same span length requires additional prestressing.

The main strength of the DPPCG system and the reason it is being investigated in this NCHRP Project is an alternate resolution of the deck replacement issue. This system is being investigated because, as included in the first line of the Problem Statement, speed of construction, particularly for the bridge replacement and repair projects, has arisen as a much more critical issue than ever before. If and when the deck of DPPCG bridges deteriorates to a state requiring replacement, it may be much more efficient, expeditious, and economical to replace the entire girder rather than replace just the deck. Therefore, the cost of re-decking the system versus total superstructure replacement should be evaluated prior to using the re-decking option.

Task 6.2 – Development of Durable Longitudinal Joints

The objective of Task 6.2 was to develop a longitudinal joint including consideration for transverse continuity for moment and shear.

Subtask 6.2-A – Analytical Program

The objectives of Subtask 6.2-A were to determine service load demands on flange-to-flange longitudinal connections for fully continuous transverse deck behavior including critical

combinations of moment and shear considering camber leveling forces and live load forces; and to develop test procedures for static and fatigue loading of laboratory test specimens.

Subtask 6.2-A1 – Study for Camber Leveling Forces

Introduction - The objective of this study is to determine the shear forces transferred across the joint due to leveling of differential camber. The work was accomplished using finite element models to simulate the leveling process. The computer models were used to perform a parametric study to determine range of forces in the longitudinal joint for different girder geometry. Appendix E provides a detailed description of the work.

Parametric Study – The following considerations were included in the parametric study:

- Magnitude of Differential Camber - Based on standards currently in use (8, 9, 10), on consultation with experts from the precast-prestressed concrete industry, and on studies that included camber measurement data (11,12) a differential camber tolerance of 1/8 in. per 10 ft with no upper limit was used in the analyses

- Bridge Geometry - The overall width of the bridge used in the investigation of camber leveling forces is 48 ft. The bridge uses the decked bulb tee shapes developed in Subtask 6.1-B-Optimized Girder Study. Three different overall girder depths are investigated: 41 in., 53 in., and 65 in. For each girder depth, 4 ft and 8 ft spacing are considered. The study included right bridges as well as bridges with skew angles of 15^{o}, 30^{o}, and 45^{o}. The span of the bridge varied based on the girder depth and spacing to produce the maximum expected leveling shear for the girder configuration considered. For the 4 ft spacing, the bridge consisted of 12 girders, while for the 8 ft spacing the bridge consisted of 6 girders with an overall bridge width of 48 ft.

- Girder to be Leveled - Analyses were conducted to determine whether the leveling of an exterior or interior girder would produce higher shear in the longitudinal joint. Two scenarios were investigated. In both scenarios, the bridge consisted of six girders. In the first scenario, an exterior cambered girder is assumed to be leveled against five attached girders on one side. In the second scenario, one of the middle girders is assumed to be leveled against two attached girders on one side and three attached girders on the other side.

Results indicate that leveling of the middle girder results in higher shear in the joint within the span while it is the opposite near the supports. Since the shear transferred across the joint due to live load is minimal near the supports, the shear forces developed within the span due to camber leveling are of more importance than those developed near the supports. Accordingly, for the rest of the parametric study, only leveling of the middle girder was considered. For six girder bridges, one middle girder is leveled against two girders on one side and three girders on the other side. For twelve girder bridges, one middle girder is leveled against five girders on one side and six girders on the other side. It should also be noted that the joint was assumed to be rigid in this analysis. The flexibility of the joint as well as creep will significantly reduce the sharp peaks near the supports.

- Span length - Analyses were conducted to determine whether higher camber leveling shear would be expected in the shorter or longer span ranges. Results indicate that for a particular girder depth and spacing the maximum camber leveling shear will occur in the shorter spans of the span range for that girder configuration. Therefore, the shortest practical span for each combination of girder depth and spacing was used. The lower bound of the span for a given section was determined based on two criteria: minimum required concrete strength at release, f'ci, and minimum required number of strands. The minimum f'ci was limited to 1.0 ksi, and minimum number of strands was set to 18, which is number of strands in the bottom row of the modified bulb of the optimized section. While there is no hard boundary on the shortest span for a given section, these criteria were selected based on the experience of the research team to determine the practical shortest span for each section.

- Modeling Techniques - The bridges were modeled using SAP2000 finite element software. The top flange, web, and bottom bulb of all girders are modeled using shell elements as shown in Figure 3.6. All girders are fully attached to each other, i.e., full continuity is assumed along the longitudinal joints. Thermal loads are applied to only one girder to simulate leveling the camber of this particular girder against the remainder of the bridge. The girder is selected to generate the highest possible camber leveling shear. The magnitude of the thermal loads is such that if the girder was to deflect freely, i.e., not attached to any other girders,

the midpoint of the girder would move upward with a magnitude equal to the assumed camber. Since the girder is attached to the remainder of the bridge along the edges of the top flange, transverse shear stresses are generated in the longitudinal joints between that particular girder and the adjacent girders. These shear stresses are equivalent to those developed due to the camber leveling process.

Parameters for the camber leveling study are summarized in Table 1.

Results of Parametric Study - An example of the transverse shear stresses is shown in Figure 3.7. The bridge used in this example consisted of six girders with 65 in. depth, 8 ft spacing, and 84 ft span. One of the middle girders is assumed to be leveled against two attached girders on one side and three attached girders on the other side. The camber of the girder to be leveled was assumed to be 1.05 in. It is observed from Figure 3.7 that the sign of the transverse shear force across the joint is reversed near the supports.

The reversal in transverse shear stresses near the supports can be explained by studying the deformed shape of the girders and is discussed in more detail in Appendix E.

Figure 3.8 shows the transverse shear forces due to leveling for right bridges for the six scenarios investigated. The maximum joint shear ranges between 0.68 kip/ft to 0.87 kip/ft. Figures 3.9 through 3.11 show the transverse shear forces due to leveling for skewed bridges. The effect of the skew is such that the leveling shear is increased near one end of the longitudinal joint and reduced near the other end. This effect is more pronounced with the increase of the skew angle. The maximum joint shear ranges between 0.85 kip/ft to 1.01 kip/ft for 15^o skew angle, 1.04 kip/ft to 1.18 kip/ft for 30^o skew angle, and 1.28 kip/ft to 1.45 kip/ft for 45^o skew angle.

The maximum flexural stresses resulting in the girders due to camber leveling are summarized in Table 2. The maximum observed stress is approximately 890 psi. It should be noted that these are transient stresses and that the final stresses will be significantly reduced due to creep. The stress produced by an imposed deformation will relax overtime due to creep of concrete. ACI 209 Committee (13) provides a methodology for calculating the stress relaxation after sudden imposed deformation.

Based on analyses described in detail in Appendix E, shear forces would be expected to reduce to approximately 50% of the initial shear force after 100 days and 35% of the initial shear force after approximately three years.

Findings for Subtask 6.2-A1

Camber Leveling Shear Forces. The results of the camber leveling study indicate that the maximum camber leveling shear will occur in the shorter spans of the span range for each of the three girder depths of 41 in., 53 in. and 65 in. Based on the analyses, higher camber leveling shear forces occur with leveling of a middle girder against attached girders on both sides. The maximum camber leveling shear stress increases with the increase of the skew angle.

Analyses indicated the maximum joint shear for non-skewed bridges was 0.87 kip/ft. The effect of the skew is such that the leveling shear is increased near one end of the longitudinal joint and reduced near the other end. This effect is more pronounced with the increase of the skew angle. The maximum calculated joint shear was 1.01 kip/ft for 15^o skew angle, 1.18 kip/ft for 30^o skew angle, and 1.45 kip/ft for 45^o skew angle.

This upper bound magnitude of camber leveling shear force of 1.45 kip/ft results in an initial nominal shear stress of 20 psi on the 6 in. thick deck section. Due to creep, the shear forces would be expected to reduce to approximately 35% of the initial shear force after approximately three years. Therefore, based on these studies, camber leveling shear forces do not result in a high shear demand on the type of longitudinal joint under investigation. However, consideration for the presence of constant shear was included in defining the loading to be used in the joint assembly testing in Subtask 6.2-C2. Based on the study in Subtask 6.2-A1, a shear force 0.5 kips/ft was determined as a reasonable upper bound to use in the test specimen to consider the shear force transferred across the joint due to the leveling of differential camber during construction.

Although the maximum initial camber leveling shear force will reduce with time, the initial force needs to be considered in design of the camber leveling procedures. Camber leveling procedures are discussed in the Guidelines for Design and Constructions developed in Task 6.3. One procedure discussed for camber leveling is to provide temporary clamps along the longitudinal joints. An example design for temporary

clamps, using 1.5 k/ft. as the maximum camber leveling shear force, is included in Appendix E.

Flexural Stress in Girders Due to Camber Leveling. The calculated maximum change in stresses in the bottom bulb of the girders due to camber leveling forces were nominally high (a maximum calculated of approximately 890 psi). This is likely a conservatively high calculated stress considering that:

- The differential camber used to verify the 1/8 in. per 10 ft. was the maximum camber difference between any two of the girders in a group, it is unlikely that this maximum differential camber would actually occur between an interior girder and the two adjacent girders as modeled in the analyses for this study;
- The analyses assumed that 100% of the deferential camber was removed during the leveling process;
- Creep is expected to reduce camber leveling stresses to approximately 35% of the initial stresses;
- The effect of camber leveling has not been shown to be a problem in decked girder bridges presently in use;

Although the nominally high tensile stresses were calculated using conservative assumptions and creep is expected to reduce the level of these stresses in a short time, further consideration was given to these nominally high stresses.

Additional analyses were therefore performed to investigate the sensitivity of the calculated stresses to span length. A governing condition for maximum calculated camber leveling forces in the prior parametric study was a short span. The maximum forces for each girder depth analyzed were calculated using the shortest span length. The additional analyses were therefore carried out to determine if the calculated tensile stresses decreased significantly as the spans were increased. For each combination of girder depth and spacing, the span was varied from the practical shortest span to the longest possible span for that particular section. The analyses did not indicate a significant drop with increased span length. Calculated maximum tensile stresses,

ranging from approximately 400 to 500 psi at the longest possible spans, are still nominally high.

One of the reasons given above to support a conclusion that tensile stresses due to camber leveling should not be a problem is that the effects of camber leveling has not been observed to be a problem in decked girder bridges currently in use. However, it should be noted that an allowable of 0 tensile stress is commonly used in the design of decked girders under service load. This criterion allows a margin of tensile capacity to help compensate for camber leveling tensile stresses. Based on this observation and the nominally high calculated flexural tensile stresses in this camber leveling study, an allowable of 0 tensile stress is included in the design guidelines developed in this project.

Subtask 6.2-A2 – Study for Live Load Forces

Introduction - The objective of this study is to provide the database of maximum forces for determination of loading demand on the longitudinal joints due to service live loads. The effects of individual variables were researched by performing parametric studies using ABAQUS. The following variables were considered:

- Girder geometry including depth, span and spacing
- Single lane loading and multilane loading
- Skewness of the bridge
- Impact of cracking of joints

The decked bulb tee girder was chosen in the study and the development of the girder geometry was discussed in Subtask 6.1: “Develop Optimized Family of Girder Sections”. Based on the Subtask 6.1, Table 3.3 summarized the practical span ranges for optimized girder sections. Typically, there were three different girder depths: 41 in., 53 in. and 65 in. The girder section is named by the girder depth, such as section “DBT41” referring to a decked bulb tee girder with 41 in. depth. For each girder section, there were three different girder spacings, 4 ft, 6 ft and 8 ft. Figure 3.12 shows the cross section of the optimized deck bulb tee girder. Chapter 2 of Appendix F provides a detailed description of the work accomplished in this study.

Description of Modeled Bridge Parameters - Table 3.4 summarizes the seven bridge models with different girder geometry and bridge skewness developed for the parametric study. Bridges A, B, C and D are straight bridges with various girder geometry (depth, spacing and span). Bridges D, E, F and G have the same girder geometry with different bridge skewness.

All seven bridges are simply supported. One intermediate steel diaphragm (ISD) is located at the midspan of the bridge to connect the web and bottom flange of the girders. This is considered a minimum of what would be used in practice. The deck of the adjacent girders was connected by the proposed continuous longitudinal joint discussed in the following sections of this report.

All the bridge models have the same bridge width of 40 ft. Figure 3.13 shows the cross section of each bridge model. The joints between girders were labeled as “joint 1”, “joint 2” and so on from left to right. Because of the symmetry of each bridge in width direction, the forces in joints locating left half of each bridge were studied. Please note that the metal railing is not shown in these sketches since only live load was considered in the study.

Description of Loadings - The live load HL-93 according to the AASHTO LRFD Bridge Design Specifications (14) was used in the study. The live load HL-93 consists of design vehicle load and lane load. The design vehicle is either design truck or design tandem which can produce the larger forces. The dynamic load allowance is applied to the design vehicle load but not to the lane load. The length of the lane load is varied to produce the larger forces. The distance between middle wheel and rear wheel of truck load varies from 14 ft to 30 ft to produce the larger force. In the parametric study, multiple presence factors of 1.20 and 1.00 were used for single lane loading and multilane (two lane) loading respectively.

For the fatigue loading, the fatigue truck load is the same as the design truck load, but with a constant spacing 30 ft between the middle wheel and the rear wheel. The dynamic load allowance is applied to the fatigue load.

Development of Finite Element Models - Three dimensional (3D) finite element (FE) modeling was completed by using ABAQUS 6.4.1. The bridge modeling consisted of three main components: intermediate steel diaphragm, decked bulb tee girder, and the

continuous longitudinal joint connection between top flanges of adjacent girders (Figure 3.14). The inclined members of steel diaphragm were modeled using 3D two-node truss elements and the horizontal member was modeled using 3D two-node beam elements as shown in Figure 3.14-a. The major portion of the decked bulb tee girder, including the bottom bulb, stem, sub-flange, and the deck directly above the sub-flange, was modeled using 3D twenty-node solid elements as shown in Figure 3.14-b.

The remainder of the deck of the girder contains the longitudinal joint that is located at the outer edges of the deck as shown in Figure 3.13. This is the main area of interest in this study. It was considered that use of shell elements in lieu of solid elements would facilitate the determination of moments and shear forces in the longitudinal joint. However, based on the results of a sensitivity study comparing results with shell elements and results with solid elements, this area of the deck, including the continuous longitudinal joint connection, was modeled using 3D eight-node thick shell elements as shown in Figure 3.14-c.

The bridge models were simply supported at the ends. The developed 3D FE models were calibrated and discussed in details by Ma et al. (15)

Parametric Study - Based on the bridge models and vehicle loading discussed above, parametric studies were conducted to determine the maximum forces in the longitudinal joint. The following parameters were considered:

- Effect of loading locations including location of Lane Loading and location of Truck or Tandem Loading,
- Effect of bridge width,
- Truck and Lane Loading vs. Tandem and Lane Loading,
- Effect of girder span,
- Effect of girder depth,
- Effect of girder spacing,
- Effect of bridge skewness,

- Single Lane Loading vs. Multilane Loading, and
- Effect of cracking in longitudinal joint

Results of Parametric for Subtask 6.2-A2 Study for Live Load Forces

Live Load – A detailed discussion of the effects of each parameter is provided in Chapter 2 of Appendix F of this report. Table 3.6 to Table 3.9 summarized the maximum forces in the joint in the 7 bridge models under different loading locations using uncracked section in the longitudinal joint. Through Table 3.6 to Table 3.8, the maximum positive moment (M) with corresponding shear (CS) and the maximum shear (S) with corresponding moment (CM) were included.

In a summary, the maximum positive moment, negative moment and shear in the longitudinal joint under live load HL-93 was 7.922kips-ft/ft, -2.152kips-ft/ft and 6.091kips/ft, respectively. For comparison, based on the DECK SLAB DESIGN TABLE A4-1 in AASHTO (14), the maximum positive live load moment in the bridge deck supported by 8ft spacing girders is 5.69kips-ft/ft.

Based on the results of the analyses using uncracked sections for the longitudinal joints, it is anticipated that the joints would be cracked under service loading. Therefore, the forces in the joint would be expected to be reduced compared with the forces calculated with uncracked sections. The difference of structural behaviors before and after crack is due to the change in the joint stiffness.

In the FE models where the largest maximum forces in the joint were found, the impact of cracking of the joint was studied by changing the modulus of elasticity (E) while keeping the moment of inertia (I) the same. Figure 3.15-(a) and Figure 3.15-(b) show the impact of cracking on the maximum moment (positive moment and negative moment) and maximum shear respectively.

From Figure 3.15, it can be seen that the cracking has influence on the maximum forces in the joints. With the reduction of the EI, the forces decrease at a different rate. The reduction of the forces becomes faster and faster when the EI reduction increased. The EI reduction has more influence on moment than on shear. When the EI reduction

reached up to 95%, the residual moment and residual shear are 35.4% and 75.7% of the values calculated by uncracked section properties respectively.

Based on results of testing trial joints in Subtask 6.2-C1: “Laboratory Testing of Trial Joints” (16), with different reinforcement details at the joint zone, the 6 in. lap length headed bar detail was selected for the further study as discussed in following sections of this report. Based on the moment-curvature test data for the 6 in. lap length headed bar specimen, (H-6-6) and continuous reinforcement specimen, (Control), the EI reduction after cracking was approximately 90%.

Considering the force reduction due to the joint cracking, the maximum positive moment, negative moment and shear in the longitudinal joint under live load HL-93 was 4.001kips-ft/ft, -1.137kips-ft/ft and 5.056kips/ft respectively.

Fatigue Loading. The Articles in AASHTO (14) referenced to the fatigue loading are listed below:

- 3.4.1 FATIGUE-Fatigue and fracture load combination relating to repetitive gravitational vehicular live load and dynamic responses under a single design truck having the axle spacing specified in Article 3.6.1.4.1

- 3.4.1 A load factor of 0.75 (Table 3.4.1-1) shall be applied to fatigue load combination

- 3.6.1.2.1 Vehicular live loading on the roadways of bridges or incidental structures, designated HL-93, shall consist of a combination of the design truck or design tandem, and design lane load.

- 3.6.1.4.1 The fatigue load shall be one design truck or axles thereof specified in Article 3.6.1.2.2, but with a constant spacing of 30.0 feet between the 32.0-fip axles.

- 3.6.2.1 The static effects of the design truck or tandem shall be increased by 15% (fatigue and fracture limit state) for dynamic load allowance (Table 3.6.2.1-1). The dynamic load allowance shall not be applied to pedestrian loads or to the design lane load.

The fatigue loading was determined by the following equation according to the above Articles:

0.75[Lane Load + 1.15 (Fatigue Truck Load)]

In a summary, the maximum positive moment, negative moment and shear in the longitudinal joint under fatigue live load HL-93 was 2.143 kips-ft/ft, -0.453 kips-ft/ft and 2.326 kips/ft respectively.

It should be noted that the loads above are probably conservatively high in that Lane Load was included. A strict interpretation of the definition of Fatigue in Article 3.4.1 indicated that live load (i.e. Lane Load) be included. A strict interpretation of Article 3.6.1.4.1 indicates however, that fatigue load consists of only load from the fatigue design truck and Lane Load is not included. This second interpretation is more common. Therefore, the loads described above are marginally higher than they need to be.

Also, it should be noted that, as described in detail in Appendix F, revisions to the fatigue loading criteria were accepted by AASHTO subsequent to the testing carried out in this project. The revisions consist of inclusion of two levels of fatigue load in Table 3.4.1-1. These are Fatigue I and Fatigue II. Fatigue II retains the current Load Factor of 0.75 and is to be applied to represent an effective stress range caused by the fatigue truck with respect to a large but finite number of stress range cycles. Fatigue I has a Load Factor of 1.5 (or 2 times 0.75) and is to be applied to the stress range caused by the fatigue truck with respect to an infinite number of stress range cycles. The implications of the use a Load Factor of 1.5 are discussed further in following presentation of Subtask 6.2-C2 in this report.

Finding for Subtask 6.2-A2 - A total of seven bridge models with different girder geometry were developed and loaded by HL-93 loading in the parametric study. The purpose of the study was to provide the database of the maximum forces in the longitudinal joints for determination of loadings on the static and fatigue slab tests in Subtask 6.2-C2: “Laboratory Testing of Joint Assemblies”. The following parameters were considered: different loading locations, effect of bridge width, design truck and lane loading vs. design tandem and lane loading, girder geometry (depth, spacing and span), bridge skewness, single lane loading vs. multilane loading, and impact of cracking of the

joints. Based on the parametric study discussed above, the following findings are summarized below:

1. The maximum forces in the joint were not sensitive to the length of the lane load. Typically, the lane load fully applied along bridge length direction produced a larger moment while the lane load stopped at the rear wheel of truck load produced a larger shear.

2. In longitudinal direction, the influence of the location of the vehicle load (truck or tandem) on the maximum forces in the joint was not significant. The truck with heavy wheels (middle wheel or rear wheel) or the tandem locating around midspan of the bridge produced a larger moment and shear.

3. The truck plus lane load produced larger forces than the tandem plus lane load and it dominated the loading for the practical span ranges of the optimized decked bulb tee girders.

4. Increasing the bridge width would decrease the maximum negative moment in some degree. However, the effect of bridge width on the maximum positive moment and the maximum shear was negligible.

5. The maximum forces in the joints were not sensitive to the span of the bridge. However, they were influenced significantly by the spacing and the depth of the girder. Girder with a larger spacing and a shallower depth produced a larger moment and shear.

6. The shear was not sensitive to the skewness of the bridge. Increasing the skewness, the maximum positive moment would increase; however, the maximum negative moment would decrease.

7. Single lane loading produced larger forces than multilane loading and it dominated the loading level.

8. The maximum forces in the joints decreased after the joint cracking. However, the impact of cracking had more effect on moment than on shear.

9. Before cracking, the maximum positive moment was 7.922 kips-ft/ft; the maximum negative moment was -2.152 kips-ft/ft; the maximum shear was 6.091 kips/ft. After cracking, the maximum positive moment was 4.001 kips-ft/ft; the maximum negative moment was -1.137 kips-ft/ft; the maximum shear was 5.056 kips/ft. The maximum forces before and after cracking were used to determine the static loading demand for test specimens in Subtask 6.2-C: “Laboratory Testing”

10. The maximum positive moment, negative moment and shear in the longitudinal joint under fatigue live load HL-93 was 2.143 kips-ft/ft, -0.453 kips-ft/ft and 2.326 kips/ft respectively. The corresponding moment (CM) occurring with the maximum shear was 2.887 kips-ft/ft. These forces were used to determine the fatigue loading demand for test specimens in Subtask 6.2-C: “Laboratory Testing”.

As discussed in the previous section of this report, a separate analytical parametric study was carried out to determine the shear force transferred across the joint due to the leveling of differential camber during construction. Based on that study, a shear force 0.5 kips/ft was determined as a reasonable upper bound to consider in the test specimen.

Subtask 6.2-A3 – Development of Laboratory Testing Protocol

Introduction - The objective of this subtask is to define details of testing apparatus, to determine the level of load, load variation, and locations of load points to be used in static and fatigue load tests for the selected trial continuous longitudinal joint. This section of the report provides the initial plan for testing. Further details are provided in Sections 3.2.6 and 3.2.7 of Appendix F.

Testing Plan and Setup - A total of four slab test specimens were planned. Each slab specimen consisted of two concrete panels connected with the selected trial continuous longitudinal joint. During the test setup, each panel was placed on the steel I-beam, which was leveled to ensure that the two panels are on the same plane. The two panels were positioned to satisfy the overlapped length and the spacing of the trial joint. Wood forms were provided at the bottom and at both ends of the joint for placing joint grout. After grouting, the slab specimen consists of 2 panels connected by the joint and was ready for testing. Since each panel has the trial joint details along two edges, each set of two panels were used to fabricate two test specimens. After completion of testing the

first joint, the panels were separated, and another joint reassembled by the other two edges to create the second test specimen.

Four slab specimens were planned for testing under different parameters: 1) flexure static (F-S) test; 2) flexure-shear static (FS-S) test; 3) flexure fatigue (F-F) test, and 4) flexure-shear fatigue (FS-F) test. Figure 3.16 shows the testing setup and the linear voltage displacement transducers (LVDT) instrumentation for each test. All slab specimens were simply supported with a 72 in. span and the joint zone located in the center of the span. The neoprene pad, with two layers of plastic sheets placed between the wood support and slab bottom, was used at one end; only the neoprene pad was used at the other end. The 10 in. by 20 in. neoprene pad and steel plate were used to simulate the truck tire contact area and the pressure loading

The F-S specimen was loaded with two equal loads spaced at 12 in. about the center of the span using Material Test System (MTS) rams until the specimen failed. The joint zone experienced the maximum constant moment without shear. The FS-S specimen was loaded with one load located at 12 in. about the center of the span until the specimen fails. The joint zone experienced the combination of moment and shear. The F-F specimen was loaded with two equal loads spaced at 12 in. about the center of the span. Figure 3.17 shows the apparatus to apply the fatigue forces to the joint zone of the specimen. Further details of the loading apparatus are provided in Section 3.2.6 of Appendix F.

The FS-F specimen was loaded with two loads spaced at 12 in. about the center of the span. Two loads (P1 and P2) were applied out-of-phase on each side of the joint during the fatigue test. For example, when “P1” reached the maximum force, “P2” was zero. The joint zone experienced the fatigue shear in reversing directions.

Fatigue Loading Determination - FE models of the test specimens (Figure 3.18) were developed to determine the loadings in fatigue tests and produce the maximum moment or the maximum shear in the joint zone corresponding to the results from previous parametric studies discussed in previous sections of this report. Results indicate that the moment along the joint resulting from the concentrated pad loads does not vary significantly from the average or nominal moment along the joint .However; shear from the concentrated pad load varies significantly along the joint length. The ratio of average

or nominal shear along the length of the joint to the peak or maximum shear near the pad load is 3.33/7.3 = 0.46. This ratio was used to determine the pad load in the test specimens required to produce the shear loads resulting from the live load study in Subtask 6.2-A2. Further discussion of results using these FE models is provided in Section 3.2.7 of Appendix F.

For the F-F specimen, a static loading was applied in several increments up to 22.7 kips in order to produce the maximum positive moment of 7.922 kips-ft per unit length in the joint and to crack the joint. After unloading to zero, a negative static load of -6.2 kips, corresponding to a negative moment of -2.152 kips-ft per unit length, was applied and unloaded to zero.

During the fatigue test, the applied load was cycled between 6 kips corresponding to a positive moment of 2.143 kips-ft per unit length and -1.2 kips corresponding to a negative moment of -0.453 kips-ft per unit length for a total of 2 million cycles at a frequency of 4Hz. At the end of 0.5, 1.0, 1.5, and 2.0 million cycles, an interim static loading test was conducted. During each of these static tests, the static loading was applied in several increments up to 11.3 kips corresponding to a positive moment of 4.001 kips-ft per unit length after cracking. After unloading to zero, a negative static load of -3.3 kips corresponding to a negative moment of -1.137 kips-ft per unit length after cracking was applied and unloaded to zero. Finally, the slab specimen was loaded to failure.

Figure 3.19 shows the first few cycles of the fatigue loading history for the FS-F specimen. As discussed previously, fatigue loads “P1” and “P2” were applied by the two MTS rams having the same frequency but out-of-phase. The slab was under the fatigue loading with the magnitude of “P1+P2” as shown in Figure 3.19.

The peak P1 was 27.1 kips and the peak P2 was -18.9 kips. The “Average” value of “P1+P2” was 4.10 kips. Using the results of analyses with the finite element model shown in Figure 3.18, and described in more detail in Appendix F, the maximum shear in the joint associated with P1 was 3.303 kips/ft, the maximum shear in the joint associated with P2 was -2.302 kips/ft, and the shear associated with the “Average” value of “P1+P2” was the 0.5 kips/ft. Therefore the camber leveling shear of 0.5 kips/ft was applied at the middle of the joint zone all the time with the fatigue shear oscillating at approximately ±

2.8 kips above and below this average. The target oscillating shear was ± 2.326 kips/ft. Therefore, the loading applied to the FS-F specimen was conservatively high.

Similar to the F-F specimen, an interim static loading test (applying “P1” and “P2” separately) was conducted at the end of 0.5, 1.0, 1.5, and 2.0 million cycles. Again, the specimen was loaded to failure after the fatigue cycles. Also, it should be noted that, due to the shear spans used in the FS-S and FS-F tests, the maximum moment accompanying the maximum shear in the test specimens was higher than the maximum moment accompanying the maximum shear in the analytical models. Therefore, the FS-S and FS-F tests are considered conservative.

Subtask 6.2-B Selection of Trial Alternate Longitudinal Joint Systems

The objectives of Subtask 6.2-B were to define alternate longitudinal joint systems and details for trail testing. Figure 3.20 shows a typical DBT bridge consisting of five DBTs connected by four longitudinal joints with welded steel connectors and grouted shear keys (17, 15). The current longitudinal joint has the strength needed to transfer shear and limited moment from one girder to adjacent girders. The width of the joint zone is small so that it facilitates accelerated construction. However, since welded steel plates are located 4 feet from each other and at mid-depth of the flange, they can not help to control flexural cracks along the longitudinal joint. Although performance of this type of joint was reported as good to excellent in a survey of current users, problems with joint cracking have been reported in the literature (17, 18). This joint cracking along with joint leakage is perceived to be an issue limiting a wider use of this type of bridges. As a result, the State of Washington has set limitation on the use of DBT for roads with high ADT and for continuous bridges. As part of a research project to address issues that influence the performance of DBT bridges, a specific objective was defined to develop improved joint details which allow DBT bridge systems to be more accepted as a viable system for accelerated bridge constructions. This section describes the process of selection of trial longitudinal joint system. Further detail on the process of the selection is provided in Section 1.2 of Appendix F.

Proposed New Joint Details. To improve the current joint detail, the proposed new details should control joint cracking better, and maintain the accelerated construction features. The main concept of an alternate joint is to replace the current welded steel connectors with

distributed reinforcement to provide moment transfer as well as shear transfer across the joint. Obviously, well distributed reinforcement can control cracks much better than widely spaced welded steel connectors. However, straight lap-spliced reinforcement requires a much wider joint to develop its strength.

The width of the joint for lap spliced reinforcement is determined by the lap length which typically depends on development length L_d of reinforcement (19). For a typical DBT, the compressive strength of the deck flange and the grout is 7000psi. If a No.5 epoxy coated bar with yielding stress 60 ksi were lapped in the 6 in. deep flange joint, the development length L_d for straight bar and hooked bar are 21.5 in. and 10.7 in. respectively. The lap length should not be less than the development length L_d, which indicates at least the same joint width needs to be provided to accommodate the lap spliced reinforcement. A straight lap-spliced joint would be much wider than the current joint width, which does not facilitate accelerated construction.

It was considered that the proposed alternate joint width to be as narrow as possible. Joint width minimization will reduce the required expensive grout which results in a reduction of cost and faster construction time. As a result, options to reduce the joint width have been explored. Such options include bars with hook (U bar), bars with headed terminations, and bars with spiral.

As discussed earlier, the hooked bar has a much smaller development length compared to the straight bar. However, it is not possible to have a standard hook for No.5 bar within the 6 in. deep flange while still satisfying the cover requirements. As a result, a non-standard U bar with a smaller bend radius was considered as shown in Figure 3.21-a.

U bars are spliced with the transverse deck reinforcement in the top flange of the DBT. They are bent to contact with the opposite U bars in the adjacent girder. Two longitudinal bars were laced through the interlocking U bars. Figure 3.21-b shows a non-overlapping headed bar connection detail proposed for consideration. Two layers of transverse deck reinforcement project out of the top flange of the girder with a head on the end. The adjacent girders will be placed with the opposing headed bar abutting each other. One welded wire reinforcement (WWR) is spliced with each layer of headed bar for force transfer. Figure 3.21-c shows a proposed joint detail with spirals confining lapped splices. Einea (20) performed an experimental program to determine lap length of the rebar confined in spirals. With the concrete compressive strength of 8660psi, they found that the lap length for No. 4, No. 6, and No. 8 bars confined with circular spirals can be as short as 4in., 5in., and 7in. respectively. In this proposed detail, two layers of transverse deck

reinforcement project out of the top flange of the girder and abut with the opposite projecting transverse deck reinforcement in the adjacent girder. The two abutting transverse deck reinforcements are spliced with two straight bars confined by the spiral wire.

In order to better understand the rapid constructability of proposed details, a survey was distributed to a variety of bridge professionals in different states. The bridge professionals were asked to comment on constructability, cost and any available performance data. Approximately 80% of the 28 agencies that were questioned responded to the survey. According to the feedback, it would be desirable to minimize or eliminate the joint zone to expedite construction and reduce cost. Field placement of reinforcement within longitudinal joint zone after erection could be tedious. Cumulative fabrication and erection tolerances, particularly differential camber, will result in some degree of vertical flange mismatching. Any connection detail must have sufficient tolerance to account for the mismatch.

The feedback almost universally indicated concerns with the connection using spiral wire. The respondents felt that the complexity of construction would cause difficulties with effective installation. Assembling the splice bars and spiral wire seemed too difficult and time consuming in the limited space of the joint strip. When the joint is very congested, it is very difficult to achieve full grout penetration throughout the assembly. For the 6 in. deep flange, the use of spiral wire will probably result in violation of the cover requirement: 2 in. at top and 1 in. at bottom, and it would be more realistic to use a thicker flange. It also would be very difficult to provide proper alignment of the opposing transverse deck reinforcements when erecting the bridge girders. It is highly unlikely that this connection would work for skewed bridges.

The primary concern with the U bar detail was achieving the desired bend radius within the 6 in. deep flange and still achieving the desired top and bottom cover requirement. The flange must be thickened substantially for a reasonable pin diameter to work, or the bars would have to be rotated sideways to maintain the required cover. Contact lapping of U bars will present construction problems in both making laps match up and difficulty in the setting operation for the girders. Much labor may be required in the field to bend bars at all contact locations. A joint with spacing completely out of phase by half a space between adjacent girders should be considered. Large amounts of differential camber may complicate lacing the longitudinal bar though the U bar interlocking, and eliminating longitudinal bar is suggested. Also, the thin, un-reinforced part of the flange under the joint would be very vulnerable to damage at all stages of fabrication and construction. Female-to-female shear key details would be preferred.

From a structural and ease of installation point of view, the headed reinforcement option appeared to be the most favorable. However, several respondents expressed concern for a detail with headed bars that do not overlap. This concept is good for setting assemblies but it does not provide a good load path with reliance on WWR for force transfer. Also, field placement of the inner layer of WWR (above lower headed bars) may be difficult. In addition, the heads of the bars appear to violate cover requirement.

Based on the feedback from the survey, a headed bar detail was selected for further investigation. Considering the limited flange depth, it was decided to investigate use one layer of overlapping headed reinforcement (Figure 3.22-a). Interlocking WWR detail as shown in Figure 3.22-b was also chosen for further investigation.

Since contact lapping will present construction problems, headed bar spacing completely out of phase by half a space is proposed shown in Figure 3.22-a, however, the lap length (measured from inside head to inside head) needs to be studied. Research on anchorage behavior of overlapping headed reinforcement was conducted by Thompson et al (21). The anchorage capacity of headed bar consisted of head bearing and bond. Based on this work, as further described in Section 1.2 of Appendix F, the development length L_d is 3.75 in. for both 4 in. spacing headed bar and 6 in. spacing headed bar.

As shown in Figure 3.22-b, the WWR detail includes three sheets of WWR with “Sheet 3” is put on the top of “Sheet 1” and “Sheet 2” which are abutted with each other. Each sheet is spliced to an adjoining sheet with two interlocking cross wires. The spacing between cross wires of the overlap sheets shall be at least 2 in. (19). In this case, width of WWR connection (distance between outermost cross wires) should be 16 in. plus the diameter of the wire. However, in order to reduce width of connection, so it is comparable with that of headed bar detail which is measured from outside head to outside head, the spacing of cross wires in WWR detail was reduced from 2 in. to 1 in. The lap length in WWR detail is defined as the distance between the center of the outermost cross wire to the center of middle wire, which was reduced to 4 in. The trial alternate joints were evaluated in a test program in Subtask 6.2-C1 as described in the following section of this report.

Subtask 6.2-C – Laboratory Testing

The objectives of Subtask 6.2-C were to investigate performance of selected alternate longitudinal joint systems and demonstrate performance of proposed improved joint system with full-scale tests under static and fatigue loading.

Subtask 6.2-C1 – Laboratory Testing of Trial Joints

Introduction – The objective of this subtask is to select trial joint details based on simple joint tests. The selected trial joint detail is then subjected to further testing in Subtask 6.2-C2. In addition, resulting data on moment curvature relationships were used in the analytical Subtask 6.2 - A2 to model the cracked stiffness of the longitudinal joints.

The following section of this report provides a summary of the test program and results of the testing. A more detailed description of this Subtask is provided in Section 1.3 of Appendix F.

Experimental Program

Testing Plan. Figure 3.23 shows a model specimen in two adjacent DBTs with the dashed line representing the longitudinal joint. Typically, the spacings of the DBT are 4 feet, 6 feet, or 8 feet respectively. The model specimen with 8 feet span was selected to evaluate the behavior of the proposed longitudinal joint details.

Figure 3.24 shows details of the three types of specimens. Each specimen was 2 ft wide, 10 ft long, and 6 in. deep with 2 in. cover at the top and 1 in. cover at the bottom.

All the specimens had four layers of reinforcement both at the left side and the right side to simulate the deck reinforcement in the top flange of adjacent girders. The headed bar, WWR Sheet 1, WWR Sheet 2, and the continuous bar were spliced with the deck reinforcement long enough to avoid pulling out. The specification of deck reinforcement was as following: No. 5 bar spaced at 6 in. at top in the “transverse” direction of the bridge deck; No. 4 bar spaced at 6 in. at bottom in the “transverse” direction of the bridge deck; No. 5 bar distribution reinforcement spaced at 8 in. at top in the “longitudinal” direction of the bridge deck; and No. 4 distribution reinforcement spaced at 8 in. at bottom in the “longitudinal” direction of the bridge deck. All the reinforcement was

grade 60 and epoxy coated. The headed reinforcement was No.5 bar with a standard 2 in. diameter circular friction welded head. The head thickness was 0.5 in.

Table 3.10 shows the main variables of the tested specimens. For the headed bar detail (Figure 3.24-a), the primary variables were the lap length and the spacing of the reinforcement. “H” means headed reinforcement and “W” means WWR. For example, the notation “H-6-4” means headed bar reinforcement with a lap length of 6 in. and a spacing of reinforcement at 4 in. A No. 5 bar with a 1.375 in. diameter circular head on each end was placed in the “longitudinal” direction both above and below the headed reinforcement at the middle of the lap length. Figure 3.24-b shows the WWR detail. As discussed in Subtask 6.2 - B, the lap length is reduced to 4 in. The spacing of WWR was the only variable in the second type of specimen. The diameter of WWR reinforcement is 5/8 in. A control specimen with a layer of continuous No. 5 rebar with a spacing of 6 in. across the joint zone shown in Figure 3.24-c was tested for comparison purpose.

All eight specimens were cast monolithically to remove the grout as a variable so the actual performance of the reinforcement in the joint zone can be focused on. The design concrete strength at 28 days was 7000psi. The concrete strength $f_c^{'}$ at the time of testing is shown in Table 3.10. Three cylinders were tested to get the compressive strength of each specimen on the testing day. The compressive strength of the control specimen was not available. Since the control specimen and Specimen H-6-6 were cast from the same batch of concrete on the same day and they were tested within five days, the compressive strength of Specimen H-6-6 was used in calculation for the control specimen.

Instrumentation and Test Setup. Steel strains were measured on selected bars in the joint zone. Figure 3.25-a shows the strain gauge layout in the control specimen. Figure 3.25-b shows the example of strain gauge layout in headed reinforcement specimens. The strain gage layout used in WWR specimen was similar to the control specimen layout. Further details on strain gage layout and notation are provided in Section 1.3 of Appendix F.

All specimens were simply supported with a 8 feet span (Figure 3.26). Neoprene pads were placed between the support concrete blocks and steel girders to ensure the boundary condition was achieved. The specimens were loaded with two equal loads

spaced at 40 in. about the center of the span using Material Test System (MTS) rams. The joint zone was located in the center of the span and experienced the maximum constant moment without shear. Linear voltage displacement transducers (LVDT) were employed to measure the specimen deflection and curvature. The dial gauges were used to measure the settlement.

Results of Testing - Subtask 6.2-C1

Moment Capacity and Curvature. Table 3.11 compiles the moment capacity and measured curvatures of each specimen. The curvatures reported include the measured curvature at maximum moment and the maximum curvature prior to failure. Four of the specimens failed suddenly and the maximum curvature could not be reported. A joint with a high moment capacity and a low curvature is undesirable because the failure is brittle and sudden.

Figure 3.27 compares the moment curvature response for each of the headed bar specimens and control specimen. It can be clearly seen that the 6 in. lap length specimens (H-6-4, H-6-6 and control specimen) provided much more ductility than the 2.5 in. or 4 in. lap length specimens (H-2.5-4, H-2.5-6 and H-4-6). The maximum curvatures in 6 in. lap length specimens were almost twice as large as those in specimens with 2.5 in. or 4 in. lap length. In the 6 in. lap length specimen moment curvature response curve, there was considerable flattening of the curve followed by a dropping off which meant that the reinforcement yielded after the specimen reached the nominal moment until the compression zone of concrete crushed and the specimen could not take any more load.

The maximum curvatures in specimens with 2.5 in. or 4 in. lap length were very close and had a relatively small value about 3810×10^{-6} rad/in. The curves did not exhibit a flattening part indicating that the steel did not fully develop before concrete crushing.

Also, the 4 in. reinforcement spacing specimens (H-6-4 and H-2.5-4) provided higher moment capacities than the 6 in. reinforcement spacing specimens because the smaller spacing provided more steel in the same cross section, which can increase the nominal moment.

Figure 3.28 show the moment curvature data for 6 in. reinforcement spacing specimens compared with results of analyses with Response 2000. Response 2000 (22) is a sectional analysis program that can calculate the strength and ductility of a reinforced concrete cross-section subjected to shear, moment, and axial load. This program was used to predict the moment curvature behavior of a continuously reinforced specimen with either 4 in. or 6 in. reinforcement spacing. The measured reinforcement yield stress of 68 ksi and elasticity modulus of 29809 ksi were used in the Response 2000 analysis.

The specimen results were split into two graphs due to the different compressive strength of the concrete. Figure 3.28-a shows the behaviors of the control specimen and H-6-6 which had a compressive strength of 10,542psi. Both specimens had a higher moment capacity and higher ductility than Response 2000. H-6-6 had a little bit more moment capacity (3%) than control specimen. The control specimen was more ductile than H-6-6 with a maximum curvature which was 36% larger than that of H-6-6. However, the 6 in. lap length had considerable anchorage to provide desirable moment capacity and ductility.

Figure 3.28-b compared the moment curvature curve between H-2.5-6, H-4-6 and Response 2000 with average compressive strength of 8,355psi. The moment capacities of both specimens were close to each other and a little bit smaller than that in Response 2000. Both specimens had only about half ductility capacity compared with Response 2000. Because of the short lap length, there was not enough anchorage between opposing headed reinforcement in the joint. As the load increased, the concrete between the opposing headed bars began to crush and failed to transfer the force between the overlapping headed reinforcement. So the two specimens exhibited relatively brittle failures with small curvatures.

Figure 3.29 shows the moment curvature data for 4 in. reinforcement spacing specimens (H-2.5-4 and H-6-4) and Response 2000 with average compressive strength of 8,900psi. H-6-4 had a larger moment capacity and ductility compared with Response 2000. It confirmed the discussion above that 6 in. lap length had the desirable anchorage capacity to yield the steel in the joint. H-2.5-4 had enough moment capacity; however, its ductility was only about 60% of that in Response 2000. Based on the review of the failed specimen, it appears that the connection failed suddenly because of the anchorage

failure due to the short lap length, which can be recognized by the abrupt stop in the moment curvature curve.

Figure 3.30 shows the moment curvature behavior of the WWR specimens. Neither specimens performed like the expected behavior of Response 2000 and failed prematurely. As noted previously, the spacing between cross wires in the joint zone of 1 in. did not meet the requirement in ACI. If WWR connection is used in the joint, it is suspected that the width of joint needs to be increased to accommodate 2 in. spacing cross wires. In addition, as shown in Figure 3.22-b, the WWR detail includes a significant shift in the location of the transverse wires in Sheet 3 as compared to Sheets l and 2. It is also suspected that providing a fourth sheet below Sheets 1 and 2 would improve behavior but diminish the constructability of the joint.

Strain Comparisons. The results from the strain gauge readings were plotted against the corresponding moment. Figure 3.31 compares the moment versus steel strain at different location in Specimen H-6-6. Steel within 0 to 2 in. away from the head (Figure 3.31-a and b) developed strain with initial load indicating the head bearing provided significant anchorage capacity. Strain in the steel 4 in. to 10 in. away from the head (Figure 3.31-c, d, e) did not indicate significant strain until the applied moment of approximately 7.41 kips-ft. This moment corresponds with first significant cracking following which the reinforcement strains away from the head increased to two to three times the strains measured near the head indicating that a combination of head bearing and bond provided the whole anchorage. Also strains measured away from the head indicated significant yielding before ultimate load.

In Figure 3.31-d, the strain development in bar 1 and bar 3 was not as rapid as bar 2 and bar 4. This was because in Specimen H-6-6, there were 4 bars (bar 1, bar 3, bar 5 and bar 7) on the right side and 3 bars (bar 2, bar 4 and bar 6) on the left. To balance the total tension force, the bars on the left which had smaller area needed to develop more strain/stress to produce the same force as the steel on the right side. Figure 3.31-f shows measured strain in the longitudinal bars was relatively low during the test. Therefore the force in the joint in this direction was relatively low.

Figure 3.32 compares the moment versus strain response at SH66-4-4 in Specimen H-6-6 with 2-4L and 2-4R in the control specimen. The three moment-strain curve matched

very well which confirmed steel 4 in. away from the head would fully develop in the 6 in. lap length headed bar connection. The joint detail in Specimen H-6-6 can transfer moment as effectively as a continuously reinforced joint.

Similar to Specimen H-6-6, the steel close to the head in Specimen H-6-4 developed strain at low load indicating the head bearing provided significant anchorage capacity. Steel away from the head indicated higher strain demonstrating that bond also contributed to the anchorage. Measured strain, greater than yield were measured at location as close as 2 in. from the head and indicated the rebar fully developed by the combination of head bearing and bond.

As discussed before, the spacing of the headed reinforcement was one of the variables that had effect on the lap length. The smaller spacing, the smaller lap length was required. Since Specimen H-6-4 had smaller reinforcement spacing than Specimen H-6-6, the steel at 2 in. away from the head yielded in H-6-4 while the steel at 4 in. away from the head yielded in H-6-6.

For Specimen H-2.5-6, strain data indicates the steel did not yield until failure, which confirms this specimen did not reach the full moment and curvature capacity because of the short lap length. Specimens H-2.5-4 and H-4-6 performed better than H-2.5-6 with respect to the more moment capacity; however, both of them had a sudden, brittle failure due to the short lap length. The 2.5 in. or 4 in. lap length was not adequate to develop the steel and could not provide desirable moment capacity and ductility. For WWR specimens, the strain gauge readings in W-4-4 and W-4-6 indicated the steel did not develop any significant strain.

Load-Deflection. Figure 3.33 compares the load-deflection curves of all the tested specimens. Note however, that the string connecting LVDT for deflection measurement for the control specimen was broken when the control specimen had a deflection around 1.2 in. and therefore does not indicate the actual deflection achieved.

Similar to the moment-curvature data, the deflection data clearly shows that for headed reinforcement, 6 in. lap length specimens (H-6-4 and H-6-6) were more deformable than the 2.5 in. or 4 in. lap length specimens (H-2.5-4, H-2.5-6 and H-4-6). The maximum deflections in 6 in. lap length specimens were almost twice the deflections measured for specimens with 2.5 in. or 4 in. lap length. In the specimen with the 6 in. lap length, load

deflection curves show obviously ductile behavior before reaching the ultimate load. The WWR specimens had low load capacity and ductility.

Observed Cracking. The first cracks developed at in the mid-span region when the moment was between 3.5 kips ft to 5 kips ft, depending on the different specimens. For 2.5 in. lap length specimens (H-2.5-4 and H-2.5-6), cracks usually consisted of flexural cracks in the “longitudinal” direction in the constant moment zone. The numbers on specimens shown in Figures 3.34 to 3.37 represent the applied loads with the unit of kips. There was not much transverse cracking (Figure 3.34-a) which means the concrete cover was sufficient to develop the bond stress that occurred. Prior to failure, a wide crack propagated along the midspan. However, the top concrete was still good until failure (Figure 3.34-b). This behavior indicates the 2.5 in. lap length was too small to provide enough anchorage (combination of head and bond). Before the top concrete crushed, the concrete between overlapping headed reinforcement failed and the overlapping reinforcement could not transfer force.

Figure 3.35 shows the cracking behavior for 4 in. lap length specimen H-4-6. Several cracks formed in the “transverse” direction in the constant moment zone indicating a loss of bond stress with load close to failure (Figure 3.35-a). These results show that a 4 in. lap length could provide some degree of bond in the lap zone prior the failure. Failure occurred with crushing of the top concrete (Figure 3.35-b) confirming a reasonably large anchorage capacity was provided by combination with head and bond in 4 in. lap length. However, this lap length was not long enough to develop the steel to fully yield.

Crack behavior for 6 in. lap length specimens (H-6-6 and H-6-4) are shown in Figure 3.36. Longitudinal flexural cracks were well-distributed along the constant moment zone. Failure occurred with crushing of the top concrete (Figure 3.36-a). Results indicated anchorage (combination of head and bond) was sufficient for the specimens to behave as continuously reinforced. Figure 3.36-b shows the maximum crack width in the constant moment zone against the applied load. Under the failure load, the maximum measured crack width is about 0.2 in. However, the measured crack width under estimated service load moment is about 0.004 in.

In WWR specimens, a large crack propagated at the center of the span until a brittle failure occurred (Figure 3.37).

Failure Types. Typically, the specimens exhibited two different failure types during testing. Figure 3.38-a and Figure 3.38-b display the ductile, slow failure and the sudden, brittle failure, respectively. The Specimens H-2.5-4, W-4-4, and W-4-6 experienced a sudden, brittle failure and broke into two pieces. The control specimen, H-6-6 and H-6-4 had a ductile failure. H-2.5-6 and H-4-6 experienced a brittle failure with small curvature but it did not break into two pieces. The testing program indicated that both the reinforcement lap length and the spacing had effects on the failure type. 2.5 in. and 4 in. lap lengths could not provide enough anchorage to fully develop the reinforcement. Since the reinforcement did not yield, as the load increased to a certain value, the anchorage was lost and the load could no longer be carried, and failure occurred suddenly. 6 in. lap length could provide desirable anchorage and had a ductile behavior.

Subtask 6.2-C1 Findings - Based on the survey and the experimental program, the following conclusions were made:

1. The headed bar detail can provide a continuous force transfer in the longitudinal joint for DBT bridge system while minimizing the width of the joint to accelerate DBT bridge construction.
2. The lap length for the headed bar detail is recommended to be 6 in. This lap length provided full development of the bars to produce full load capacity and significant ductility.
3. The reinforcement spacing had an effect on the structural behavior. The smaller spacing provided more load resistance with less ductility because more steel was provided in the same cross section.
4. In the tested WWR connection details, the joint width accommodating 1 in. spacing between cross wires failed to provide the required moment capacity. Therefore, a WWR connection detail with the same joint width as the headed bar detail cannot be recommended.
5. According to the moment capacity, curvature, cracking, deflection and steel strain comparison, the headed bar detail with a 6 in. lap length was recommended for replacing the current welded steel connector detail as the improved longitudinal joint detail for DBT bridges.

Subtask 6.2-C2 – Laboratory Testing of Joint Assemblies

Introduction – The objectives of this subtask are to determine the static load strengths and fatigue characteristics for the selected alternate longitudinal joint system. Previous sections of this report present the results of a study that assesses potential alternate joint details for decked bulb tee (DBT) bridges based on constructability, followed by testing of selected details. Seven reinforced concrete beam specimens connected with either lapped headed reinforcement or lapped welded wire reinforcement (WWR) were tested along with another specimen reinforced by continuous bars for comparison. Based on that study, a headed bar detail with a 6 in. lap length was recommended for additional testing to further investigate replacing the current welded steel connector detail. This section of the report describes the test program and presents results of this additional testing.

In this study, four full-scale slabs connected by a headed reinforcement detail utilizing a 6 in. lap length were fabricated and tested. The analytical parametric studying Subtask 6.2-A was conducted to provide the database of maximum forces in the longitudinal joint. These maximum forces are used to determine the loading demand necessary in the slab testing due to the service live load. Static and fatigue tests under four-point pure-flexural loading, as well as three-point flexural-shear loading, were conducted. Test results were evaluated based on flexural capacity, curvature behavior, cracking, deflection and steel strain. Based on these test results, the improved longitudinal joint detail is a viable connection system to transfer the forces between the adjacent DBT girders. Further details of work accomplished in this subtask are provided in Chapter 3 of Appendix F.

Experimental Program

Slab Dimension. A total of four slabs with the same dimensions were fabricated for the static and fatigue testing. Each specimen consists of two panels as shown in Figure 3.39. Each panel is 72 in. wide, 64 in. long, and 6 in. deep. The female-to-female shear key was provided at the vertical edge of both ends in the specimen length direction. This allowed each slab to be used for two tests.

Reinforcement Layout and Strain Gage Instrumentation. Figure 3.40 displays the reinforcement layout used in the slab specimen. There are five layers of reinforcement in each panel along the specimen depth direction with a 2 in. cover at the top and 1 in.

cover at the bottom. The top two layers and bottom two layers of reinforcement simulate the deck reinforcement in the top flange of DBT girders. The middle layer of the reinforcement consists of epoxy coated headed bars which project out of the panel to splice with the headed bars in the adjacent panel in the longitudinal joint. All the epoxy coated reinforcement has a nominal yield stress of 60 ksi. The spacing of the headed bar is 6 in. and the splice length (inside head to inside head) is also 6 in. One longitudinal headed bar was placed along the center line of the joint both above and below the spliced headed reinforcement. The headed reinforcement is a No. 5 bar with a standard 2 in. diameter circular friction welded head. The head thickness is 0.5 in.

Steel strains were measured on selected bars in the joint zone. Figure 3.41 depicts the strain gauge layout in the slab for the four-point pure-flexure test (the left figure in Figure 3.41 and the three-point flexure-shear test (the right figure in Figure 3.41). Chapter 3 of Appendix F provides further detail regarding the strain gage layout and nomenclature used to define gage positions.

Panel Fabrication. The concrete panels were fabricated locally at Ross Prestressed Concrete Inc. in Knoxville, TN. Figure 3.42-a shows the panel reinforcement before placement of the concrete. The two ends of the wood form, in the length direction, were slotted at a spacing of 6 in. to fix the headed reinforcement in place. Foam wedges were used to form the configuration of the shear key at the vertical edge of the panel. The design concrete compressive strength at 28 days was 4000 psi. A total of 18 concrete cylinders were made with the pouring of panels (Figure 3.42-b).

Joint Surface Preparation. The surfaces of the shear key were sandblasted to prepare the joint for the closure pour. The purpose of the surface preparation is to remove all contaminants that can interfere with adhesion and to develop a surface roughness to promote a mechanical bond between the grout and base concrete. After the removal of the deteriorated concrete, proper preparation should provide a dry, clean and sound surface offering a sufficient profile to achieve adequate adhesion. There are many methods of surface preparation such as chemical cleaning, mechanical cleaning and blasting cleaning. Sandblasting uses compressed air to eject the high speed stream of sand onto the surface which needs to be prepared. This method is very effective to process the surface of precast members under industrial conditions. Black Beauty 2050

sand was chosen for sandblasting to prepare the surface in this study. The profiles of the surface before and after sandblasting are shown in Figure 3.43

Closure-Pour Materials. The longitudinal joint, which is filled with closure-pour materials connecting the top flange of the adjacent DBT girders, is considered to be the structural element of the bridge deck. It is important for the selected closure-pour material to reach its design compressive strength in a relatively short time for the purpose of accelerated bridge construction. As described in Section 3.2.5 of Appendix F, it was decided to use two grout materials, SET 45 HW (SET) and EUCO-SPEED MP (EUCO), for trial testing (23). Both of these materials are magnesium phosphate-based materials and were used with a 60% extension of pea gravel as described in section 3.2.5 of Appendix F.

Based on the results of a comparative study described in Section 3.2.5 of Appendix F, the grout SET was selected in this study. The selection was based primarily on setting time of the grout.

The compressive strength of grouted joint $f_{cj}^{'}$ at the time of testing for each specimen, along with the compressive strength of concrete panel $f_{c}^{'}$ are shown in Table 3.12.

Testing Plan and Setup and Fatigue Load Determination. A total of four slab specimens were made. Each slab specimen consists of two concrete panels connected with an overlapping headed reinforcement and the SET 45 HW extended grout. The four slab specimens were tested under different parameters: 1) flexure static (F-S) test; 2) flexure-shear static (FS-S) test; 3) flexure fatigue (F-F) test, and 4) flexure-shear fatigue (FS-F) test.

Details of the Test Plan, Setup, and Fatigue Load Determination are provided in the previous discussion of Subtask 6.2-A3 – Development of Laboratory Testing Protocol of this report and in Sections 3.2.6 and 3.2.7 of Appendix F. As pointed out in the discussions of the testing protocol, due to the shear spans used in the FS-S and FS-F tests, the maximum moment accompanying the maximum shear in these flexure-shear test specimens was higher than the maximum moment accompanying the maximum shear in the analytical models of the bridge decks. Therefore, the loading used in the flexure-shear test specimens is more severe than the loading determined in the live load

analyses, and results of the FS-S and FS-F tests are considered conservative. Also, as described in the previous discussion of Subtask 6.2-A3, for the FS-F test, the camber leveling shear of 0.5 kips/ft was applied at the middle of the joint zone all the time with the fatigue shear oscillating at approximately ± 2.8 kips above and below this average. The target oscillating shear was ± 2.326 kips/ft. Therefore, the loading applied to the FS-F specimen was conservatively high.

Further, however, Section 2.5.10 of this Appendix F includes a discussion of revisions accepted by AASHTO Bridge Committee, Technical Committees T-5 Loads, and T-14 Steel subsequent to panel tests. The revisions consist of inclusion of two levels of fatigue load in Table 3.4.1-1. These are Fatigue I and Fatigue II. Fatigue II retains the current Load Factor of 0.75 and is to be applied to represent an effective stress range caused by the fatigue truck with respect to a large but finite number of stress range cycles. Fatigue I has a Load Factor of 1.5 (or 2 times 0.75) and is to be applied to the stress range caused by the fatigue truck with respect to an infinite number of stress range cycles.

Section 2.5.10 of Appendix F presents factored fatigue loads using the revised Load Factor of 1.5 for Fatigue I of 3.419 kips-ft/ft, -0.568 kips-ft/ft and 4.382 kips/ft for maximum positive moment, negative moment and shear respectively. In addition, the maximum factored fatigue moment would be coincidental with the maximum shear of 4.382 kips/ft is 2.201 kips-ft/ft.

For the F-F test, the Fatigue I moment of 3.419 kips-ft/ft is 60% higher than the maximum 2.143 kips-ft/ft used in the test. Therefore, the F-F test is not adequate to demonstrate infinite life per the accepted AASHTO revisions. For the FS-F test the Fatigue I shear of 4.382 kips/ft is 33% higher than the maximum shear of 3.303 kips//ft used in the test. However, during the FS-F test, moment was cycled between 3.150 and 4.521 kips-ft/ft while the shear was reversed. These moments are 43% and 105% higher than the maximum of 2.201 kips-ft/ft. that would be coincidental with the maximum shear. Therefore, although the shear was low for Fatigue I loading, the flexure was very high. Therefore, in the opinion of the researchers, the FS-F test was a very robust test to demonstrate the viability of the improved longitudinal joint detail.

Results of Testing - Subtask 6.2-C2

Moment Capacity and Curvature. Figure 3.45 shows the curvature-fatigue cycle curves (C-N) for the fatigue tests. The curvature represents the average curvature of the joint zone after a different number of fatigue cycles under a specific loading. For example, the curve labeled with "M=0.5 k-ft/ft" in Figure 3.45-(a) represents the change of the curvature of the joint zone with numbers of fatigue cycles, which was measured at the loading level corresponding to a moment of 0.5 kips-ft/ft of the joint for the F-F specimen during each of the interim static load tests.

As shown in Figure 3.45, the curvature increased with the increasing of the joint moment for all specimens. Comparing among different joint moment levels, the impact of fatigue on the curvature is about the same for all specimens. It appears that fatigue loading has no effect on the curvature for the F-F specimen while it increases the curvature for the FS-F specimen. For the FS-F specimen under "P1", the first set of one-million cycles increases the curvature more than the second set of one-million cycles. For the FS-F specimen under "P2", however, the first set of 1.5-million cycles have more impact. Damage accumulations due to fatigue loading cycles cease after that point. In general, there is no significant influence of fatigue cycles on the curvature after the first one-million to 1.5-million cycles.

Figure 3.46 compares the moment-curvature curves between the specimens (F-F and FS-F) subjected to fatigue loading after 2,000,000 cycles with the specimens (F-S and FS-S) subjected to static loading without fatigue cycles. The y axis labeling "Moment/Joint Length" represents the nominal distributed moment along the joint, which is the applied moment divided by the length of the joint. Both the F-S specimen and FS-S specimen were loaded with un-cracked section while the F-F specimen and FS-F specimen were loaded with cracked section after 2,000,000 fatigue cycles. As a result, the slope of the curve (stiffness of the slab) for F-S and FS-S is steeper (larger) than the F-F and FS-F at the beginning of the load. After the applied moment exceeds the cracking moment level, the slopes of the two curves are about the same, indicating that the fatigue cycles had no significant effect on the curvature development, as discussed earlier. The Service Load shown in Figure F-3.46-(a) is the maximum positive calculated moment after cracking of 4.001 kip-ft/ft reported in Finding for Subtask 6.2-A2.

As shown in Figure 3.46-(a), when the joint moment reaches about 10.4 kips-ft per unit length, the reinforcement in both specimens (F-F and F-S) is yielded, indicating that fatigue cycles have no significant influence on the yielding load. After yielding of the reinforcement, the F-S specimen shows a larger curvature development than the F-F specimen. The maximum curvature of the F-F specimen is about 50% of the maximum curvature of the F-S specimen. At service loading, the two specimens have essentially the same curvature.

Unfortunately, this kind of comparison cannot be made for flexure-shear tests in Figure 3.46-(b) because the LVDTs measuring curvature in the FS-S specimen were removed before specimen failure; therefore, the maximum curvature cannot be reported. As shown in Figure 3.46-(b), for the range of loading for which curvature was measured, there is no obvious flat part of the two curves. The Service Load shown in Figure 3.46-(b) is the corresponding moment (CM) occurring with the maximum shear is 2.887 kips-ft/ft. after cracking reported in Finding for Subtask 6.2-A2

Load Deflection Relationships. Figure 3.47 compares the load-deflection curves between the fatigue slab after 2,000,000 cycles and the slab under static loading without fatigue cycles. The y axis labeling “Load/Joint Length” represents the nominal distributed load along the specimen, which is the applied load, P, divided by the length of the specimen. Note that the load P is the load applied to one loading pad as shown in Figure 3.16.

The beam theory (labeled “Theoretical Analysis” in Figure 3.47) was utilized to predict a load-deflection curve consisting of three parts: before cracking, after cracking until yielding of the reinforcement, and the stage of plastic hinge development at midspan after reinforcement yielding. The deformation capacity of the theoretical analysis was based on crack section property for conservative purpose. Similar to Figure 3.46, the slope of the curve for F-S and FS-S is steeper than the slope of the curve for F-F and FS-F from the initial loading until cracking load is reached. After cracking, the development of the deflection between static slab and the fatigue slab is the same, and the slopes of the two curves are about the same. This indicates that the fatigue cycles have no significant effect on the deflection in this stage.

The Service Load shown in Figure 3.47-(a) is the Load/Joint Length of 1.894 kips/ft which corresponds with the maximum positive calculated moment of 4.001 kips-ft/ft after cracking reported in Section 2.6. The Service Load shown in Figure 3.47-(b) is the Load/Joint Length of 2.306 kips/ft. This Service Load /Joint Length corresponds with the maximum calculated shear near the pad load of 5.056 kips/ft based on analyses using the finite element model shown in Figure 3.18 and discussed under Subtask 6.2 A3.

After yielding of the reinforcement, the plastic hinge is developed fully at the joint zone of the F-S specimen with large deformation until failure, while the F-F specimen failed without significant development of the plastic hinge. The F-S specimen has 113% load capacity and 112% deformation capacity of the theoretical calculations while the F-F specimen has 101% and 82%, respectively. Under the flexure loading (F-S and F-F), the fatigue cycles have impact on the slab ductility and the development of the plastic hinge after the yielding of the reinforcement. The fatigue cycles prevent the development of the plastic hinge after the yielding of the reinforcement and reduce the ductility significantly.

Under service load, the deflection of the F-F specimen is larger than the F-S specimen. The deflection difference between the F-S and F-F specimen is caused by the un-cracked section property and cracked section property for each slab at the initial loading.

Under the flexure-shear loading (Figure 3.47 b) both FS-S and FS-F reached the maximum load near the load capacity of the theoretical analysis. Prior to failure, the maximum loads in FS-S and FS-F was 11.2 kips-ft per unit length and 11.6 kips-ft per unit length respectively. The fatigue cycles have no influence on the curvature development before yielding of the reinforcement and the yielding load. However, the deformation capacity in FS-S and FS-F were 77% and 70% of the theoretical value due to the shear failure with limited plastic hinge development.

Figure 3.48 shows the relative displacement (RD) between the two sides of the joint interface versus fatigue-cycle (N) curves for FS-F under specific loading levels during interim static load tests. For the F-F specimen, the relative displacement of the joint interface is zero under service live load. Figure 3.48-(a) and Figure 3.48-(b) are the curves for the FS-F specimen under “P1” and “P2”, respectively.

From Figure 3.48, it can be seen that the relative displacement of the joint interface is dependent upon the applied load. The relative displacement increases with the increasing of the applied load. However, under the same loading level, the curve is very flat. The relative displacement after different fatigue cycles is the same under the same load, so there is no influence of fatigue cycles on the relative displacement under service live load.

Load Crack Width Relationship. During the tests, the cracks at the interface between the grouted joint and the concrete panel were observed and crack widths were measured. The two cracks marked as “14” and “12” shown in Figure 3.49 are labeled as either “Crack 1” with larger crack width or “Crack 2” with smaller crack width.

Figure 3.50 (a) and (b) show the load-crack width relationship for the F-S specimen and the FS-S specimen, respectively. The Service Load shown in Figure 3.50-(a) is the Load/Joint Length of 1.894 kips/ft which corresponds with the maximum positive calculated moment of 4.001 kips-ft/ft after cracking reported in Section 2.6. The Service Load shown in Figure 3.50-(b) is the Load/Joint Length of 2.306 kips/ft. This Service Load /Joint Length corresponds with the maximum calculated shear near the pad load of 5.056 kips/ft based on analyses using the finite element model shown in Figure 3.18 and discussed under Subtask 6.2 A3.

The crack width was measured by DEMEC mechanical strain gauges. From Figure 3.50-(a), it can be seen that the width of the two cracks is developed at a different rate with the increasing of the loading. The width of “Crack 1” grows faster than the width of “Crack 2” due to the reinforcement yielding that is developed at the joint interface of the “Crack 1” location. The crack widths at the Service Load level of 1.894 kip /ft are relatively small.

In Figure 3.50-(b), the two cracks are widened at the same rate with the increasing of the loading when the load reaches about 7.4 kips per unit length, the width of “Crack 2” decreases suddenly by 23% due to the flexural-shear crack that developed across the joint zone, as shown in Figure 3.51. After the formation of the flexural-shear crack, the two cracks continue to develop with the same rate until the specimen fails. The crack widths at the service load level of 2.306 kip/ft are relatively small.

Figure 3.52 shows the crack width-fatigue cycle curve (CW-N) for the fatigue tests representing the maximum crack width at the joint interface after a various number of fatigue cycles under specified loadings.

From Figure 3.52, it can be seen that the width of the crack at the joint interface is dependent upon the applied load. The crack width increases with the increasing of the loading, however, the curve is very flat under the same loading. So the influence of fatigue cycles on the crack width of the joint interface is negligible under service live load.

Moment-Strain Curve. Figure 3.53 shows the strain-fatigue cycle curves (S-N) for the fatigue tests representing the reinforcement strain in the joint after a various number of fatigue cycles under service live load. The strain gauge number and the loading are shown in the figure. For example, “2-1” represents the strain gauge #1 at the headed bar #2 and “M = 3 k-ft/ft” means the joint of the slab is subjected to a joint moment of 3 kips-ft per unit length.

From the Figure 3.53, it can be seen that all the curves are again flat and the variation of the reinforcement strain after different fatigue cycles is not significant. All reinforcement under the loading zone and the longitudinal headed bar experience a very low strain compared with the reinforcement in the joint.

Failure of Specimen. As shown in Figure 3.54-(a), the failure mode of the F-S specimen is a typical flexure failure. After the headed reinforcement yields, both the concrete in the panel and the grout in the joint crushes. The grout under the reinforcement spalls off along the joint due to the bending of the spliced headed bars. The slab specimen experiences a ductile failure and spliced headed bars hold the crushed concrete to prevent the separation of the panels.

The failure mode of the FS-S specimen is a typical flexural-shear failure. Figure 3.54-(b) shows that the shear crack crosses the joint zone when the slab fails. It can be seen that the shear crack is widened from the lower part of the joint interface. Then, it crosses the whole grouted joint and reaches to the top part of the joint interface.

The failure mode of the F-F specimen is a flexure failure. However, by comparing with the F-S specimen, there is little development of plastic hinge at the interface of the joint

(Figure 3.54-c). This confirms that the fatigue cycles inhibit the development of the plastic hinge at the joint zone. The grout in the joint zone is crushed at top. There is a large crack along the interface of the joint at the bottom of the slab. The grout under the reinforcement does not spall off along the joint.

The failure mode of the FS-F specimen is a shear failure. Figure 3.54-(d) shows the shear cracks in the joint zone when the slab fails. It can be seen that the shear crack is developed from the lower part of the joint interface, then crosses the concrete panel and reaches to the top concrete. It can be seen that there is no spalling along the joint.

Subtask 6.2-C2 Findings - Based on the experimental program, the following conclusions were made:

1. The fatigue loading has little influence on the structure behavior including average curvature of the joint, deflection at midspan, relative displacement of the joint interface as well as reinforcement strain under service live load.

2. The fatigue loading has no effect on the loading capacity of the structure. The slab, after 2,000,000 fatigue cycles, has the same loading capacity as the slab under static load test.

3. The fatigue loading inhibits the development of the plastic hinge under pure-bending load. The fatigue cycles reduce the ductility capacity significantly.

4. Based on these tests, the improved longitudinal joint detail is a viable connection system to transfer the forces between the adjacent decked bulb tee (DBT) girders.

Task 6.3- Design and Construction Guidelines

Subtask 6.3-A – Documentation of Design and Construction Practices

Background

Construction and geometry control were identified as key issues for further work in Task 6. There are certain issues involved in erection/construction that are relatively unique to this type of bridge. Current non-users have little experience with these issues and need guidelines as to how to handle these issues. In particular, construction geometry control for differential camber, skewness, and cross-slope needed to be addressed. Therefore, Task 6.3

was included in the Detailed Work Plan. This task was carried out to document best practices for existing systems based on successful methodology currently being used.

Results

Data was collected using interviews with designers, and precasters, with significant experience with this type of bridge. The practicality of the existing practices was assessed based on results of interviews and on the knowledge and experience of the research team. Written descriptions of selected practices were developed to address previously defined issues such as:

- Geometry control issues (cross-slope, skew, camber).
- Weight and length limitation for loading, transportation, and erection.
- Lateral stability during transportation and erection.
- Erection schemes.
- Planning for speed of construction.
- Details and construction sequence for establishing continuity for live load.
- Girder splicing and segmental construction.
- Attachment of rail systems.
- Provisions for bridge widening.

The collected information is and presented within the Guidelines for Design and Construction of Decked Precast Prestressed Concrete Girder Bridges document provided as a separate report for this project.

Subtask 6.3-B – Design Examples

The objectives of Subtask 6.3-B were to develop an example of design and detailing procedures for a selected bridge in a clear and step-by-step fashion with respect to the guidelines. The results include a design example for a simple-span bridge. A step-by-step design example that illustrates all significant steps in the design process is provided as an appendix to the Guidelines for Design and Construction of Decked Precast Prestressed Concrete Girder Bridges document provided as a separate report for this project.

Subtask 6.3-C – Design Examples for Future Re-Decking

The objective of Subtask 6.3-C was to demonstrate the design of the interface between deck and girder considering the option of future deck replacement. The interface was designed using the detail discussed in Subtask 6.1-A Full Depth Deck Replacement, which incorporates a debonded joint between the deck and the girder to facilitate deck removal and shear keys with reinforcement for horizontal shear transfer across the interface. The design horizontal shear was based the maximum horizontal shear anticipated for this type of bridge girder as obtained from the parametric studies in Subtask 6.1-B Optimized Girder Study. Two examples are presented. The first considers the optimized section developed in Subtask 6.1-B and the second considers a typical AASHTO type section. Figures 3.55 and 3.56 illustrate the shear key geometry and reinforcement for the optimized section while Figures 3.57 and 3.58 illustrate the shear key geometry and reinforcement for AASHTO Type II girder.

The design results indicated that for the optimized section under maximum shear condition, the bars crossing the interface near sub-flange tips will serve as both connecting reinforcement and horizontal shear reinforcement. It should be noted that the sub-flange is not acting composite with the top flange for transverse bending. However, this connecting reinforcement is needed so that the sub-flange can work in parallel with the top-flange for transverse bending moments that put the bottom of the sub-flange in tension. The narrow top surface of AASHTO Type II section results in high horizontal shear stress demand. In order to accommodate such high shear stress, the shear keys are spaced at a shorter distance as shown in Figure 3.58. These designs demonstrate the maximum reinforcement and shear key geometry required for selected connection details. The examples indicated that the proposed details for facilitating future deck replacement are adequate for horizontal shear transfer across the interface between the two casting stages. Further details of the designs are provided in Appendix G of this report.

Table 3.1 Parameters for Camber Leveling Study

Girder Depth (in.)	Girder Spacing (ft)	Span (ft)	Diff. Camber (in.)
65	8	84	1.05
65	4	108	1.35
53	8	76	0.95
53	4	98	1.23
41	8	64	0.80
41	4	84	1.05

Table 3.2 Girder Flexural Stresses Due to Camber Leveling (psi)

Girder			Skew Angle							
Depth	Spac.	Span	0^o		15^o		30^o		45^o	
(in.)	(ft)	(ft)	Tens.	Com.	Tens.	Com.	Tens.	Com.	Tens.	Com.
65	8	84	800	-551	814	-559	843	-658	889	-785
65	4	108	734	-598	737	-599	744	-620	756	-695
53	8	76	742	-480	756	-483	786	-595	832	-710
53	4	98	663	-538	666	-539	673	-560	686	-625
41	8	64	685	-439	702	-443	734	-557	785	-670
41	4	84	596	-488	600	-489	609	-513	623	-570

Table 3.3 Practical Span Ranges for Optimized Decked Bulb Tee Girders

Section	Spacing (ft)	Span (ft)	
		Minimum	Maximum
DBT41	4	84	124
	6	72	130
	8	64	118
DBT53	4	98	150
	6	84	156
	8	76	148
DBT65	4	108	172
	6	94	180
	8	84	176

Table 3.4 Summary of the Seven Bridge Models

Bridge	Girder		Span (ft)	Skewness (degree)
	Depth (inch)	Spacing (ft)		
A	65	8	134	0
B	65	8	84	0
C	65	4	108	0
D	41	8	118	0
E	41	8	118	45
F	41	8	118	30
G	41	8	118	15

Table 3.5: Maximum Forces in Joint 1 under Single Lane Loading

Bridge Models	Maximum Moment		Maximum Shear	
	M (kips-ft/ft)	CS (kips/ft)	CM (kips-ft/ft)	S (kips/ft)
A	5.498	0.114	3.716	6.024
B	5.034	0.094	3.373	5.646
C	2.242	0.029	1.672	4.745
D	6.304	0.227	4.492	5.768
E	6.713	0.137	5.027	5.703
F	6.512	0.178	4.693	5.718
G	6.404	0.204	4.585	5.746

Table 3.6: Maximum Forces in Joint 2 under Single Lane Loading

Bridge Models	Maximum Moment		Maximum Shear	
	M (kips-ft/ft)	CS (kips/ft)	CM (kips-ft/ft)	S (kips/ft)
A	6.286	0.112	4.206	5.856
B	5.225	0.048	3.442	5.899
C	3.386	0.299	2.432	4.738
D	7.393	0.347	5.294	5.946
E	7.922	0.421	5.464	6.091
F	7.528	0.364	5.370	6.054
G	7.432	0.348	5.305	6.041

Table 3.7: Maximum Forces in Joint 1 under Multilane Loading

Bridge Models	Maximum Moment		Maximum Shear	
	M (kips-ft/ft)	CS (kips/ft)	CM (kips-ft/ft)	S (kips/ft)
A	4.376	0.230	2.964	5.070
B	3.933	0.039	2.619	4.672
C	1.715	0.019	1.254	3.956
D	5.056	0.385	3.524	4.956
E	5.785	0.285	4.355	4.911
F	5.369	0.322	3.798	4.926
G	5.185	0.358	3.603	4.939

Table 3.8: Maximum Forces in Joint 2 under Multilane Loading

Bridge Models	Maximum Moment		Maximum Shear	
	M (kips-ft/ft)	CS (kips/ft)	CM (kips-ft/ft)	S (kips/ft)
A	4.472	0.095	2.830	4.723
B	3.936	0.056	2.525	4.888
C	2.287	0.230	2.195	3.699
D	5.219	0.517	3.492	5.128
E	6.475	0.573	4.074	5.270
F	5.703	0.510	3.760	5.221
G	5.390	0.516	3.578	5.167

Table 3.9: Maximum Negative Moment

Bridge Models	Joint 1 (kips-ft /ft)	Joint 2 (kips-ft/ft)
A	-0.371	-0.978
B	-0.389	-1.034
C	-0.078	-0.215
D	-0.785	-2.152
E	-1.400	-1.560
F	-0.939	-1.940
G	-0.824	-2.110

Table 3.10. Main Variables of Beam Specimens

Name	Reinforcement	Lap Length in.	Spacing in.	f_c' psi
Control	Straight Bar	Continuous	6	10,542
H-6-6	Headed Bar	6	6	10,542
H-2.5-6	Headed Bar	2.5	6	8,230
H-6-4	Headed Bar	6	4	8,860
H-2.5-4	Headed Bar	2.5	4	8,950
H-4-6	Headed Bar	4	6	8,480
W-4-6	WWR	4	6	7,750
W-4-4	WWR	4	4	8,352

Table 3.11. Moment Capacity and Curvature of Specimens

Specimens	Moment Capacity M_n (kips-ft)	Curvature (10^6/ in.)	
		Corresponding to M_n	Maximum
Control	25.19	10,802	12,934
H-6-6	25.83	7,653	9,490
H-2.5-6	17.39	2,167	3,715
H-6-4	39.4	6,320	8,848
H-2.5-4	32.13	3,407	Failed Suddenly
H-4-6	18.4	3,509	Failed Suddenly
W-4-4	4.74	942	Failed Suddenly
W-4-6	3.68	2003	Failed Suddenly

Table 3.12. Compressive Strength of Concrete Panel and Grouted Joint

Specimen	Panel (psi)	Joint (psi)
F-S	7495	5473
FS-S	7495	7295
F-F	5491	7021
FS-F	5491	5829

Figure 3.1 View of the Recessed Shear Key System

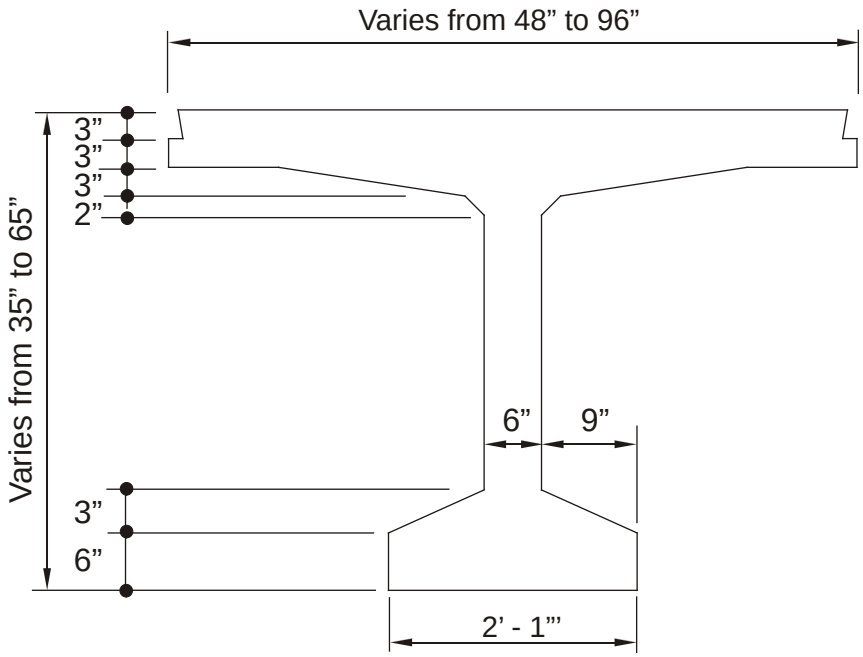

Figure 3.2. Conventional Decked Bulb Tee.

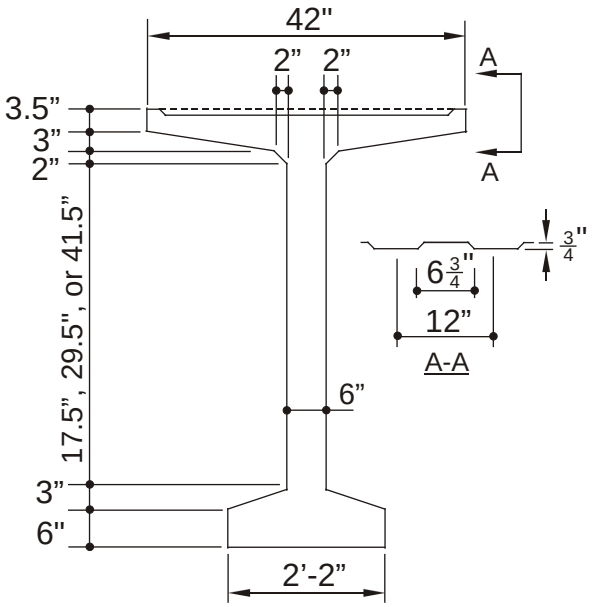

Figure 3.3. Proposed Girder: Stage 1 of Casting.

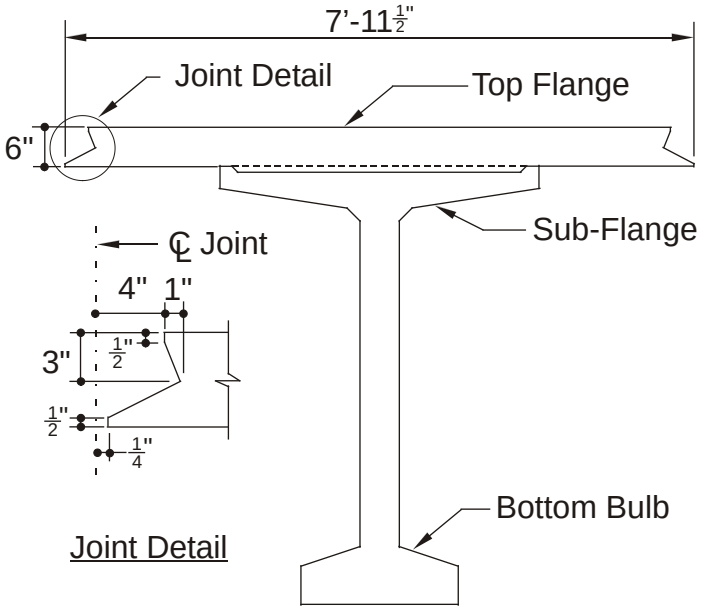

Figure 3.4. Proposed Girder: Stage 2 of Casting.

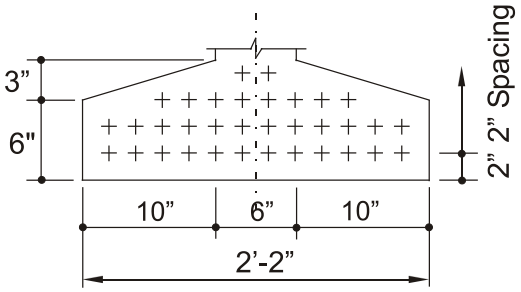

a) Standard bottom bulb

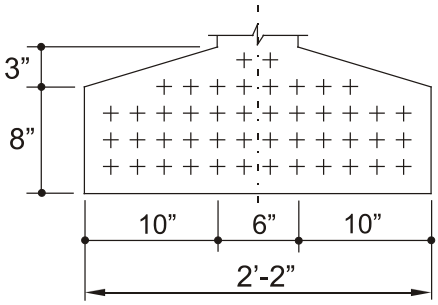

b) Tall bottom bulb with extra row of strands

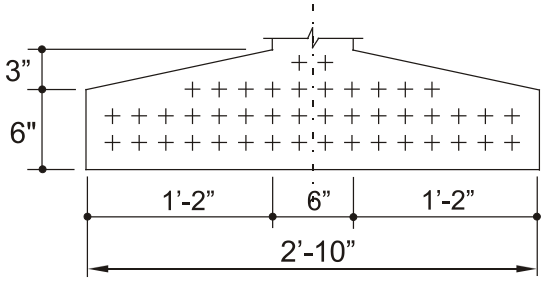

c) Wide bottom bulb with extra columns of strands

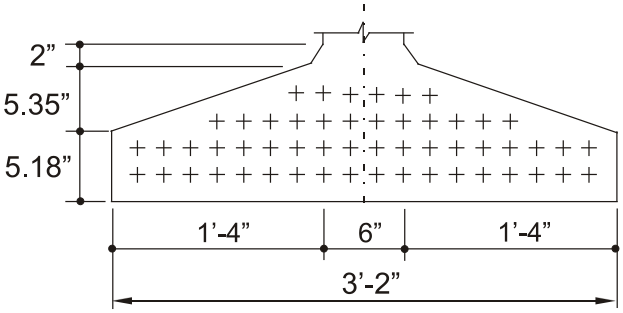

d) Modified NU bulb (no radii)

Figure 3.5 Bottom Bulb Configurations

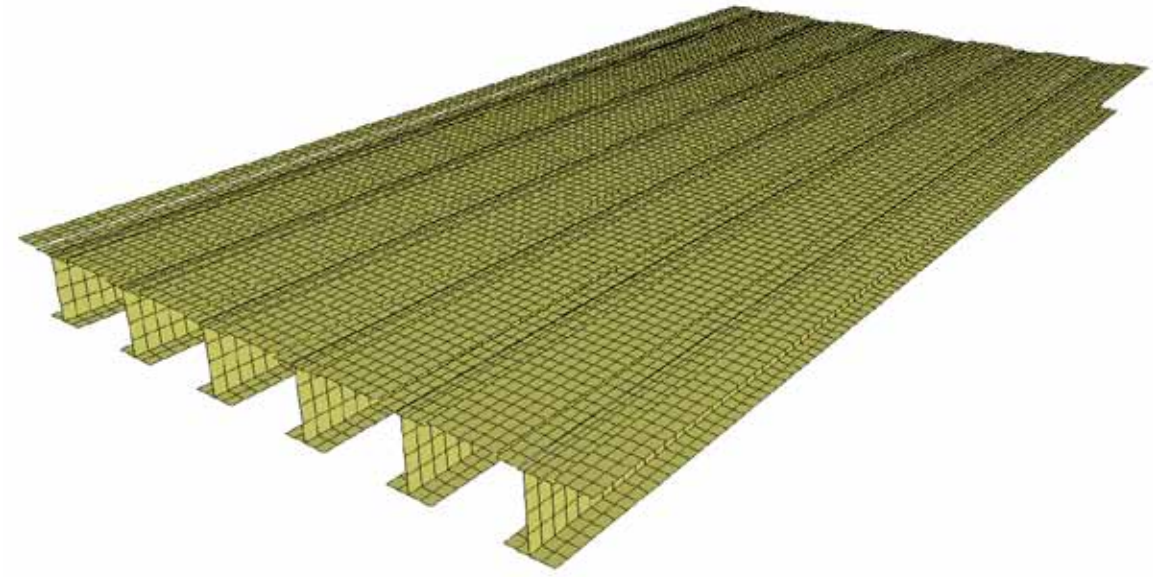

Figure 3.6 Finite element model using shell elements

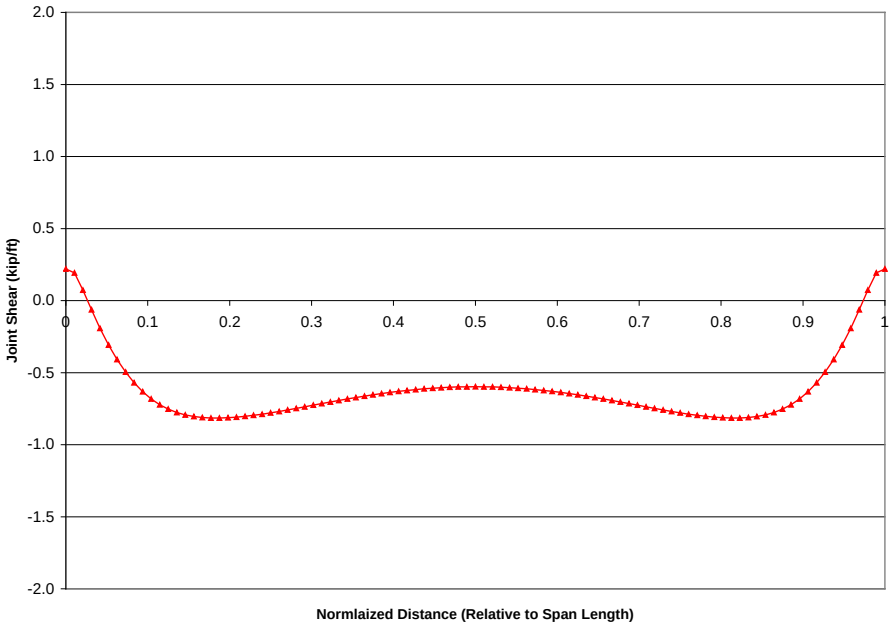

Figure 3.7 Transverse shear forces due to leveling of an interior girder

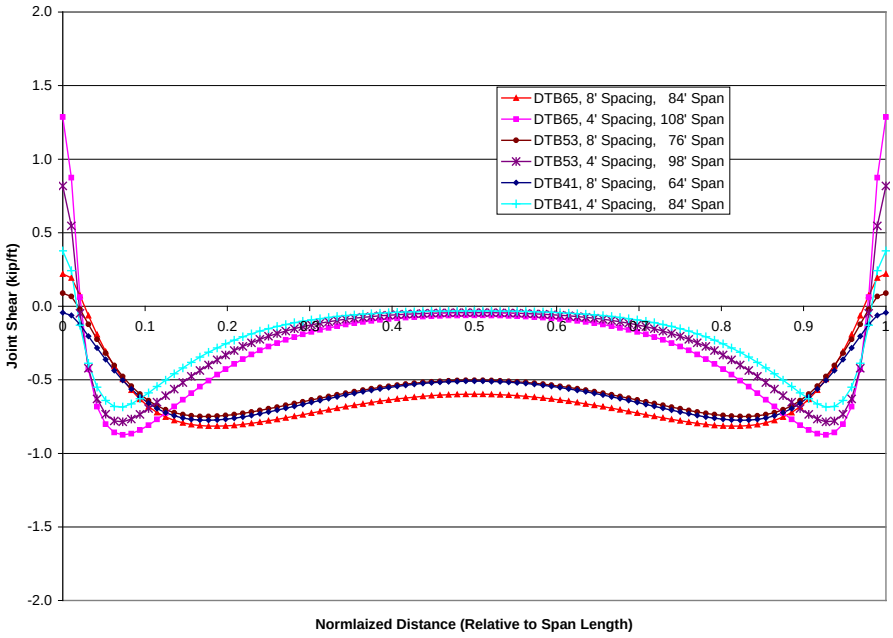

Figure 3.8 Shear forces due to camber leveling in right bridges

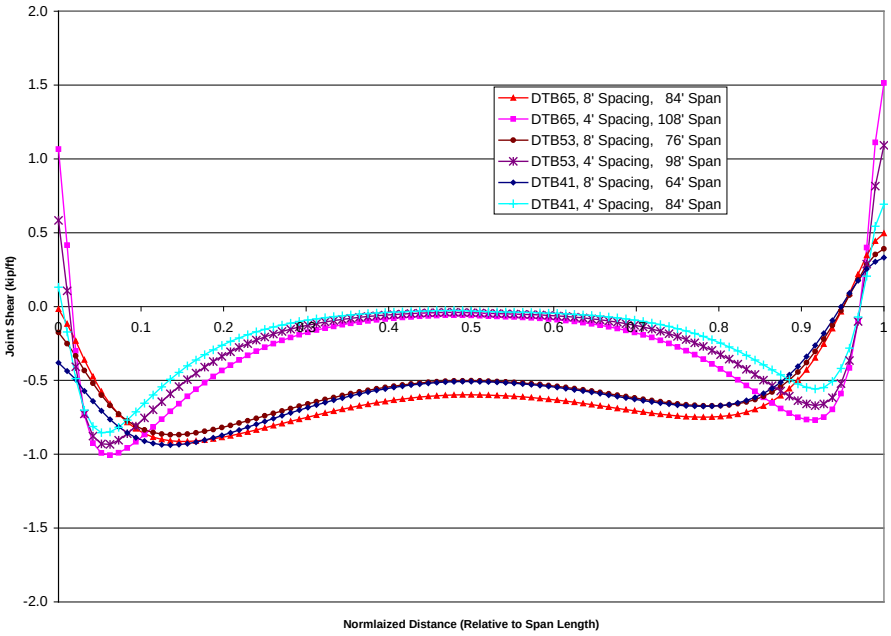

Figure 3.9 Shear forces due to camber leveling in 15^o skewed bridges

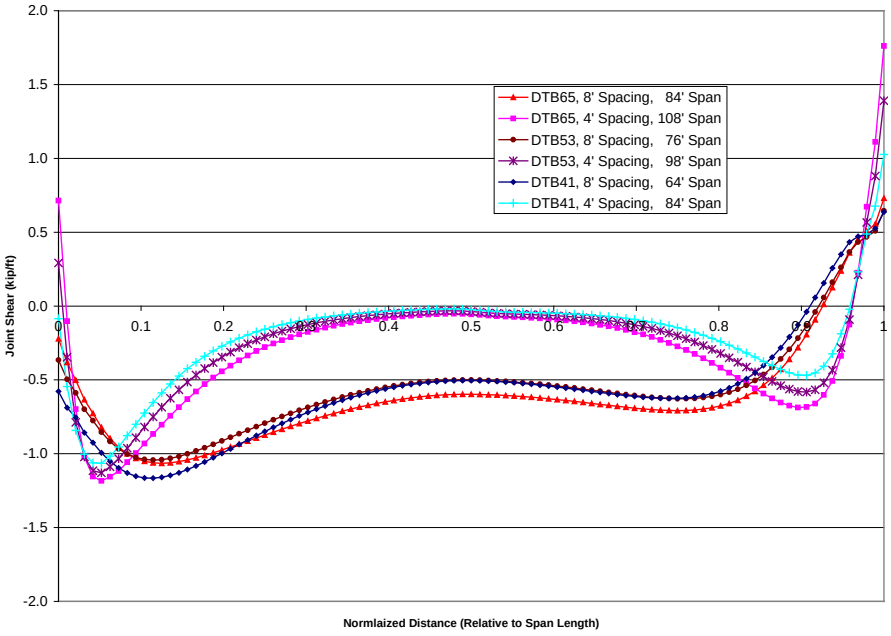

Figure 3.10 Shear forces due to camber leveling in 30^o skewed bridges

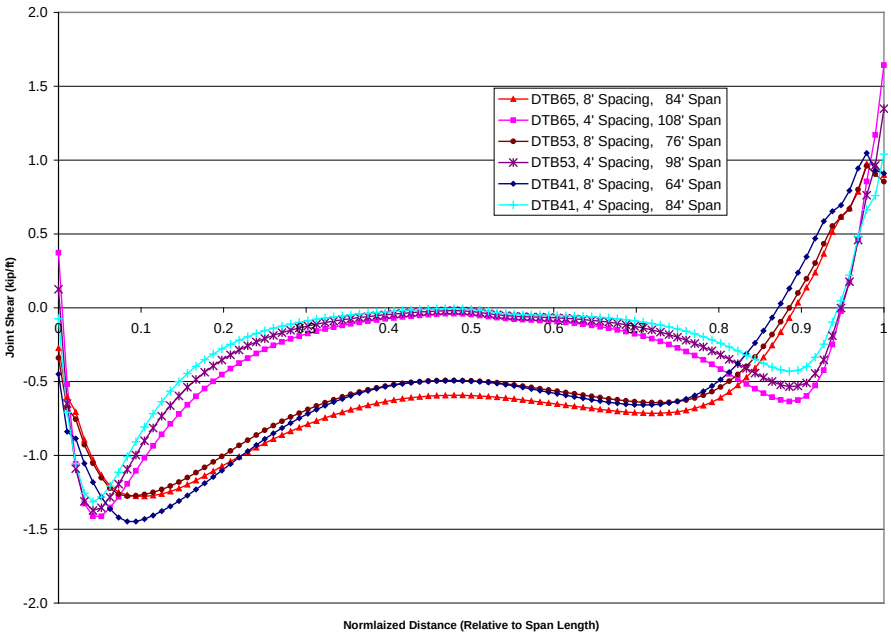

Figure 3.11 Shear forces due to camber leveling in 45^{o} skewed bridges

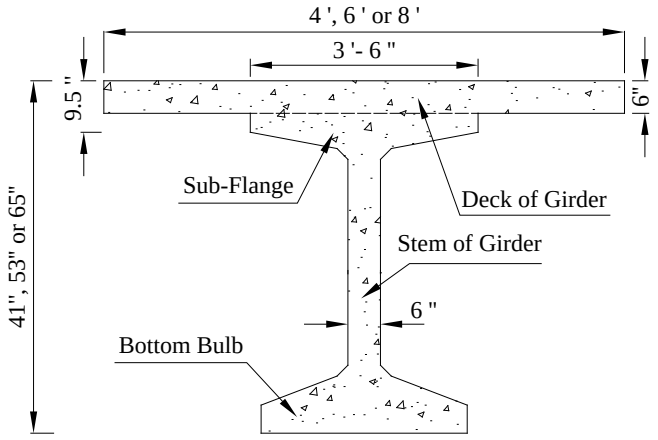

Figure 3.12: Cross Section of Optimized Decked Bulb Tee Girder

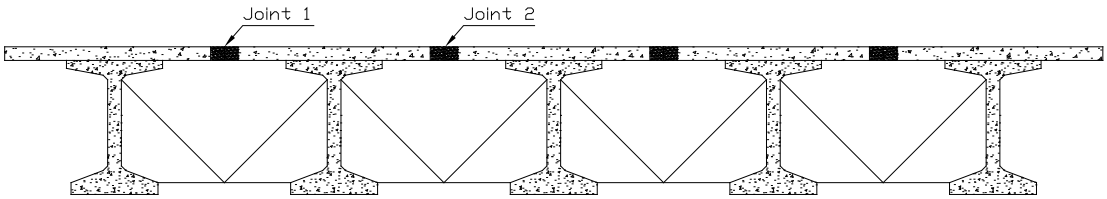

(a) Bridge A

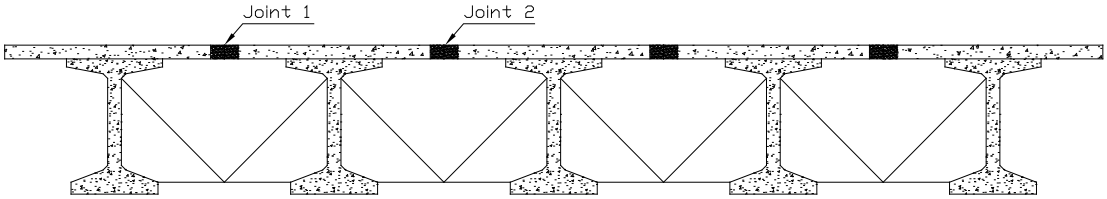

(b) Bridge B

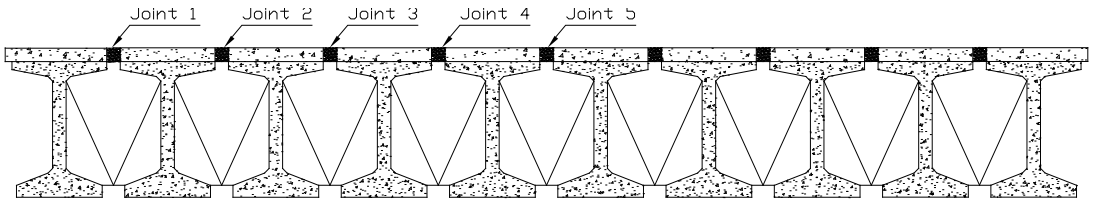

(c) Bridge C

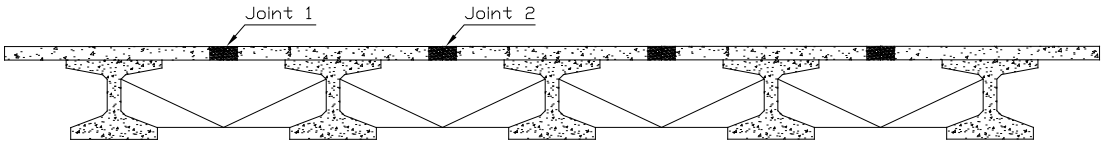

(d) Bridge D

Figure 3.13: Cross Section Sketch of Bridge Models

(a) Intermediate Steel Diaphragm

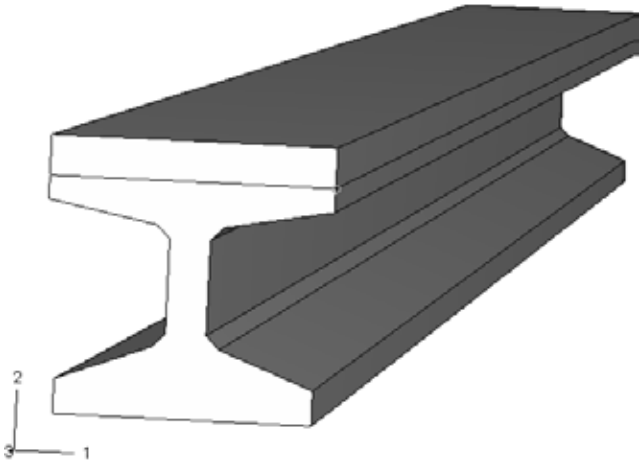

(b) Decked Bulb Tee Girder

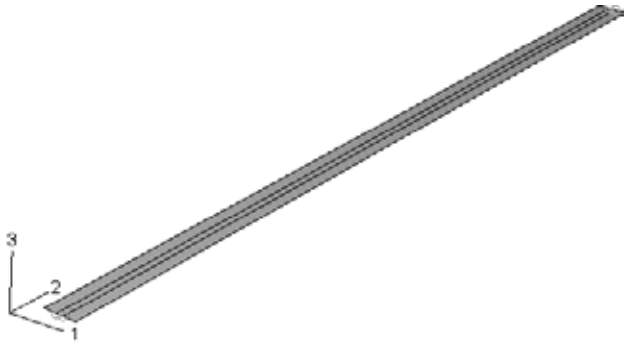

(c) Continuous Longitudinal Joint Connection

Figure 3.14: Bridge Components Modeled by 3D Finite Elements

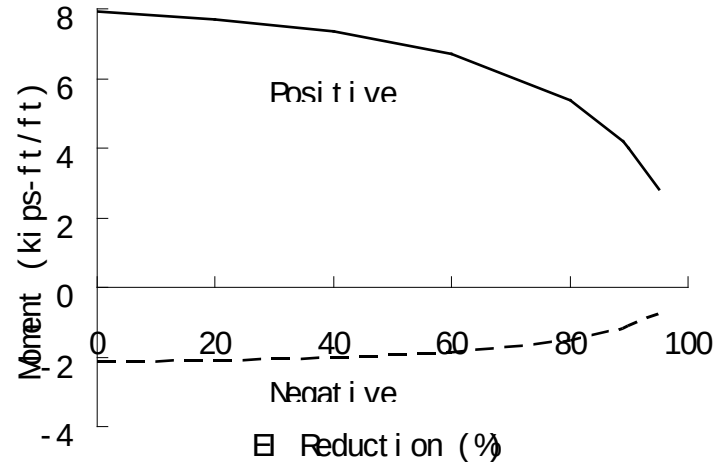

(a) Moment

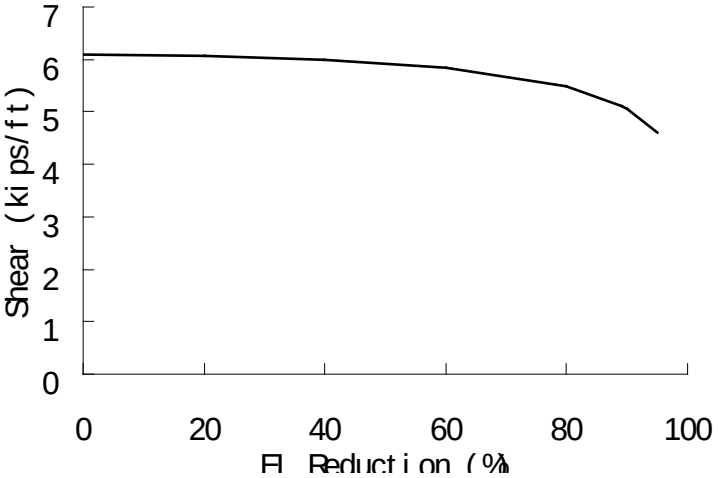

(b) Shear

Figure 3.15: Impact of Cracking on Forces

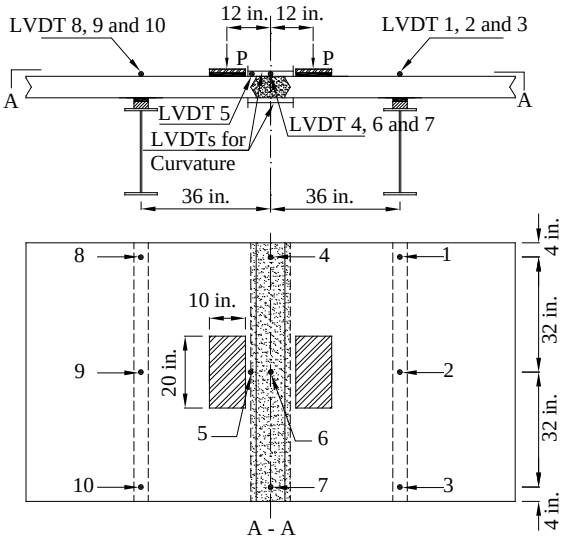

(a) Flexure Static (F-S) Test

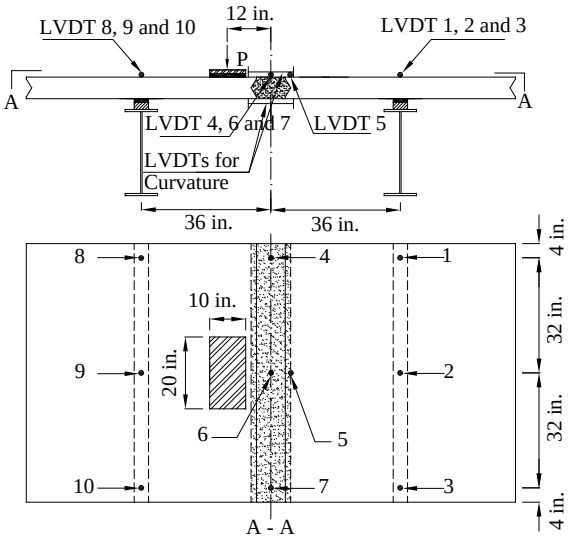

(b) Flexure-Shear Static (FS-S) Test

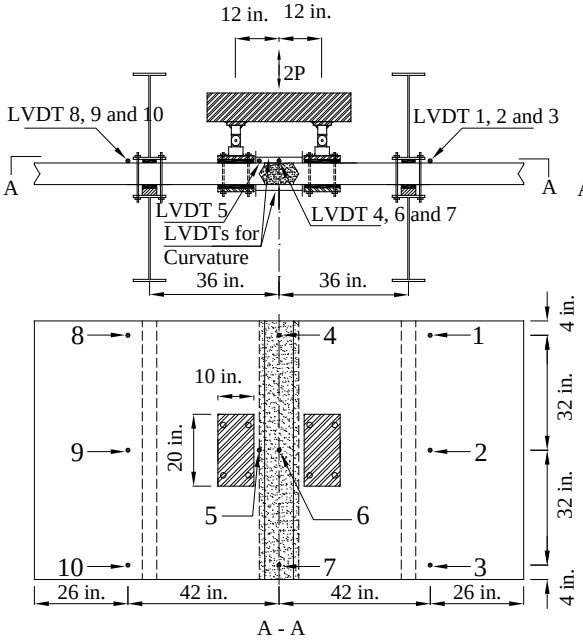

(c) Flexure Fatigue (F-F) Test

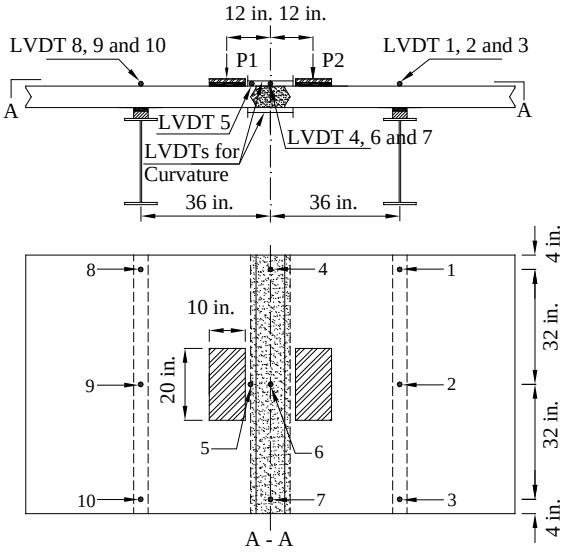

(d) Flexure-Shear Fatigue (FS-F) Test

Figure 3.16. Testing Setup

Figure 3.17. Apparatus Applying Fatigue Forces

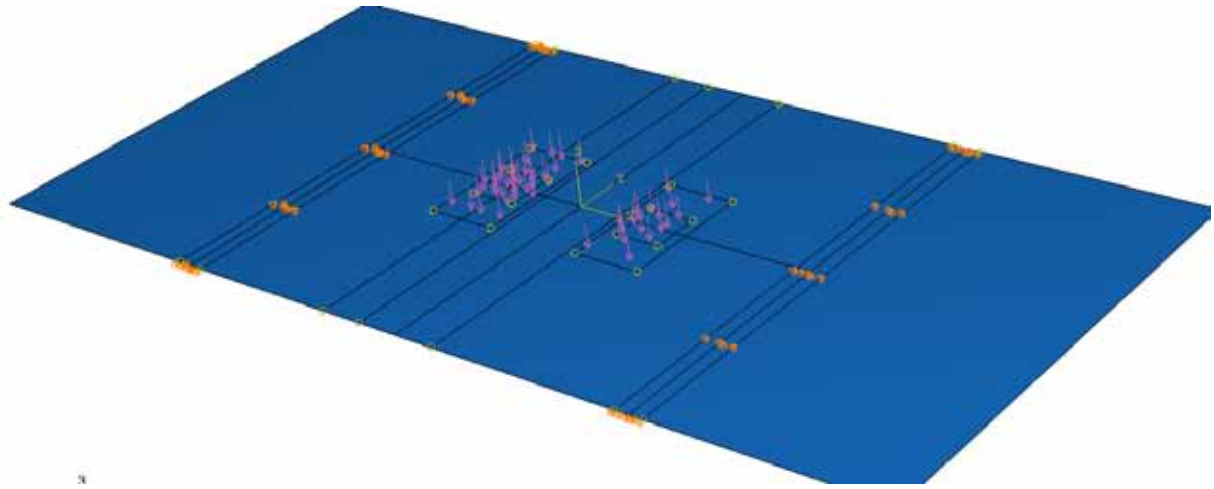

Figure 3.18. FE Model for Loading Determination

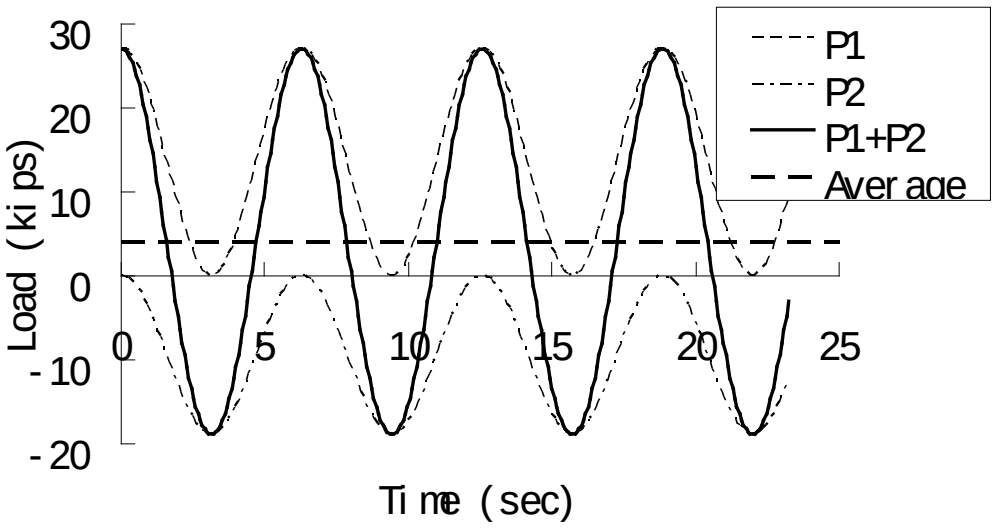

Figure 3.19: History of Fatigue Loading

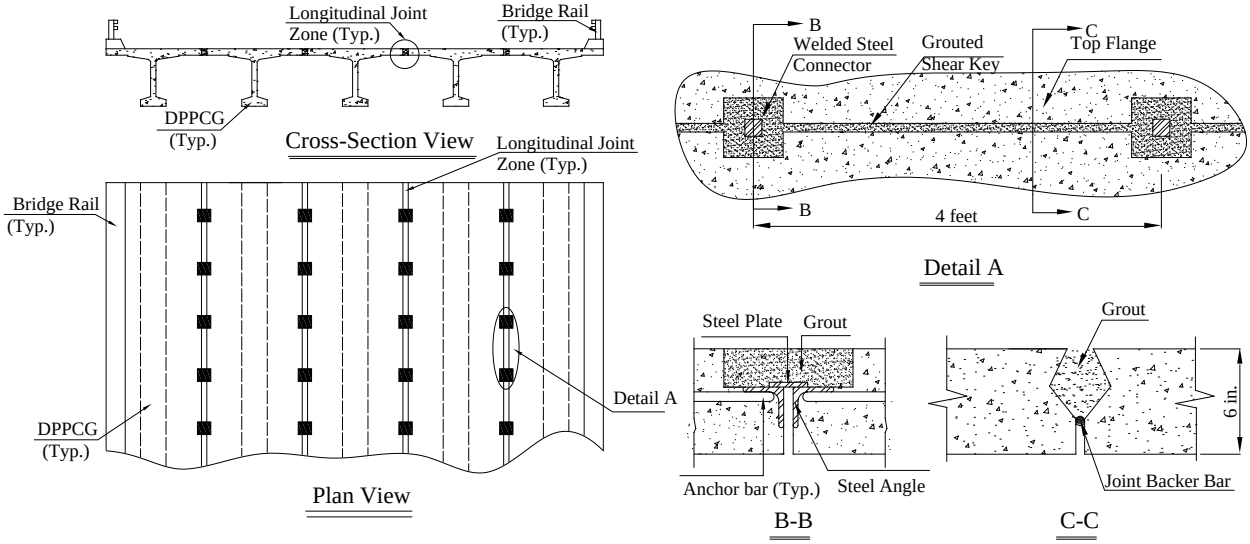

Figure. 3.20. A Typical DBT Bridge Connected by Longitudinal Joints with Welded Steel Connectors

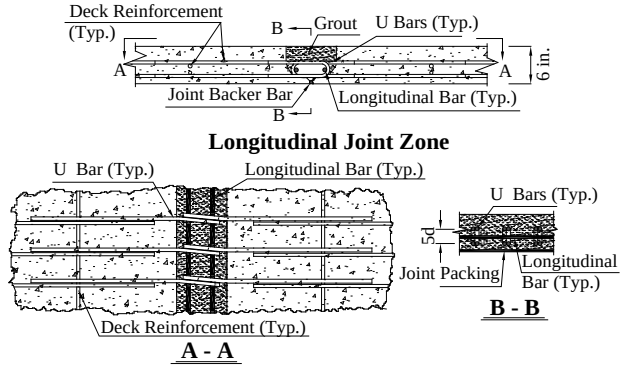

(a): U bar detail

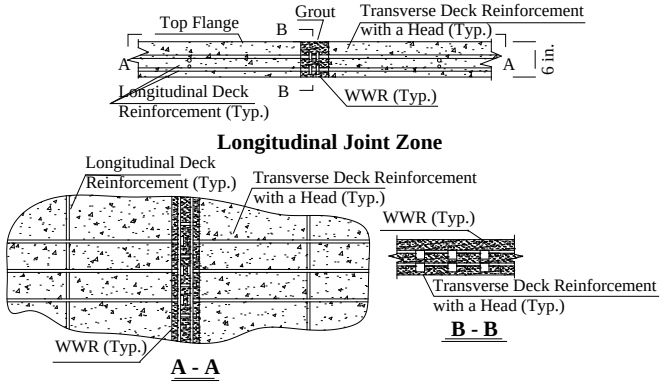

(b): Headed bar detail

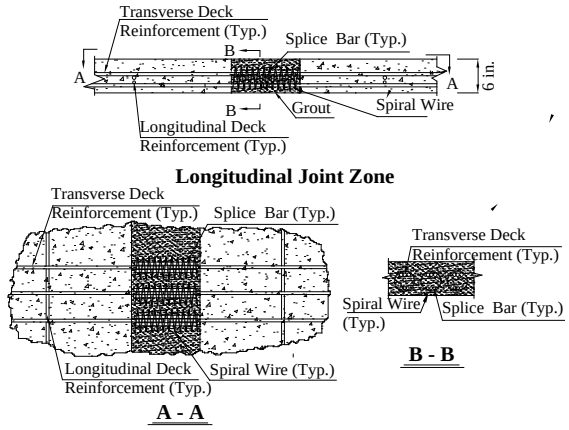

(c): Spiral bar detail

Figure 3.21. Proposed New Joint Details

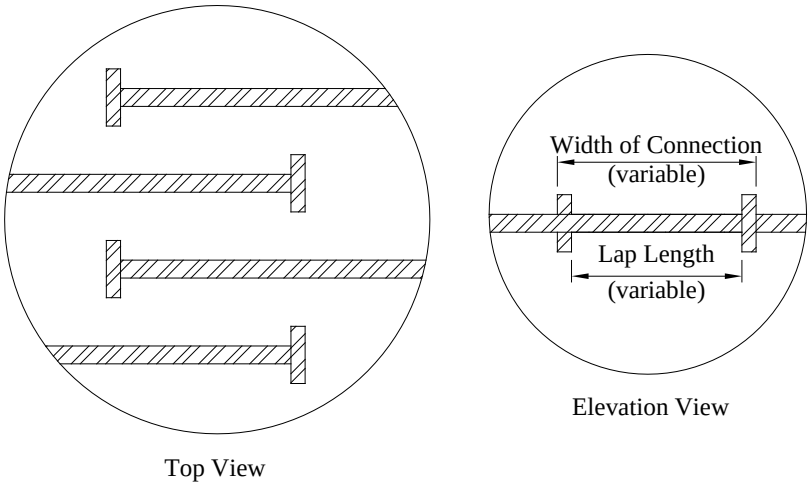

(a): Headed reinforcement connection detail

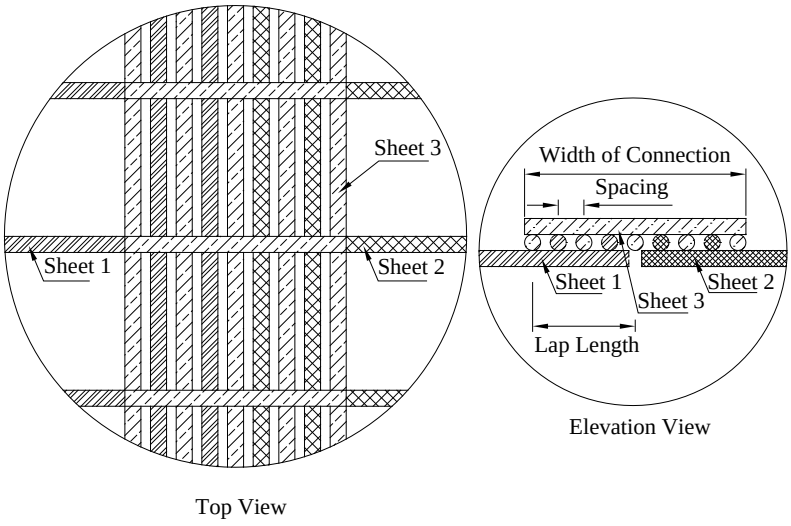

(b): WWR reinforcement connection detail

Figure 3.22. Improved Joint Details

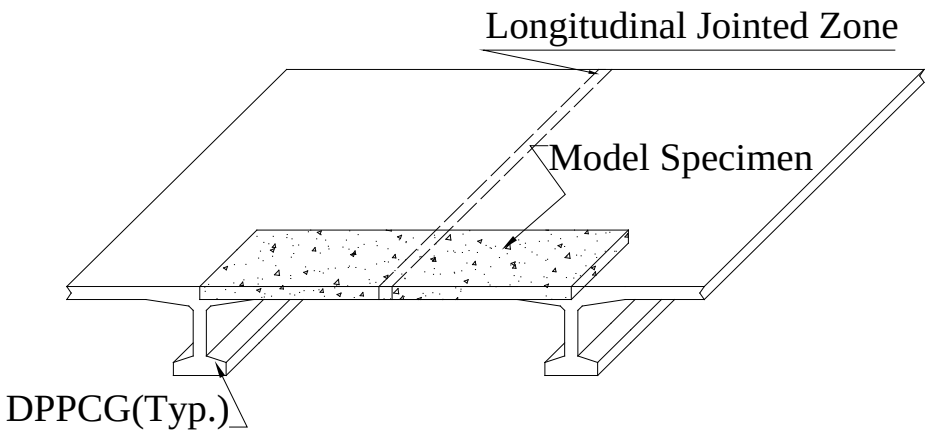

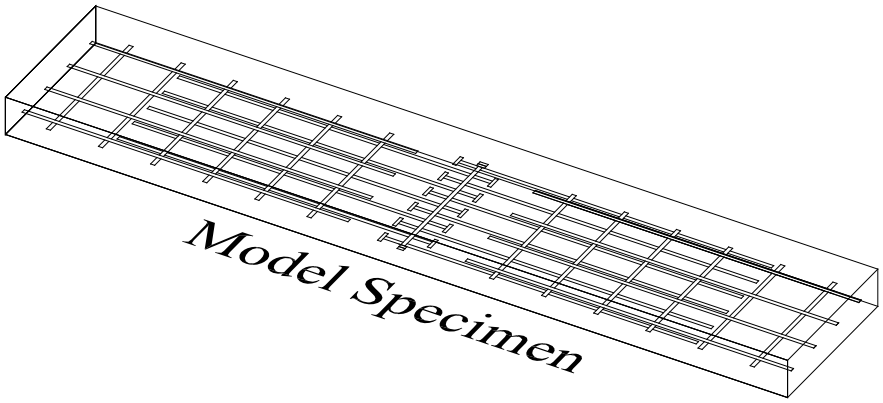

Figure 3.23. Specimen to Evaluate Joint Behavior

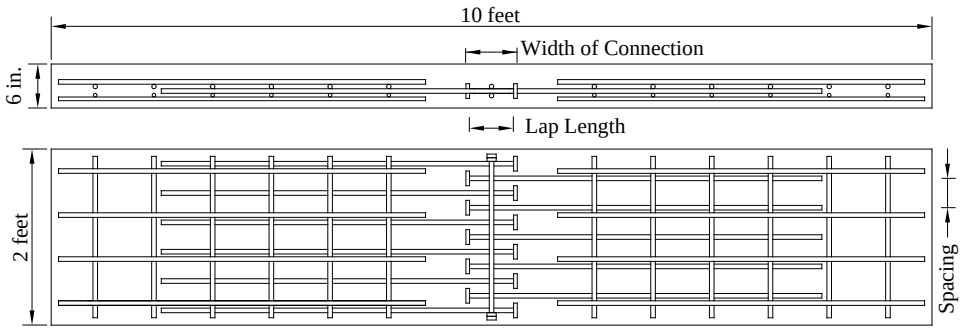

(a): Headed reinforcement connection

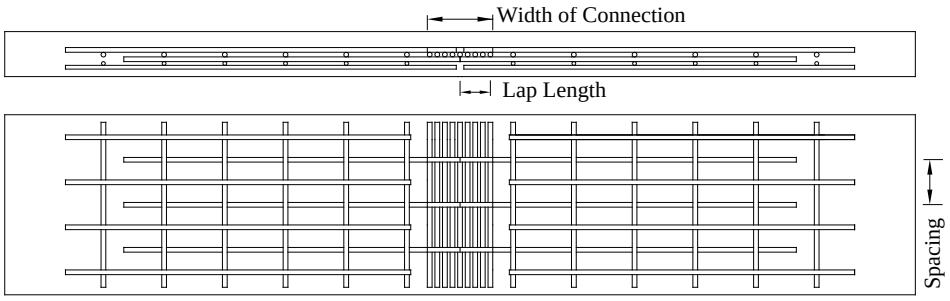

(b): WWR connection

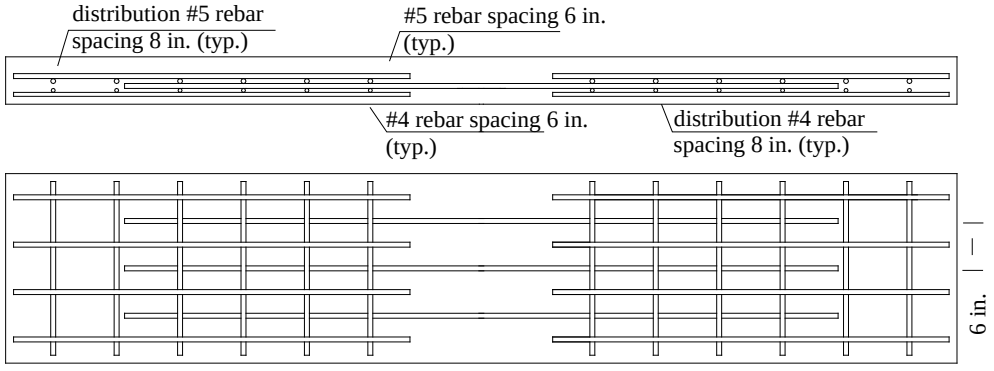

(c): Control beam

Figure 3.24. Three Types of Specimens

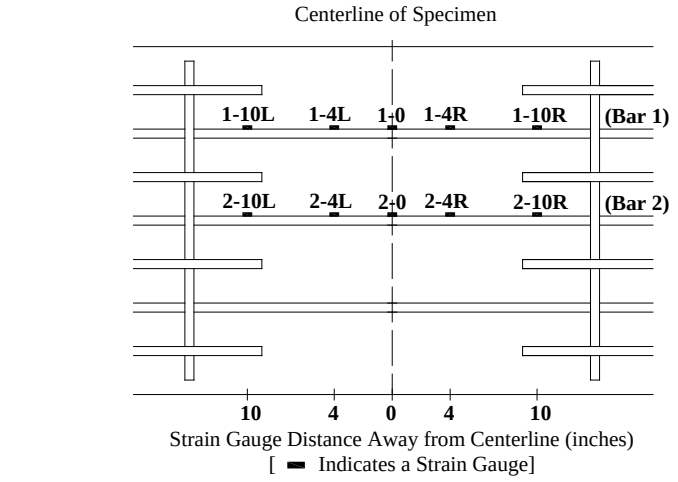

(a): Control specimen

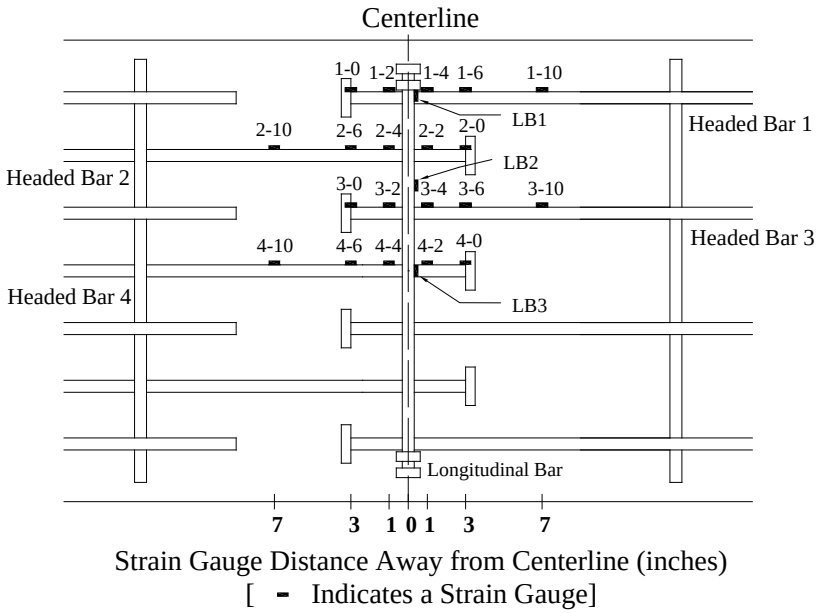

(b): Headed reinforcement specimen

Figure 3.25 Strain Gauge Layout

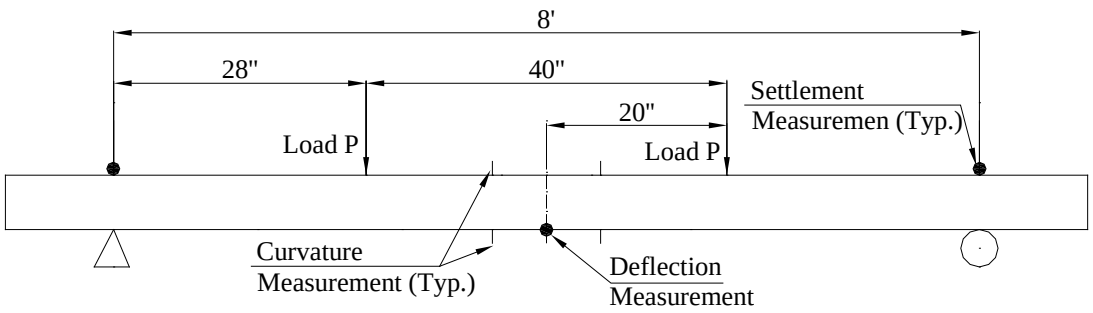

Figure 3.26. Testing Setup

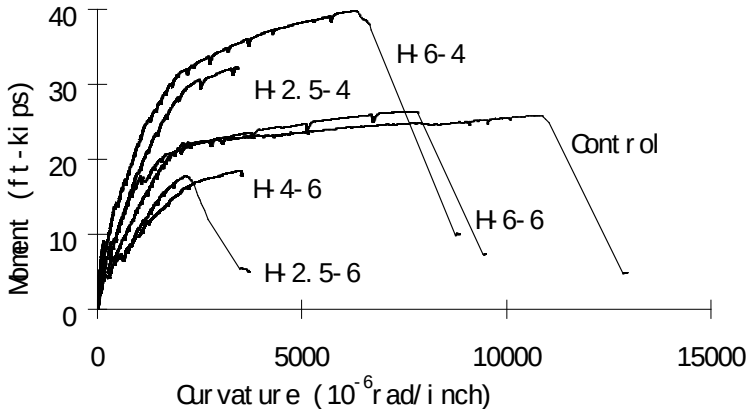

Figure 3.27. Moment Curvature Diagrams for Headed Bar Specimens

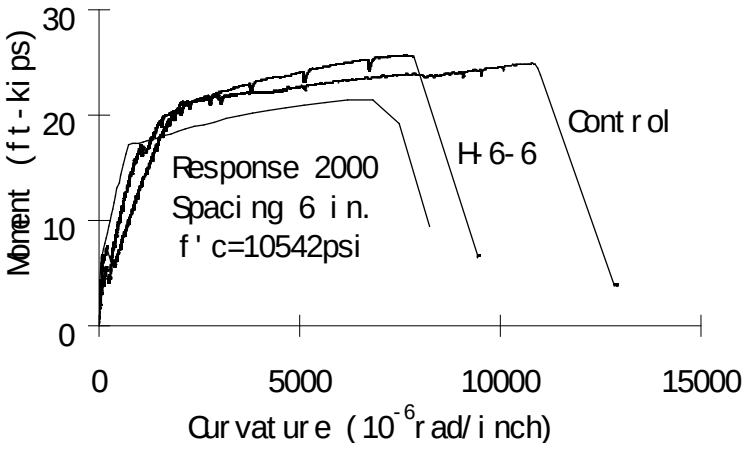

(a): $f_c^{'} = 10{,}542\,psi$

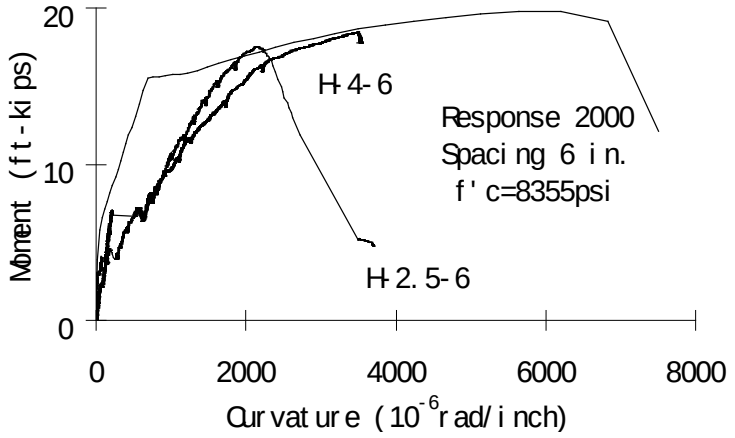

(b): $f_c^{'} = 8{,}355\,psi$

Figure 3.28 Moment Curvature Diagrams for 6 in. Spacing Specimens with Response 2000

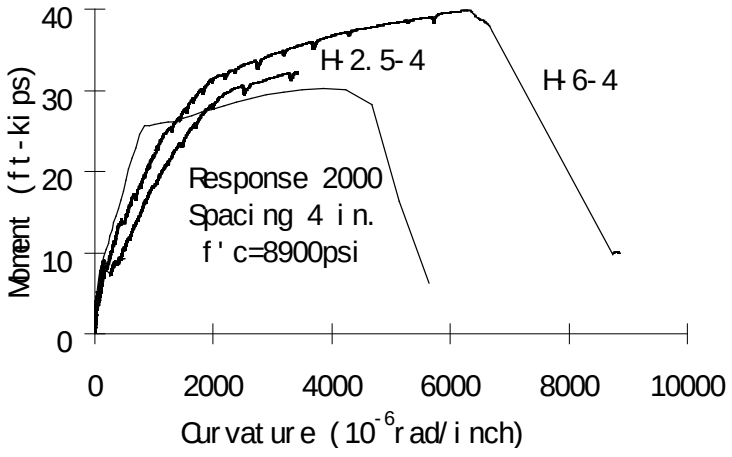

Figure 3.29. Moment Curvature Diagrams for 4 in. Spacing Specimens with Response 2000 Results

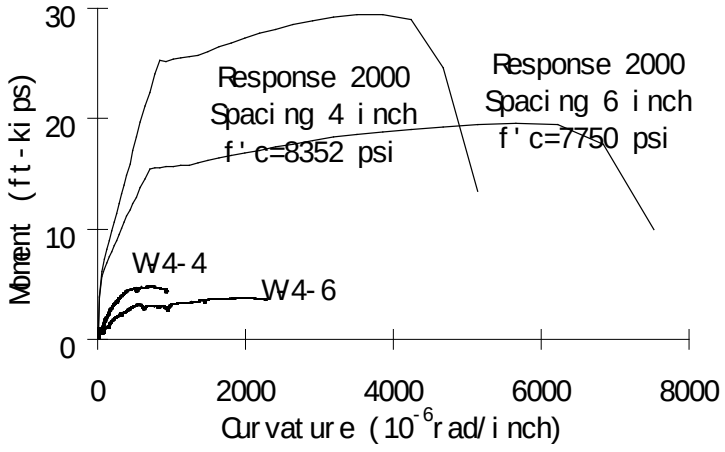

Figure 3.30. Moment Curvature Diagrams for WWR specimens

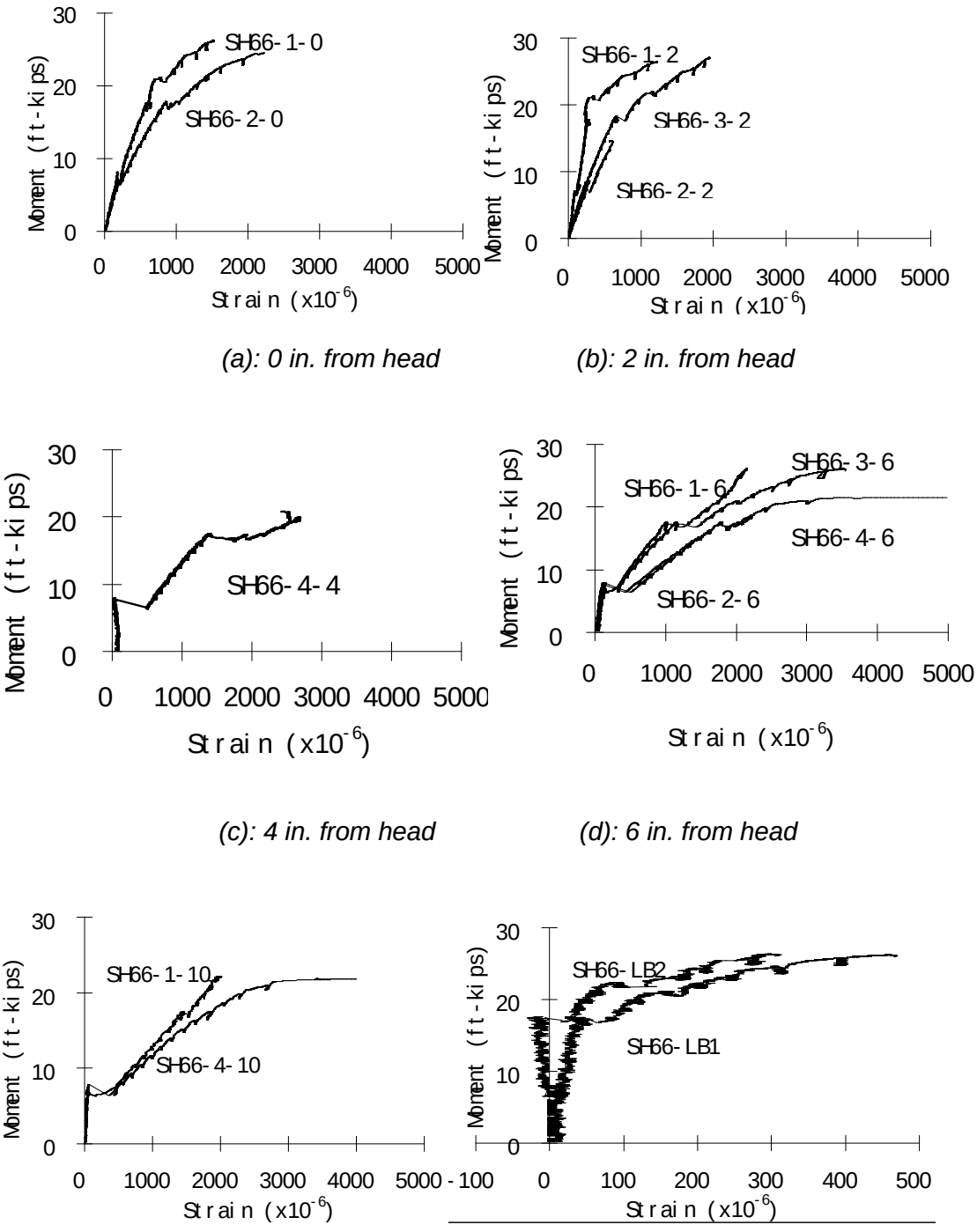

(a): 0 in. from head *(b): 2 in. from head*

(c): 4 in. from head *(d): 6 in. from head*

(e): 10 in. from head *(f): longitudinal bar*

Figure 3.31. Moment vs. Steel Strain Comparison for H-6-6

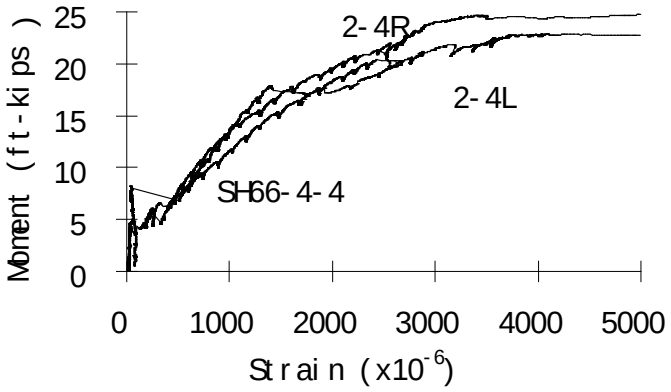

Figure 3.32. Moment vs. Steel Strain Comparison

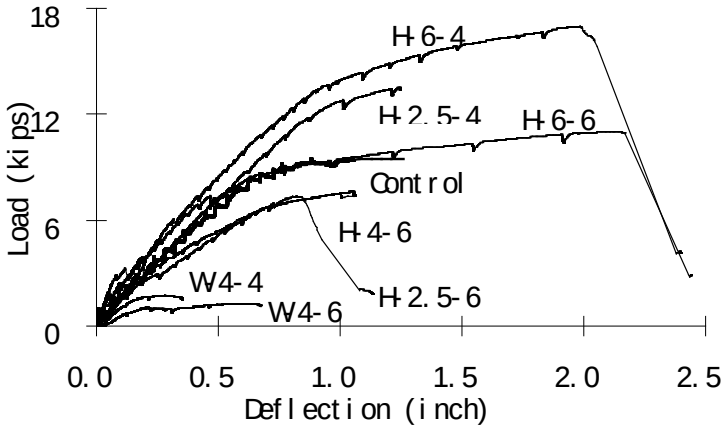

Figure 3.33. Load vs. Deflection Curve

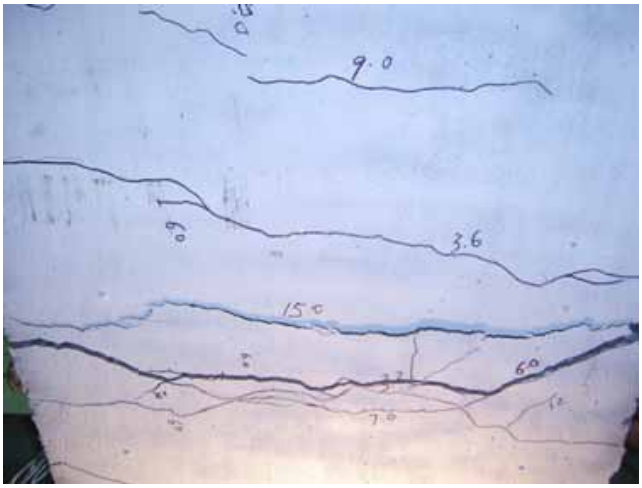

(a): Bottom view

(b): Side view

Figure 3.34. Crack Behavior for Specimen H-2.5-4 and H-2.5-6

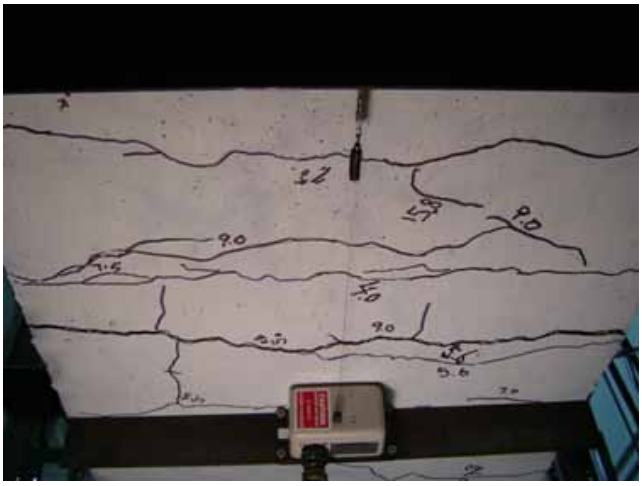

(a): Bottom view

(b): Side view

Figure 3.35. Crack Behavior for Specimen H-4-6

(a): Bottom view

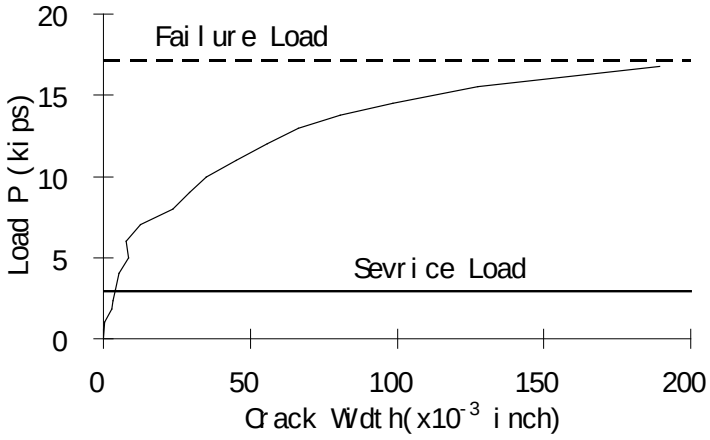

(b): Crack width-load curve

Figure 3.36. Crack Behavior for 6 in. Lap Length Specimen

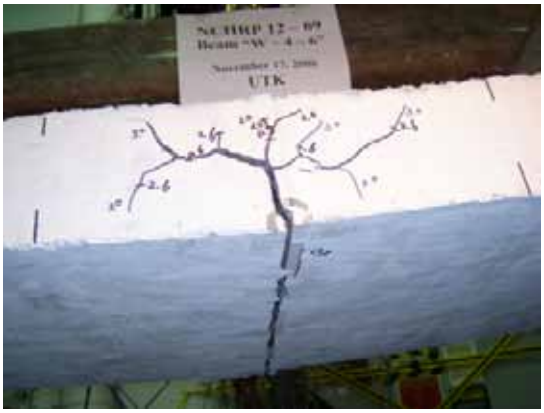

Figure 3.37. A Large Crack Propagating along Midspan in WWR Specimens

(a): Ductile failure

(b): Brittle Failure

Figure 3.38. Failure Types

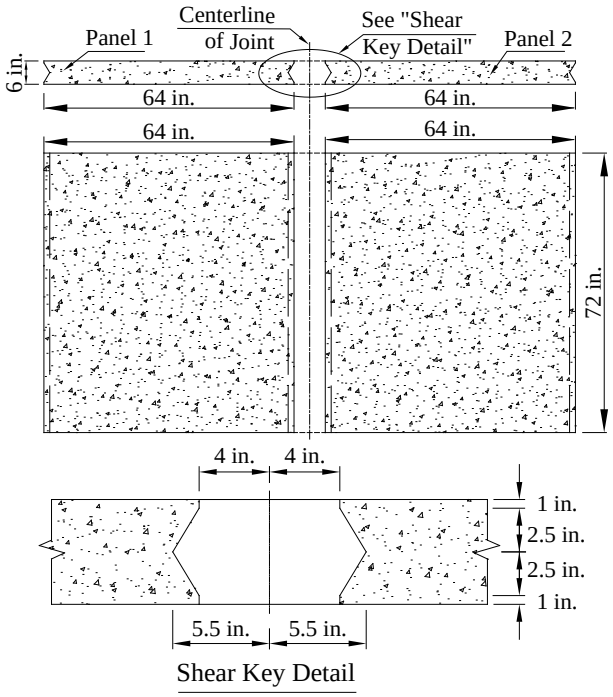

Figure 3.39. Dimension of Slab Specimen

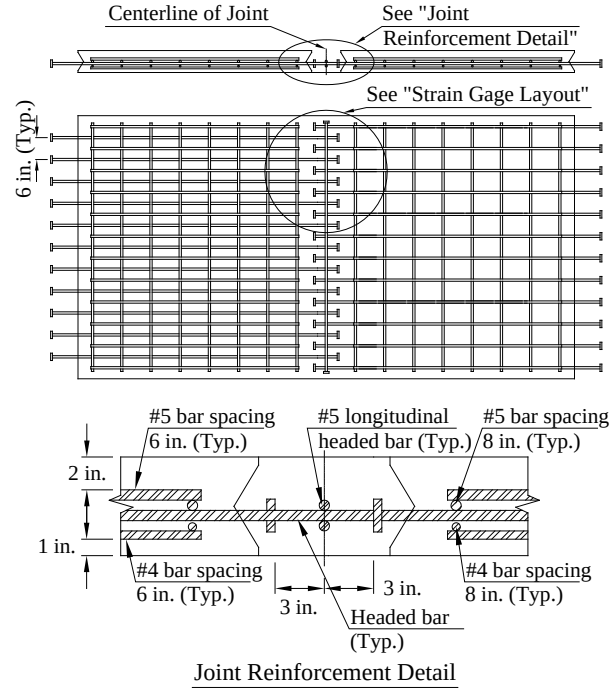

Figure 3.40. Reinforcement Layout in Slab

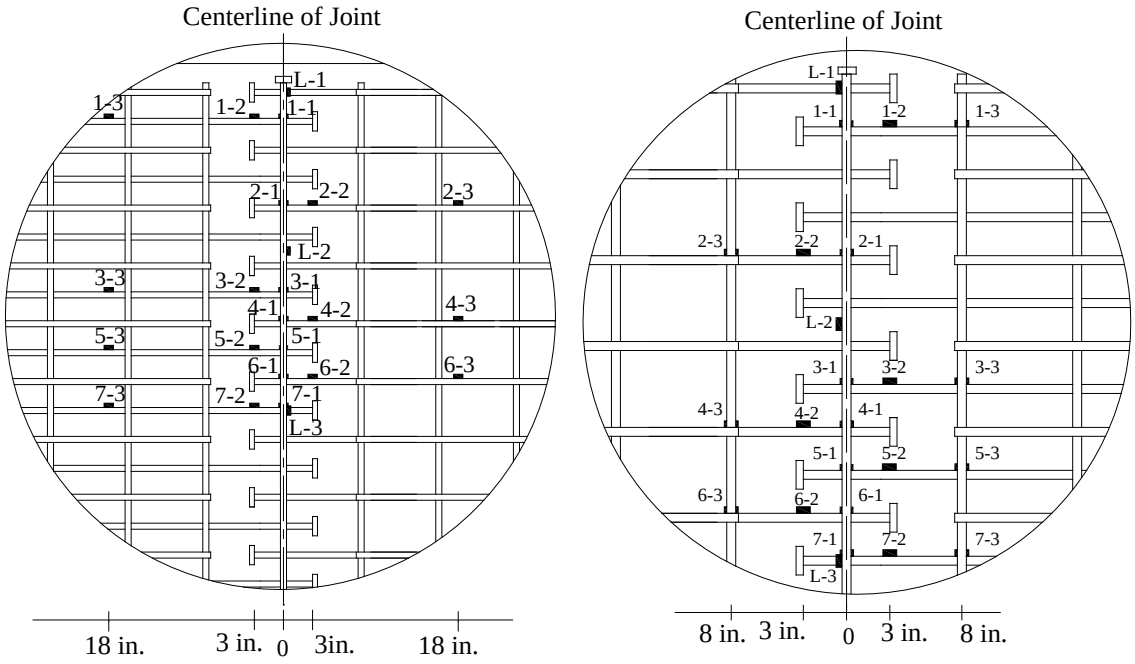

Figure 3.41. Strain Gage Layout

(a): Before Pouring (b): After Pouring

Figure 3.42. Panel Fabrication

(a): Before Sandblasting *(b): After Sandblasting*

Figure 3.43. Profile of Joint Surface

(a): Before Grouting *(b): After Grouting*

Figure 3.44. Slab Specimen

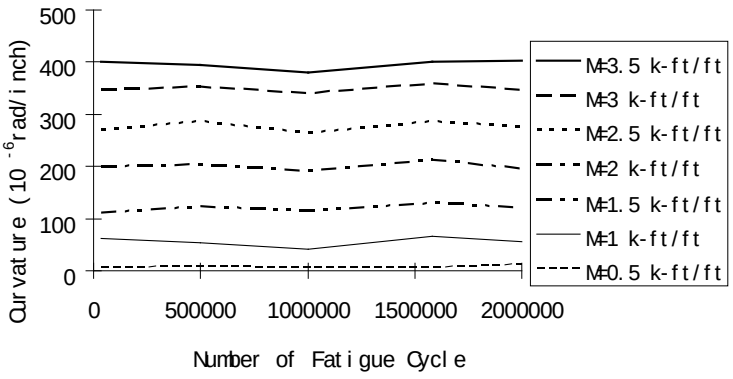

(a) F-F Specimen

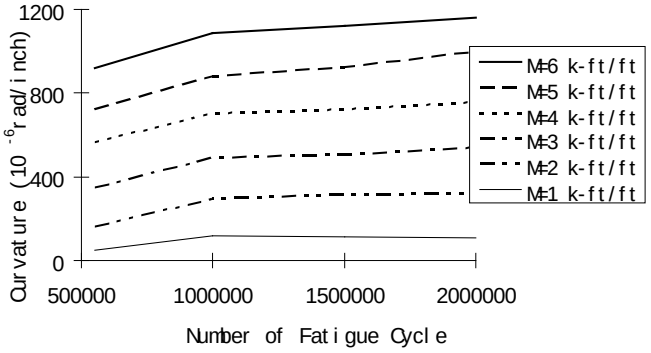

(b) FS-F Specimen under P1

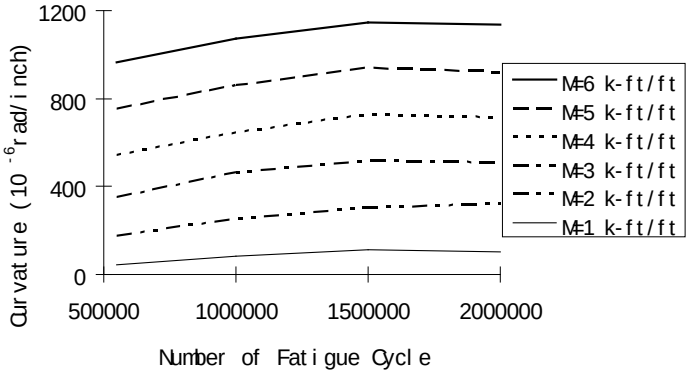

(c) FS-F Specimen under P2

Figure 3.45. C-N Curve

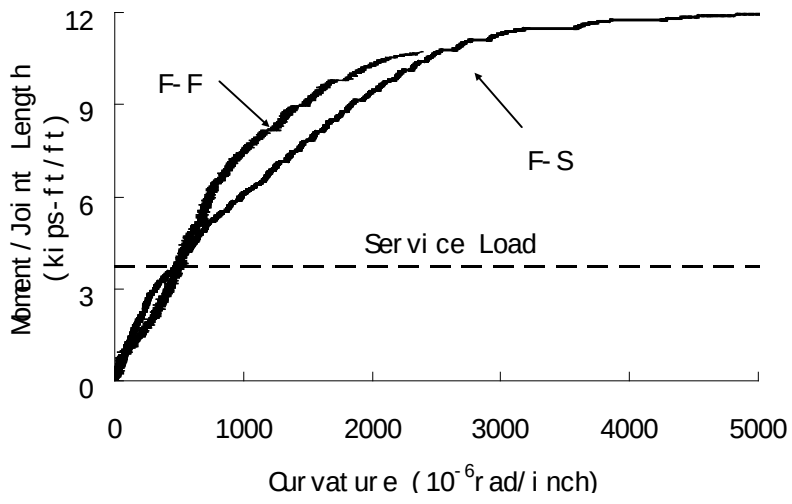

(a) Flexure Tests

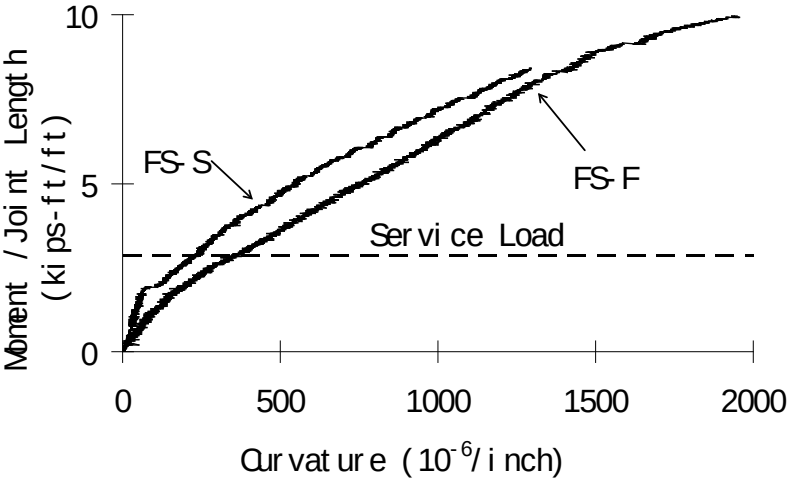

(b) Flexure-Shear Tests

Figure 3.46. Moment-Curvature Curve

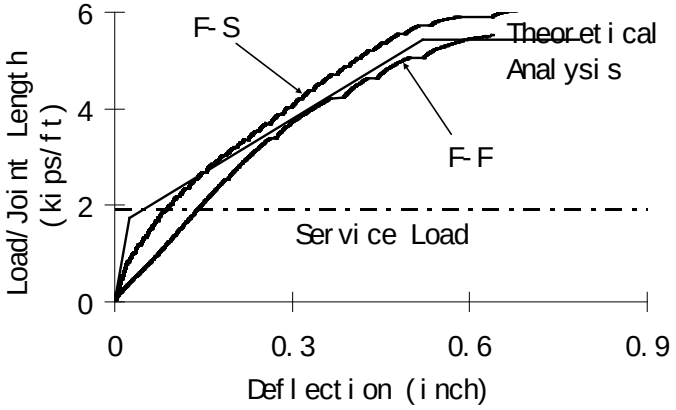

(a) Flexure Tests

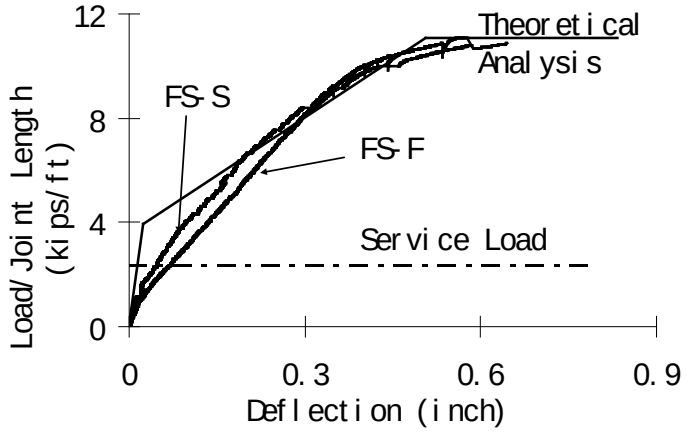

(b) Flexure-Shear Tests

Figure 3.47. Load-Deflection Curve

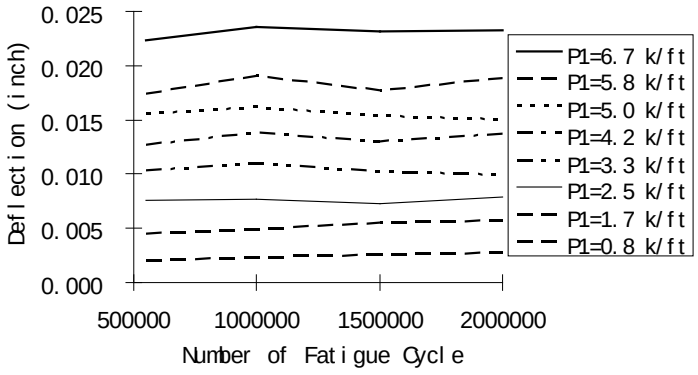

(a) FS-F Specimen under P1

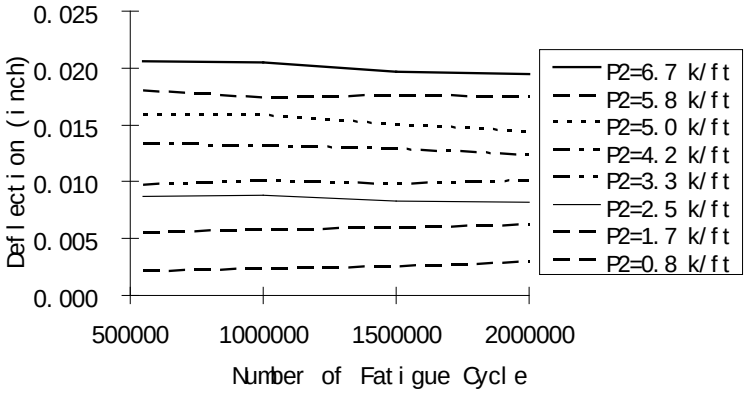

(b) FS-F Specimen under P2

Figure 3.48. RD-N Curve

Figure 3.49. Cracks at Interface of the Joint

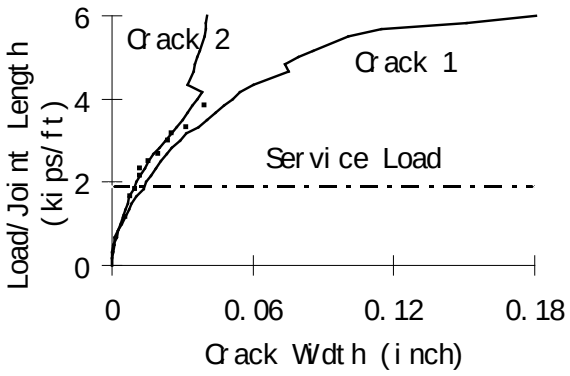

(a) F-S Specimen

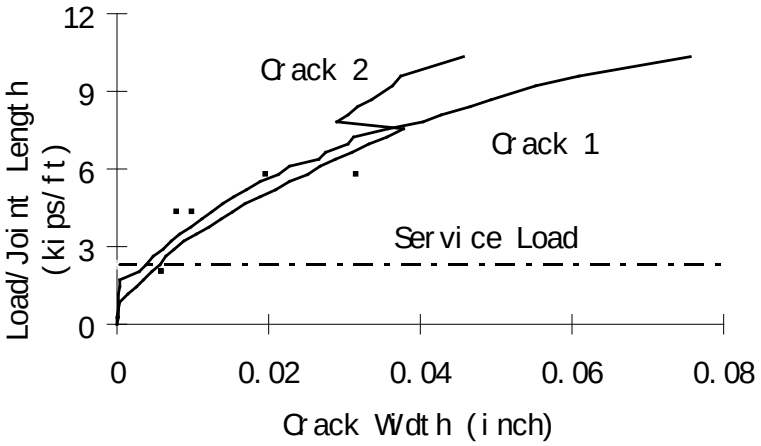

(b) FS-S Specimen

Figure 3.50. Load-Crack Width Curve

Figure 3.51. A Flexural-Shear Crack across Joint Zone

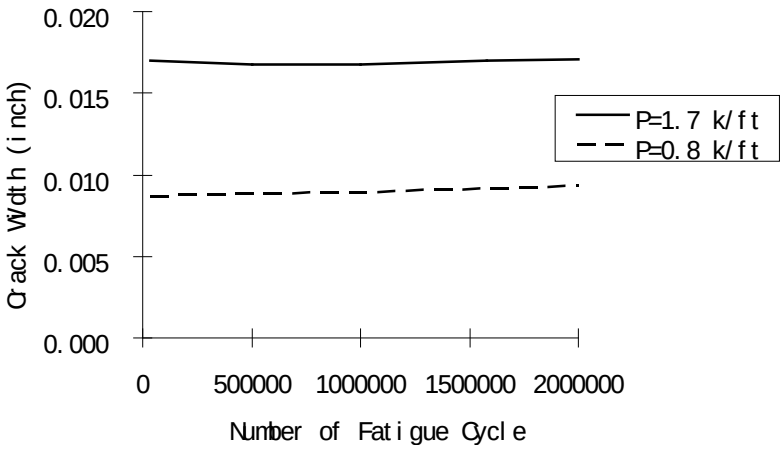

(a) F-F Specimen

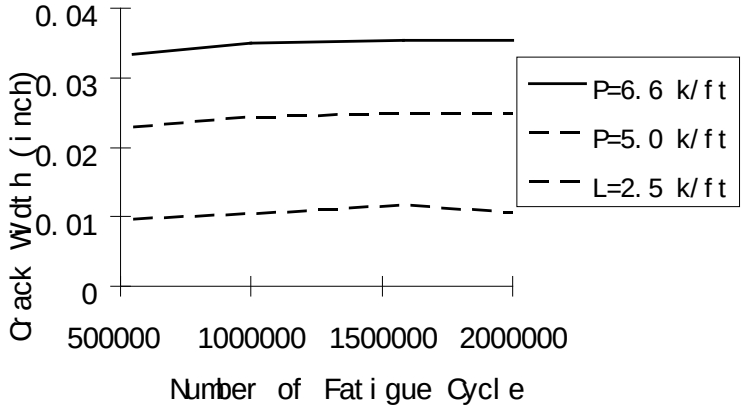

(b) FS-F Specimen

Figure 3.52 CW-N Curve

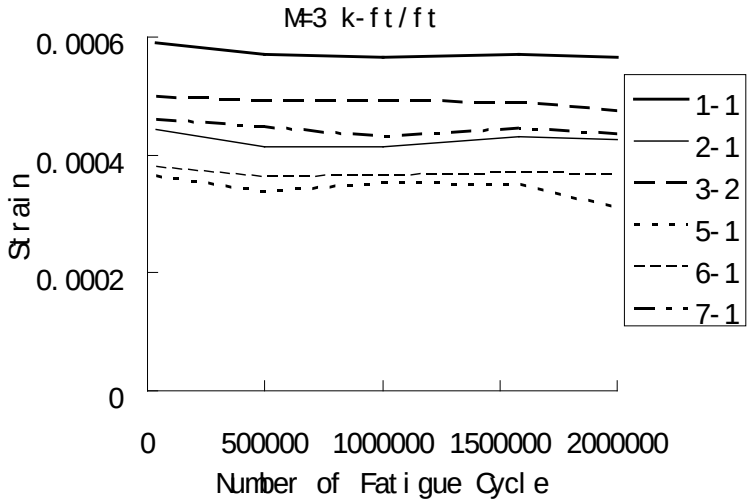

(a) F-F Specimen

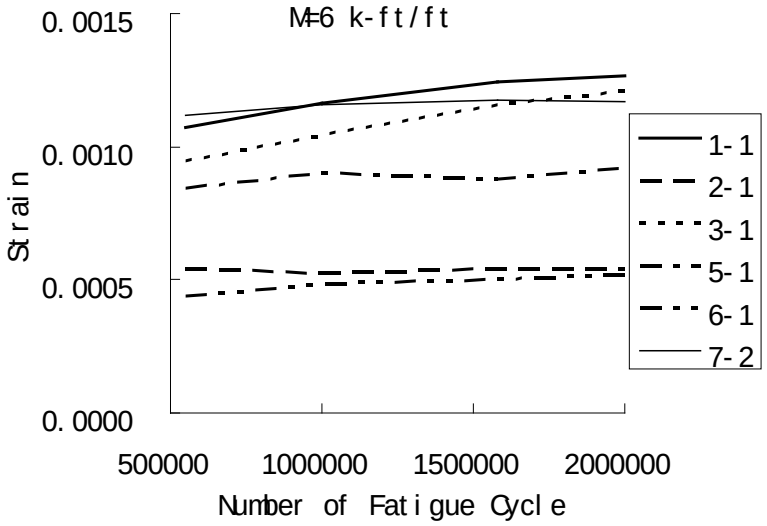

(b) FS-F Specimen

Figure 3.53. S-N Curve

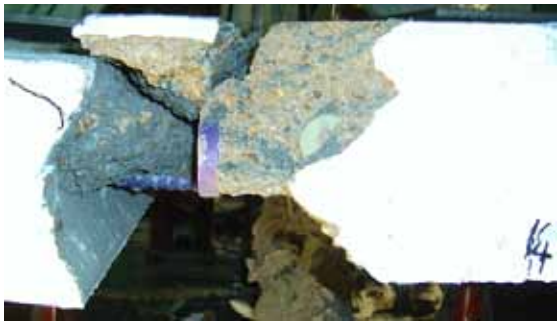

(a) F-S Specimen

(b) FS-S Specimen

(c) F-F Specimen

(d) FS-F Specimen

Figure 3.54 Specimen Failures

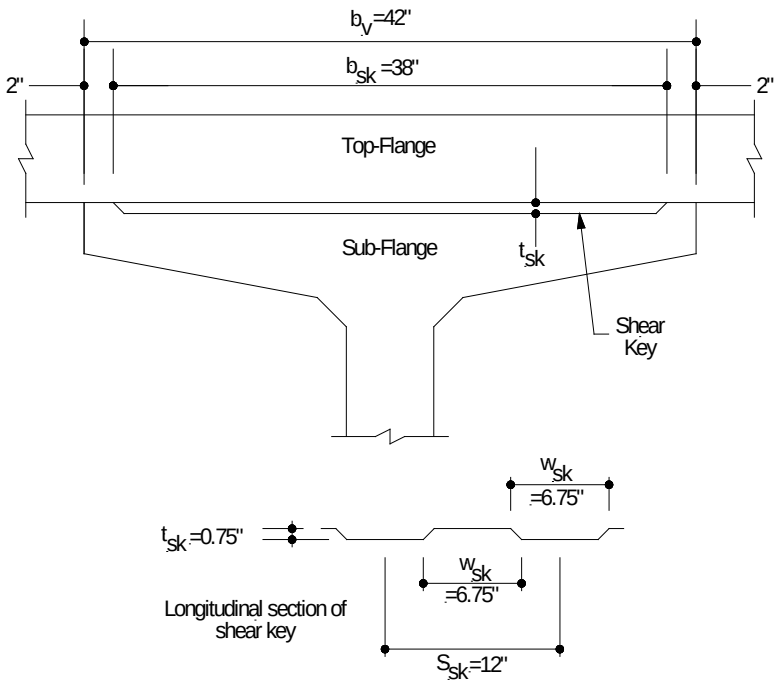

Figure 3.55 Shear Key Dimensions for Optimized Section.

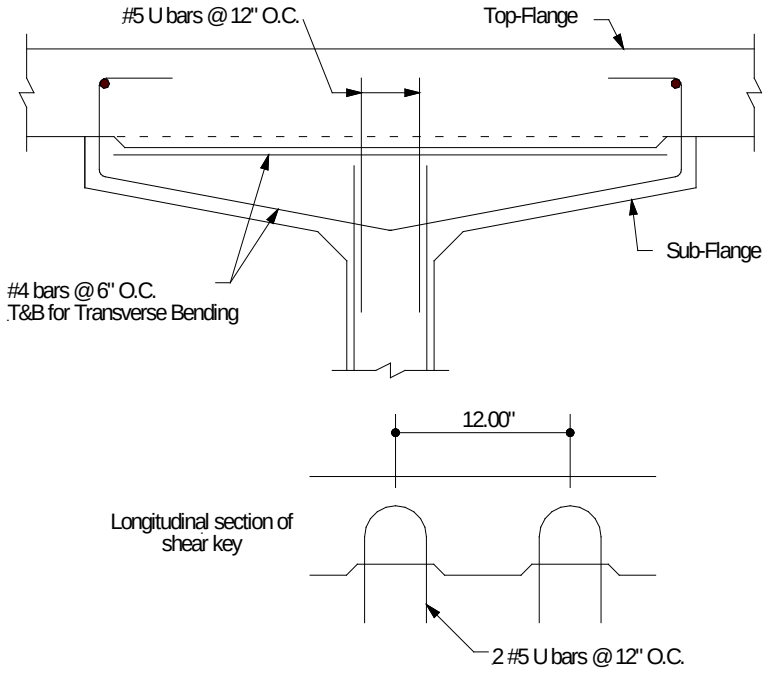

Figure 3.56 Horizontal Shear Reinforcement for Optimized Section.

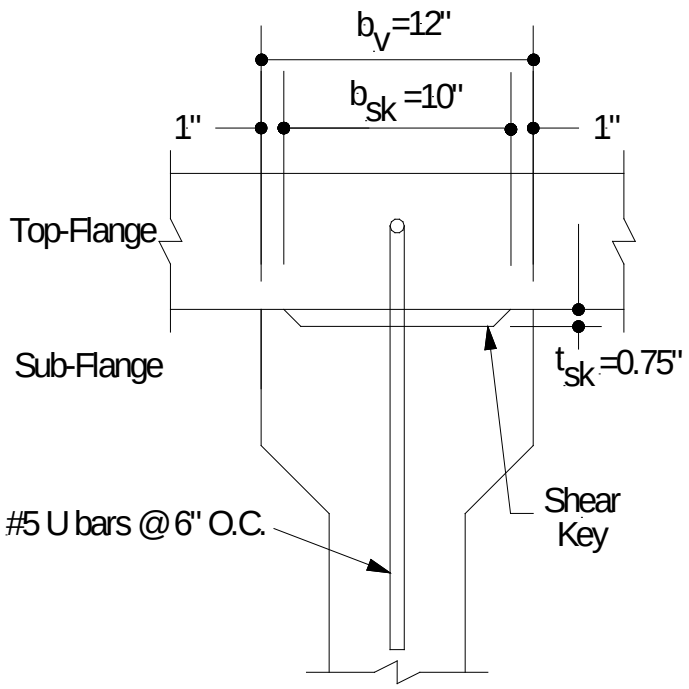

Figure 3.57 Shear Key Dimensions for AASHTO Type II Section.

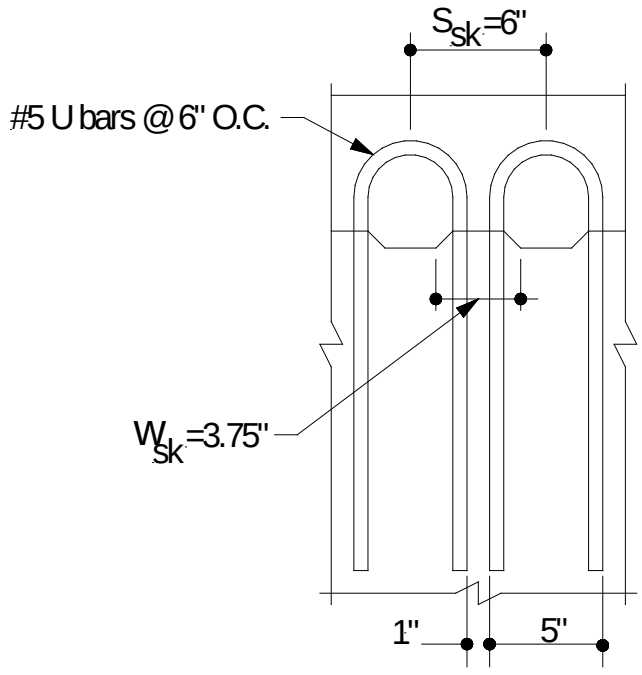

Figure 3.58. Horizontal Shear Reinforcement for AASHTO Type II Section.

CHAPTER 4

CONCLUSIONS AND SUGGESTED RESEARCH

CONCLUSIONS

The primary objective of NCHRP Project 12-69 is to develop guidelines for design and construction for long-span decked precast, prestressed concrete girder bridges. These guidelines will provide highway agencies with the information necessary for considering a bridge construction method that is expected to reduce the total construction time, improve public acceptance, reduce accident risk, and yield economic and environmental benefits.

In developing these guidelines, the NCHRP Project 12-69 had two goals. The first was to provide guidelines for design, construction, and geometry control based on successful methodology currently being used. To date, use of long-span decked precast, prestressed concrete girder bridges has mostly been limited to the northwest region of the United States where this type of bridge has been used very successfully. The first goal of the NCHRP project is to document the successful methodologies. This has been accomplished by interviews with knowledgeable designers and precasters, by collecting and reviewing existing design and construction practices, and presenting the collected information within the Guidelines for Design and Construction of Decked Precast Prestressed Concrete Girder Bridges document provided as a separate report for this project.

The second goal was to develop an improved longitudinal joint system. Currently, the most widely used longitudinal connection between precast concrete members is a combination of a continuously grouted shear key and welded connectors spaced at intervals from 4 ft to 8 ft on-center. This type of connection is intended to transfer shear and prevent relative vertical displacements across the longitudinal joints.

Implications from a survey of issues performed as part of the NCHRP Project12-69 indicated that, if this type of joint is properly designed and constructed, the performance can be good to excellent. Therefore, the guidelines for methodology currently being used address this type of connection. However, there is also a perception of cracking and leakage with this type of longitudinal joint. Therefore, an improved type of joint was a second goal within the NCHRP Project 12-69.

This goal was accomplished with a series of studies that determined:

- Key issues include the need for re-decking and the durability of longitudinal joints.

- The concept of the debonded shear key and the cast-in-place deck as described in NCHRP Report 407 (3) is the current state-of-art for replacement of decks on concrete girders that has been sufficiently tested and documented. Therefore, it is the appropriate system to be incorporated in the development of optimized family of girder sections

- The girder shape shown in Figure 4.1 and 4.2 with the modified NU bulb configuration shown in Figure 4.3 d) is structurally efficient and facilitates future re-decking of the system. The study focused on the decked bulb tee (DBT) because of the structural efficiency of this section and because this is the section that is most common in current use. The section includes a 6 in. top flange thickness based upon the historical thickness of the top flange of conventional decked bulb tee girders to minimize weight and a 42 in. sub-flange to facilitate re-decking. However, the analyses in this study show that the efficiency of these girders is decreased when the re-decking option is considered. To use the re-decking option, a two-stage casting procedure is required and to attain the same span length requires additional prestressing.

- A primary strength of the use of decked girders is speed of construction, particularly for the bridge replacement and repair projects, which has arisen as a much more critical issue than ever before. Therefore, when re-decking is needed it may be much more efficient, expeditious, and economical to replace the entire girder rather than replace just the deck. The cost of re-decking the system versus total superstructure replacement should be evaluated prior to using the re-decking option.

- To develop a more durable longitudinal joint, analytical studies were first carried out using the girder shape shown in Figure 4.1 and 4.2 to determine maximum service loads on the joint for the range of bridge parameters that are feasible for this type of bridge including girder depth, span, girder spacing, and skew. These studies indicated that:

- For camber leveling forces the maximum shear will occur in the shorter spans of the span range for a particular girder depth, and the maximum camber leveling shear stress increases with the increase of the skew angle. Based on the analyses, a shear in the longitudinal joint of 1.5 kips/ft is a maximum initial shear force needs to be considered in design of the camber leveling procedures. However, with consideration for the effects of creep, a shear force 0.5 kips/ft was determined as a reasonable upper bound long term camber leveling shear force transferred across the joint to combine with the effects of service live load.

- The camber leveling study also determined that the calculated maximum change in stresses in the bottom bulb of the girders due to camber leveling forces were nominally high (a maximum calculated of approximately 890 psi). It was also noted that an allowable of 0 tensile stress is commonly used in the design of decked girders under service load. This criterion allows a margin of tensile capacity to help compensate for camber leveling tensile stresses. Based on this observation and the nominally high calculated flexural tensile stresses in this camber leveling study, an allowable of 0 tensile stress is included in the design guidelines developed in this project.

- For HL-93 live load in an uncracked deck, the maximum positive moment is 7.922 kips-ft/ft; the maximum negative moment is -2.152 kips-ft/ft; the maximum shear is 6.091 kips/ft. However, at these levels of load, the deck is expected to crack at the longitudinal joints. Cracking would be expected even if the deck were monolithic concrete. After cracking, the maximum positive moment is 4.001 kips-ft/ft; the maximum negative moment is -1.137 kips-ft/ft; the maximum shear is 5.056 kips/ft. The maximum positive moment, negative moment and shear in the longitudinal joint under fatigue live load HL-93 was 2.326 kips-ft/ft, -0.453 kips-ft/ft and 2.542 kips/ft respectively. These forces combined with the camber leveling shear discussed above were used to determine the fatigue loading demand for full scale panel test specimens.

- To continue to develop a more durable longitudinal joint, experimental studies were then carried out including a study to define potential improved longitudinal joint systems, laboratory testing of trial joints, and further laboratory testing of a selected trial joint. The final test series included full scale panel tests with static and fatigue flexure and flexure-shear loading of the trial longitudinal joint details shown in Figure 4.4and 4.5. The details include headed reinforcement bars lap spliced and grouted within a narrow joint preformed into the longitudinal edges of the precast deck portion of the precast girders These studies indicated that the improved longitudinal joint detail has sufficient strength, fatigue characteristic, and crack control for the maximum loads determined from the analytical studies and therefore is a viable connection system to transfer the forces between the adjacent decked bulb tee (DBT) girders.

SUGGESTED FURTHER RESEARCH

Based on the full-scale panel test results, the improved longitudinal joint detail is a viable connection system for decked bulb tee (DBT) girders. As a next step, construction and monitoring of a prototype bridge to demonstrate constructability and durability may be advisable.

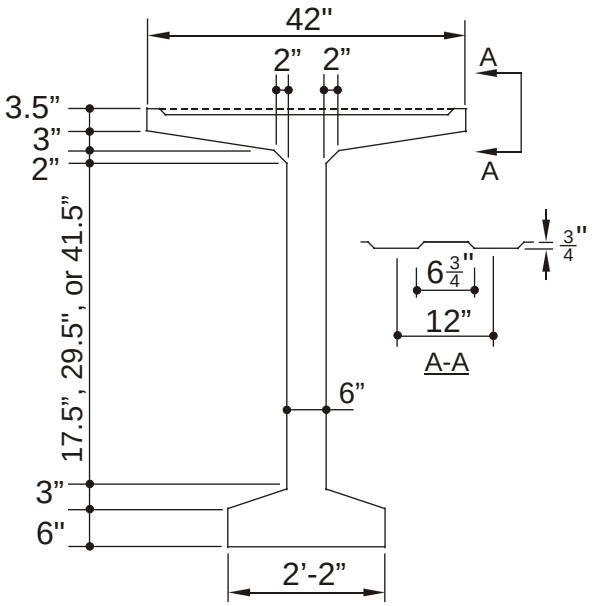

Figure 4.1. Proposed Girder: Stage 1 of Casting.

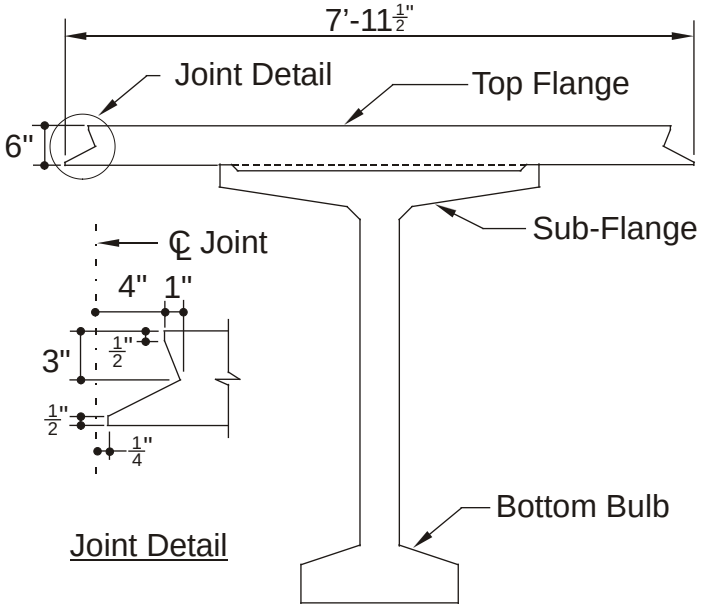

Figure 4.2 Proposed Girder: Stage 2 of Casting.

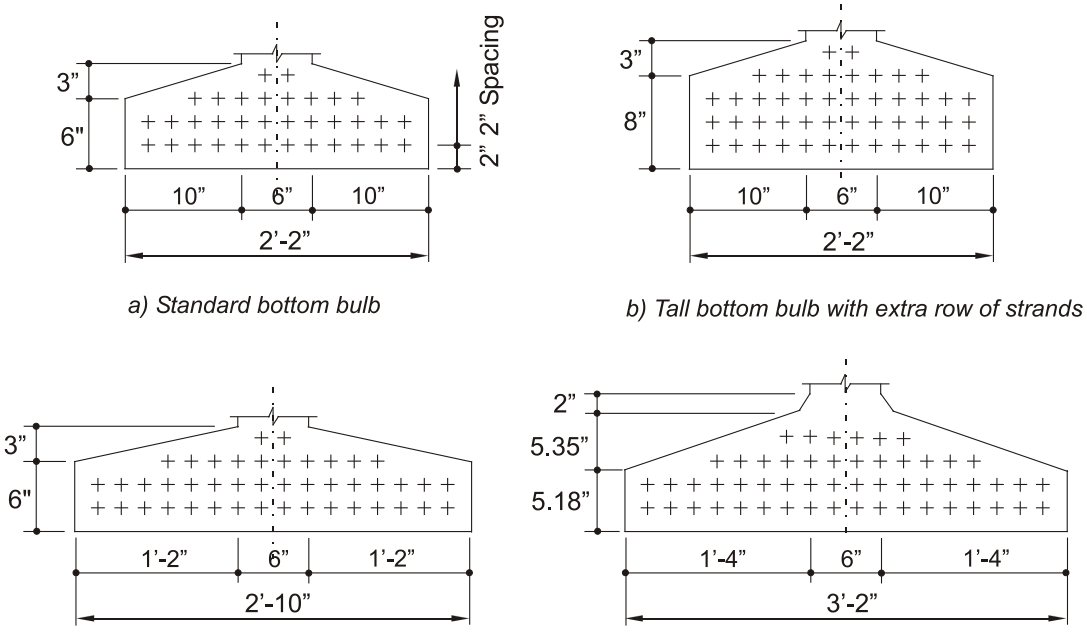

Figure 4.3 Bottom Bulb Configurations

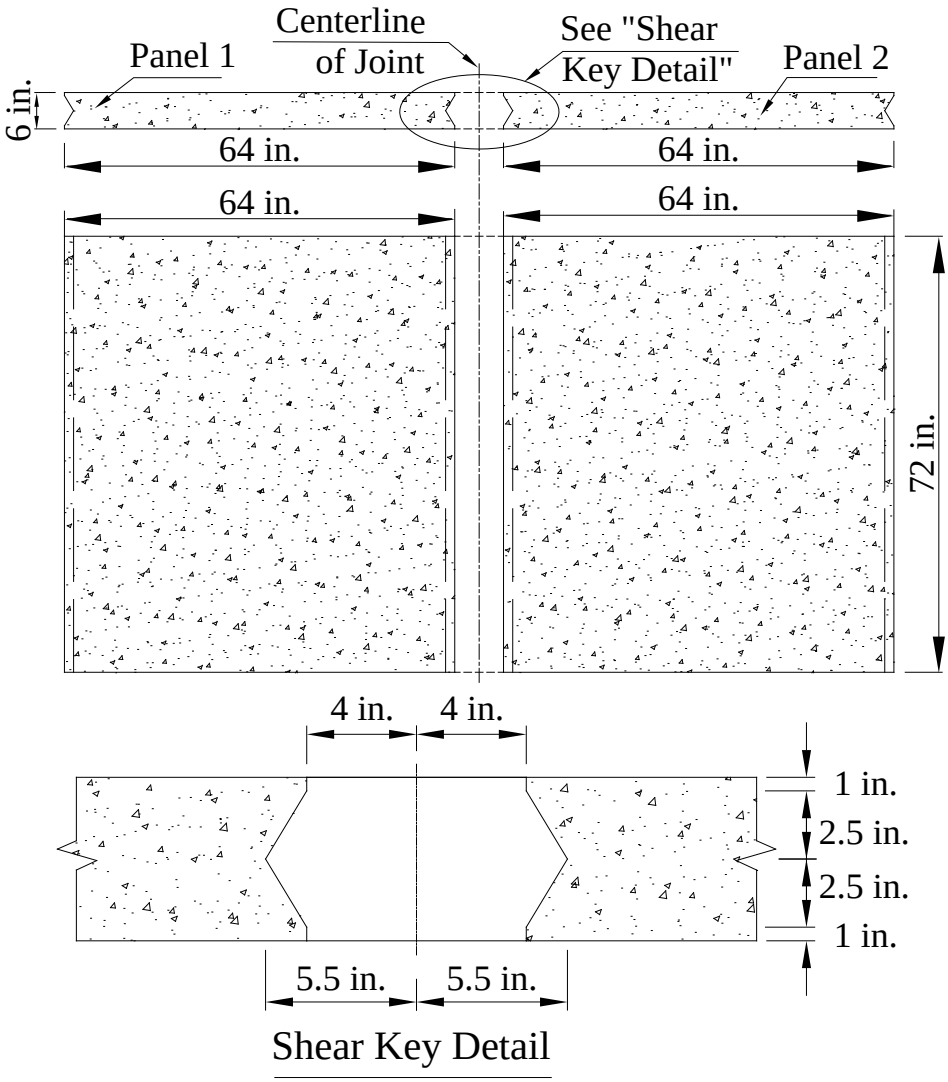

Figure 4.4 Dimension of Slab Specimen

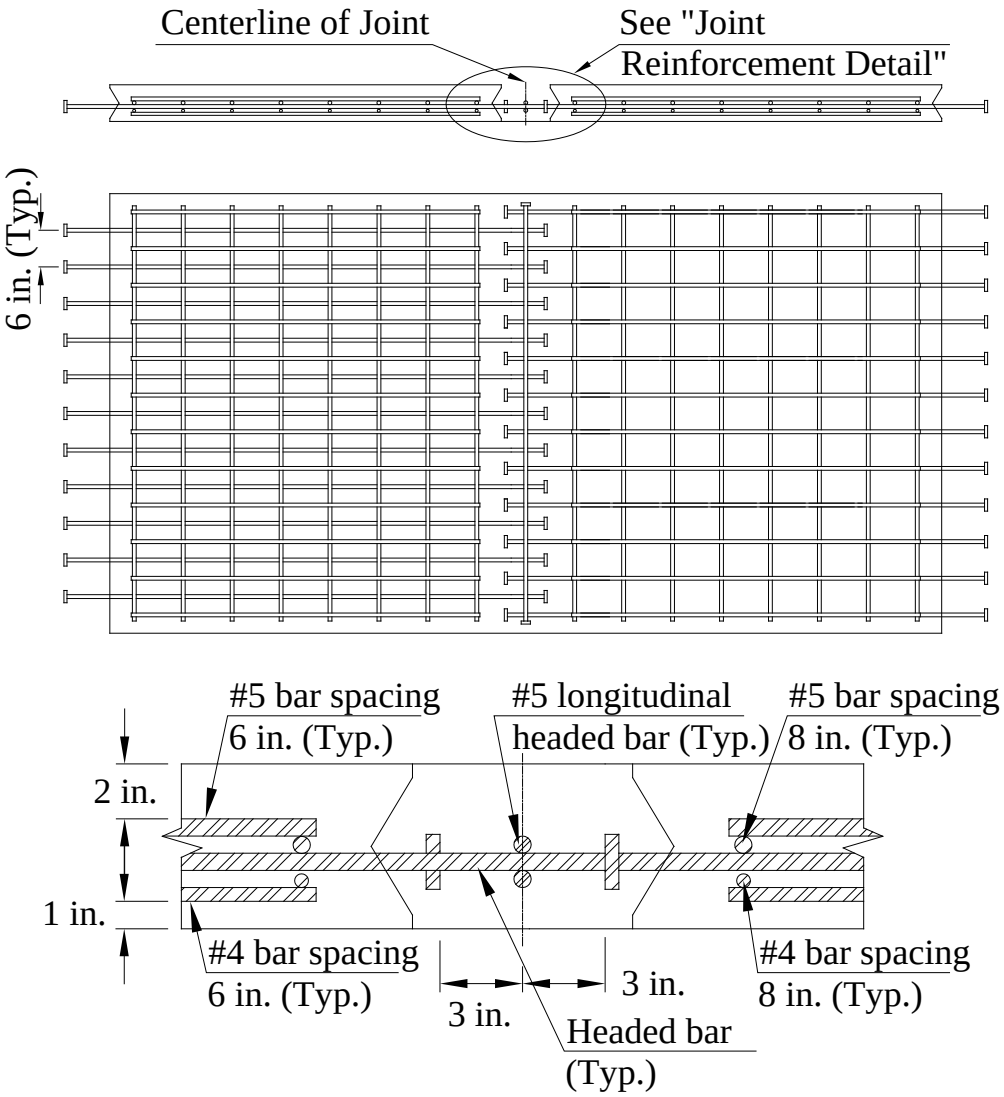

Figure 4.5. Reinforcement Layout in Slab

REFERENCES

1. Mehrabi, A.B., “Work plan,” NCHRP Project No. 12-69, Design and Construction Guidelines for Long-span Decked Precast, Prestressed Concrete Girder Bridges, June 15, 2004, 21pp.

2. AASHTO, “LRFD Bridge Design Specifications,” Third Edition, American Association of State Highway and Transportation Officials, Inc., 2004.

3. Tadros, M. K. and Baishya, M. C., “Rapid Replacement of Bridge Decks,” NCHRP Report 407, Transportation Research Board, National Cooperative Highway Research Program, 1998

4. Tadros, M. K., Badie, S. S., and Kamel, M. R., “Girder/Deck Connection for Rapid Removal of Bridge Decks,” PCI Journal, Vol. 47, No. 3, May-June, 2002, pp. 58-69.

5. “PCI Bridge Design Manual”, Prestressed Concrete Institute, Chicago, IL, Oct. 1997.

6. Mast, R. F., “Lateral Stability of Long Prestressed Beams – Part 1”, PCI Journal, V. 34, No. 1, Jan. – Feb., 1989, pp. 34-53.

7. Mast, R. F., “Lateral Stability of Long Prestressed Beams – Part 2”, PCI Journal, V. 38, No. 1, Jan. – Feb., 1993, pp. 70-88.

8. Alaska Department of Transportation and Public Facilities, Standard Specifications for Highway Construction 2004
http://www.dot.state.ak.us/stwddes/dcsspecs/assets/pdf/hwyspecs/english/2004sshc.pdf

9. Prestressed Concrete Institute, “PCI Design Handbook,” 6th Edition, Chicago, 2004.

10. Washington State Department of Transportation, Standard Specifications for Road, Bridge, and Municipal Construction, 2006.

11. Rosa, M., Stanton, J. F., and Eberhard, M. O. “Improving Predictions for Camber in Precast, Prestressed Concrete Bridge Girders,” University of Washington, Seattle, Washington, March, 2007.

12. Sethi, V., “Unbonded Monostrands for Camber Adjustment,” Master Thesis, Virginia Polytechnic Institute and State University, Blacksburg, Virginia, 2006.

13. ACI Committee 209, “Prediction of Creep, Shrinkage, and Temperature Effects in Concrete Structures,” ACI Manual of Concrete Practice, 2002.

14. AASHTO LRFD “Bridge Design Specifications,” Fourth Edition, American Association for State Highway and Transportation Officials, Washington, D.C., 2007.

15. Ma, Z. et al , “Field Test and 3D FE Modeling of Decked Bulb-Tee Bridges,” ASCE Journal of Bridge Engineering, 12(3), 306-314, 2007

16. Li, L., Ma, Z., Griffey, M. E., Oesterle, R. G., “Improved Longitudinal Joint Details in Decked Bulb Tees for Accelerated Bridge Construction: Concept Development,” ASCE Journal of Bridge Engineering (paper in print), 2009

17. Stanton, J., and Mattock, A.H. “Load distribution and connection design for precast stemmed multibeam bridge superstructures” NCHRP Rep. 287. 1986

18. Martin, L.D., and Osborn, A.E.N. “Connections for Modular Precast Concrete Bridge Decks,” Report No. FHWA/RD-82/106, US DOT, Federal Highway Administration. 1983

19. ACI Committee 318 “Building Code Requirements for Structural Concrete (ACI 318-05)”. Farmington Hills, MI: American Concrete Institute International. 2005

20. Einea, A., Yehia, S. and Tadros, M. K. “Lap Splices in Confined Concrete” ACI Structural Journal, 96(6), 947-956. 1999

21. Thompson, M.K., et al. “Behavior and Capacity of Headed Reinforcement” ACI Structure Journal, 103(4), 522-530. 2006

22. Bentz, E. C., and Collins, M.P., *Response-2000 Reinforced Concrete Sectional Analysis*. A software downloaded http://www.ecf.utoronto.ca/~bentz/r2k.htm (2006).

23. Zhu, P. and Ma, Z., “Selection of Closure Pour Materials for CIP Connection of the Precast Bridge Deck Systems,” Proceedings of PCI Concrete Bridge Conference, Orlando, Florida, October. 2008